Secondary Ice Particle Production from Rimed Ice

By
Teizi Henmi

Department of Atmospheric Science
Colorado State University
Fort Collins, Colorado

This report was prepared with support provided by National Science Foundation Grants
GA-11574, GA-26601, and GA-31460.
Principal investigator: Lewis O. Grant
June 1974

Colorado State University

Department of Atmospheric Science

Paper No. 220

SECONDARY ICE PARTICLE PRODUCTION FROM RIMED ICE

by

Teizi Henmi

This report was prepared with support provided
by National Science Foundation Grants
GA-11574, GA-26601 and GL-31460
Principal Investigator, Lewis O. Grant

Department of Atmospheric Science
Colorado State University
Fort Collins, Colorado

June 1974
Atmospheric Science Paper No. 220

ABSTRACT

SECONDARY ICE PARTICLE PRODUCTION FROM RIMED ICE

High ratios of the concentrations of ice particles to that of ice nuclei have been observed in convective type clouds, and numerous physical mechanisms have been suggested to explain these multiplication phenomena of ice particles. However, no mechanism has been able to explain satisfactorily the phenomena of ice multiplication. In this paper, the roles of the riming process and of rimed ice on ice multiplication were studied experimentally.

The purpose of the first series of experiments was to study the secondary ice particle production from ice during its growth by the riming process. The number of secondary ice particles produced during the growth of ice were fewer than 10 per milligram of ice. In terms of the accretion number of water droplets, several million accretions of water droplets were necessary for the production of one secondary ice particle. It was concluded that secondary ice particle productions during the riming growth of ice are not effective mechanisms for ice multiplication in clouds.

The purpose of the second series of experiments was to study the secondary ice particle productions due to the evaporation process of ice which had been formed by the riming process. It was found that while rimed ice with the apparent density of less than 0.2 g cm^{-3} is being ventilated with subsaturated air, secondary ice particles are commonly produced at the rate of 10 to 200 per milligram of evaporating ice. Mechanical fracturing of the surface structure of rimed ice due to ventilation with subsaturated air was responsible for the production.

The possibility was considered that some graupel particles in the atmosphere could possess favorable physical characteristics similar to those of the rimed ice which was effective for the production of a large number of secondary ice particles throughout the experiments. It was inferred that graupel particles could commonly encounter subsaturated air in and around a cumulus cloud. Simple model calculations were conducted and it was concluded an ice multiplication rate of the order of several per minute in a cumulus cloud could be explained by the production of secondary ice particles due to the evaporation of falling graupel particles.

ACKNOWLEDGEMENTS

The author wishes to express his appreciation to Professor Lewis O. Grant for his helpful suggestions and encouragement throughout this work. He is also grateful to Drs. Charles A. Knight, Myrin L. Corrin and Dale R. Winder for their helpful comments. Mr. Rene Eles is appreciated for his skillful work building the chamber. He is grateful to his wife for her encouragement and patience.

This research was supported by the National Science Foundation under Contracts GA-11574, GA-26601, and GI-31460.

TABLE OF CONTENTS

Chapter III

Chapter IV

Chapter V

LIST OF FIGURES

Figure No.		Page

Figure No.		Page

Chapter I

INTRODUCTION

A. Problem

Ice crystal formation in natural clouds has been primarily attributed to the heterogeneous nucleation by ice-forming nuclei. Measurements of the number of these primary ice nuclei indicate that there are significant spatial and temporal variations in their concentrations. Moreover, the number of ice nuclei activated in the atmosphere is strongly dependent upon temperature. In general, the average spectrum of ice-forming nuclei in the atmosphere is crudely expressed by an exponential of the form

$$n(\Delta T) = n_o \exp(\beta \Delta T)$$

where ΔT is the degree of supercooling, $n(\Delta T)$ is the number of nuclei per litre active at supercoolings less than ΔT, and β and n_o are numerical factors (Fletcher, 1962). For a mean activation spectrum Fletcher suggested that β and n_o are, respectively, about 0.6 and about 10^{-5} litre^{-1}. This gives typically a concentration of one active nucleus per litre at approximately -20°C, the concentration changing by a factor of about 10 for each 4°C of supercooling (See Figure 1-1).

However, observations of ice crystals in natural clouds by various groups have shown that the concentrations of ice crystals are often three or four orders of magnitude larger than that measured by ice nuclei counters or estimated by an empirical formula such as given by Fletcher, suggesting the existence of some very active ice crystal enhancement mechanisms. There is an uncertainty in the methods of

(1969) and Takeuchi (1972) suggested the following time sequence of ice phase development:

(i) At the initial stage of cloud development only supercooled water droplets are present.

(ii) Collision - coalescence processes take place and large water droplets of precipitation size are developed. At this stage a decrease of liquid water content is noticed and small concentrations of ice particles are observed. The types of ice particles observed are mainly rimed ice (graupel particles) or frozen water droplets.

(iii) The liquid water contents become smaller but appreciable concentrations of regular ice crystals and graupel are noticed. At this stage the liquid water contents are on the order of 0.1 gm m^{-3}, the concentrations of regular ice crystals are several 10 $litre^{-1}$ and graupel concentrations are about 1 $litre^{-1}$ (Mossop et al., 1969).

(iv) Finally, the liquid water disappears completely and the concentrations of regular ice crystals sometimes become hundreds $litre^{-1}$. At this stage the concentrations of graupel and frozen water droplets decrease to the value less than 1 $litre^{-1}$.

There are few reports concerning the rate of increase of ice particle concentrations. Mossop et al. (1970) found that it took about eight minutes for the concentration to be multiplied by a factor of 10.

On the other hand, Koenig (1963), from the observations of summer cumulus clouds in Missouri, reported an increase in the concentration of ice particles from below the limit of detection (20 m^{-3}) to $10^4 m^{-3}$ in five and a half minutes, which is a multiplication factor of 500 or more in five and a half minutes. More observational data are required to resolve the rate of increase of ice particles

d. Relationship of cloud size to ice multiplication

It is reported that wide clouds are more likely to contain ice than narrow short-lived clouds (Mossop et al., 1970, Morris and Braham, 1968). Cumulus clouds having large widths are usually multicelled, and longer-lived. This is consistent with the observation that ice multiplication is a time-dependent process. Ice particles in an old cell may be incorporated in a newly rising tower by mixing processes.

2. Suggested mechanisms and laboratory experiments

In order to explain the phenomenon of ice multiplication, many mechanisms have been suggested and laboratory experiments associated with those mechanisms have been conducted. As early as 1948 Langmuir (1948) suggested a possible mechanism to explain high concentrations of ice particles in natural clouds, namely, the fragmentation of snowflakes by contact between snowflakes.

The suggested mechanisms can be classified into two main categories. The first category is associated with the mechanisms of primary appearances of ice particles produced from the primary ice particles.

1. Mechanisms associated with the primary appearance ice include:
   a. Ice formation on slow acting ice nuclei (Warner and Newnham, 1958; Takeda, 1968)

b. Ice formation on pre-activated nuclei (Roberts and Hallett, 1968)

c. Contact nucleation by dry particles (Gohkale and Goold, 1968)

d. Freezing of water droplets due to the evaporation cooling (Hallet, 1970)

e. Electro-freezing or mechanical-freezing of supercooled water (Abbas and Latham, 1969)

The combination of mechanisms a through d should be responsible for the initiation of the ice phase. However, ice multiplication, such as that shown in Figure 1-1, cannot be explained by these mechanisms (Mossop, 1969, 1971). Concerning mechanism e it was reported that freezing probability of water droplets is enhanced only if the electrical field stronger than 10 KV/cm is applied to water droplets. It is, however, unlikely that such a strong electric field exists frequently in clouds where ice multiplication takes place (Mossop et al., 1969). To date there has been no report which describes the observation that ice multiplication is accompanied with lightning.

2. Mechanisms associated with secondary production of ice include:

a. Shedding of "whiskers" from evaporating ice particles (Cross, 1969; DeMichelli and Lincenblat, 1967; Ruskin, 1969)

b. Mechanical fragmentation of fragile ice crystals (Langmuir, 1948; Grant, 1968; Vardiman and Grant, 1972)

c. "Splintering" when drops freeze in the riming growth of ice particles (Johnson and Hallet, 1968; Mossop et al., 1969; Mossop et al., 1972; Ono, 1971).

d. Shattering of water drops freezing in free fall (Hobbs and Alkezweeny, 1968; Brownscombe and Thorndike, 1968; Takahashi and Yamashita, 1970)

e. Frost-like growth on ice particles in local supersaturation caused by contact with large drops (Koenig, 1965)

f. Accumulation of ice crystals on ice nuclei at the sampling level (Mossop and Ono, 1969)

g. Seeding by ice particles from higher clouds (Braham, 1967)

The experiments on mechanism a, shedding of "whiskers" from evaporating ice particles, have been conducted only on bulk ice. According to the experiments by Cross (1969) and DeMichelli and Lincenblat (1967), ice "whiskers" appeared on the surface of substrate ice after the ice had been continuously exposed to subsaturated air for at least 10 minutes. It is unlikely that ice particles would be continuously exposed to subsaturated air for such a long period of time. Nevertheless, these studies necessitate further studies regarding the effect of subsaturated air on ice particles for ice multiplication.

Mechanism b, mechanical fragmentation of fragile ice crystals, seems to be effective in clouds whose temperature and humidity are favorable for the growth of dendritic crystals. However ice multiplication has been observed frequently in clouds whose top temperature is warmer than -10°C. The crystal type in this temperature region is mainly column which is considered not to be fragile. Therefore, this mechanism may be one but cannot be accepted as general explanation for ice multiplication.

As has been described previously, ice multiplication may be preceded by the formation of large supercooled water drops of precipitation size. For this reason, mechanism c, the secondary ice particle production due to splintering of large water drops freezing in free fall, was hypothesized to be the most likely mechanism of ice multiplication (Koenig, 1963; Braham, 1964). This hypothesis is based on the experimental results that the water drops of 1 mm size suspended on various supports produced many ice particles by shattering during the freezing process (Mason and Maybank, 1960; Kachurin and Belyaev, 1960, Evans and Hutchinson, 1963). However, the recent studies of suspended water drops by Dye and Hobbs (1968), and Johnson and Hallett (1968) show that the previous results were produced by contamination of carbon dioxide used for cooling systems of experiments and that the splintering of water droplets during the freezing process rarely happened in the natural atmosphere.

The experimental results on shattering water drops freezing in free fall are inconclusive. According to Hobbs and Alkezweeny (1968) and Brownscombe and Thorndike (1968) drops smaller than 50 microns in diamater did not shatter on freezing in free fall at temperatures between -6 and -30°C. Of the larger drops about 10 percent did shatter, but the number of splinters produced was small. On the average, each freezing drop produced less than two ice particle (Brownscombe and Thorndike, 1968). Takahashi and Yamashita (1970) showed, on the other hand, that 37 percent of drops with 75 to 175 microns in diameter shattered during freezing in free fall at temperature of -16°C but they did not measure the number of splinters produced.

With this physical reasoning, Johnson (1972) and Brownscombe and Goldsmith (1972) conducted riming experiments. Johnson reported on experiments in which an ice substrate is ventilated with air containing supercooled water droplets with diameters of 20 to 100 microns at velocities up to 10 m sec^{-1}. It was concluded that fewer than one drop in 6 x 10^4 will eject an ice splinter larger than 10 microns in diameter. In the experiments by Brownscombe and Goldsmith ice which was formed on an insulated rod 3 mm in diameter was rotated in a supercooled water cloud which had droplets with a mean volume diameter of about 15 microns. In addition, droplets of mean volume diameter of about 40 microns were also injected into the chamber. The maximum ice crystal production rate was one crystal for every 5 x 10^4 droplets collected.

A second possibility for secondary ice particle production during the riming process is mechanical fracturing of the surface structure of ice by ventilation while ice is growing by the riming process under strong ventilation.

A third possibility for secondary ice particle production is that some of the water droplets which come in contact with an ice specimen will be bounced off resulting in frozen water droplets as secondary ice particles (Aufdermaur and Johnson, 1972). From the experiments of charge separation due to riming in an electric field, Aufdermaur and Johnson suggested that the charging events are the results of some drops colliding with an ice pellet at grazing incidence at a rate of about one to ten events per 1000 drops. In their experiments ice pellets were grown by riming of supercooled water droplets of 20 to 100 micron in diameter. The temperature of the experiments was between -5 and -15°C, and the impaction velocity was about 10 m sec^{-1}. However, they detected an insignificant number of secondary ice particles by the sugar solution method.

B. Plan of Study

The investigation includes consideration of the second and third possibilities of secondary ice production during the riming process. The first mechanism suggested by Brownscombe and Hallett has been studied extensively, resulting in no significant number of secondary ice particles. It may be reasonable to consider that since low density ice results from the weak bonding between droplets, the structure of such ice is fragile. If the surface structure of such ice is blown off by ventilation, it should occur more often when the ventilation velocity is larger.

The third possible mechanism of secondary ice particle production by the riming process, or, the bouncing-off of droplets after droplets collide with the ice surface, should be more important when the number of collision is large. The collision frequency is high when both the impact velocity and the concentration of cloud droplets are large.

From the above considerations experiments were conducted under the following conditions.

1. Temperature: -7 ± 1°C

   This temperature was chosen for the following reasons: (i) ice multiplication is often observed at a temperature warmer than -10°C, and (ii) at colder temperatures the effect of ice accumulating on the chamber is greater and the number of effective ice nuclei in the air becomes larger.

2. Impaction (ventilation) velocity: 2~5 m sec^{-1}

   This is well within the range of fall velocity of a graupel particle (See Figure 4-2) and high enough to produce a reasonably strong drag force. In addition, fragile ice can be formed by impaction velocities within this range, according to Macklin's results (1962).

3. Liquid water contents: less than 0.5 gm m^{-3}

   Low density ice is formed more easily when the liquid water content is lower.

4. Size of cloud water droplets: 3~20 microns in diameter

   This size distribution may be close to those in continental type clouds but smaller than those in maritime type clouds. Low density ice is more easily produced by cloud water drops having small diameters (Macklin, 1962). In addition, high concentrations of cloud water droplets are obtained at low liquid water contents so that large numbers of collisions can be expected.

C. Experimental System

The experimental system was set up in a cold room, as shown schematically in Figure 2-1. The following give the details.

1. The Chamber

The chamber is made of transparent plastic plates so that the inside of the chamber can be seen through the wall. Figure 2-2 is a photograph of the chamber. The lower portion of the chamber is about 20 cm x 20 cm x 40 cm. At the bottom of the chamber a sugar solution tray is placed in order to detect secondary ice particles produced from the growing ice specimen. A thick aluminum plate is

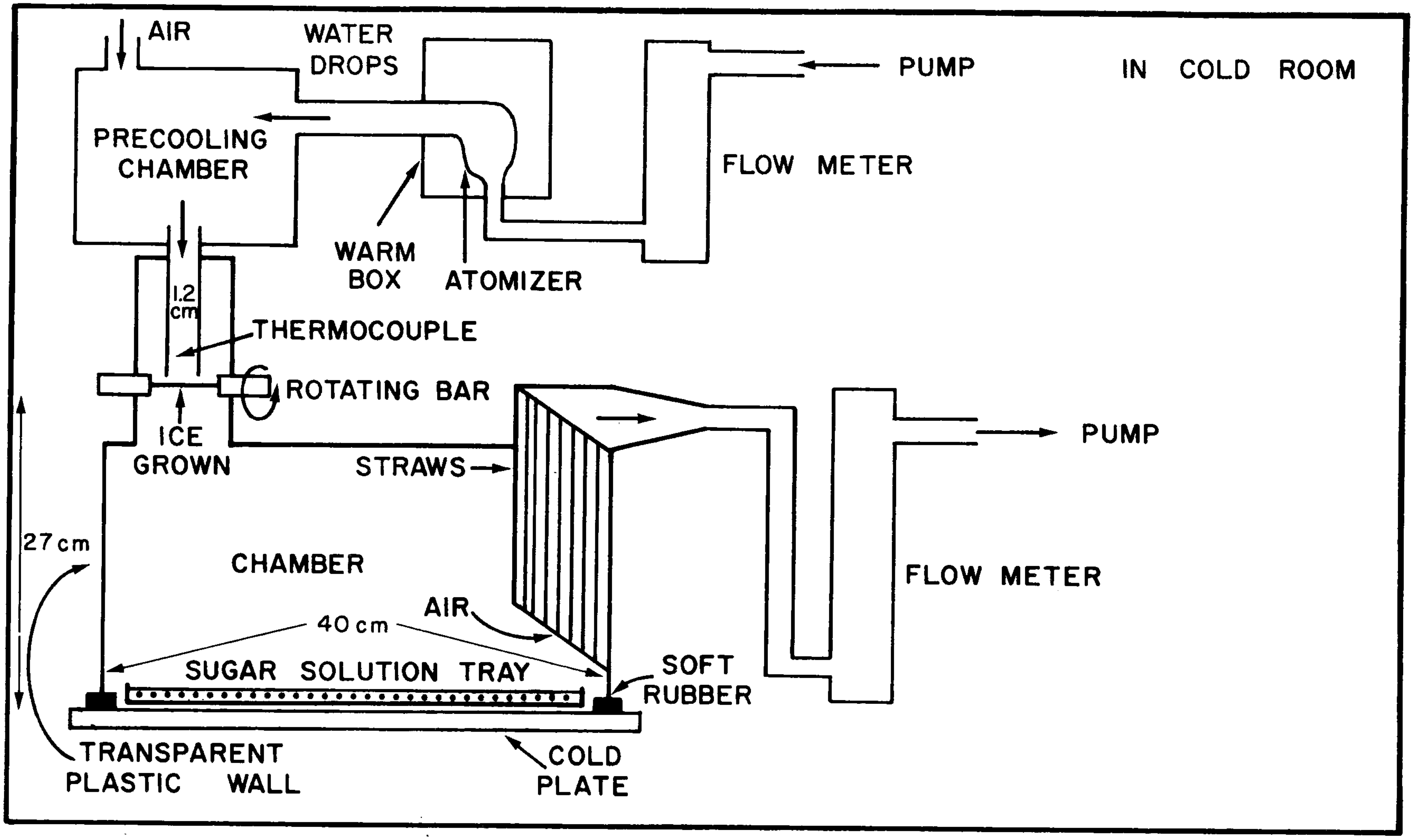

Figure 2-1. Schematic diagram of experimental system.

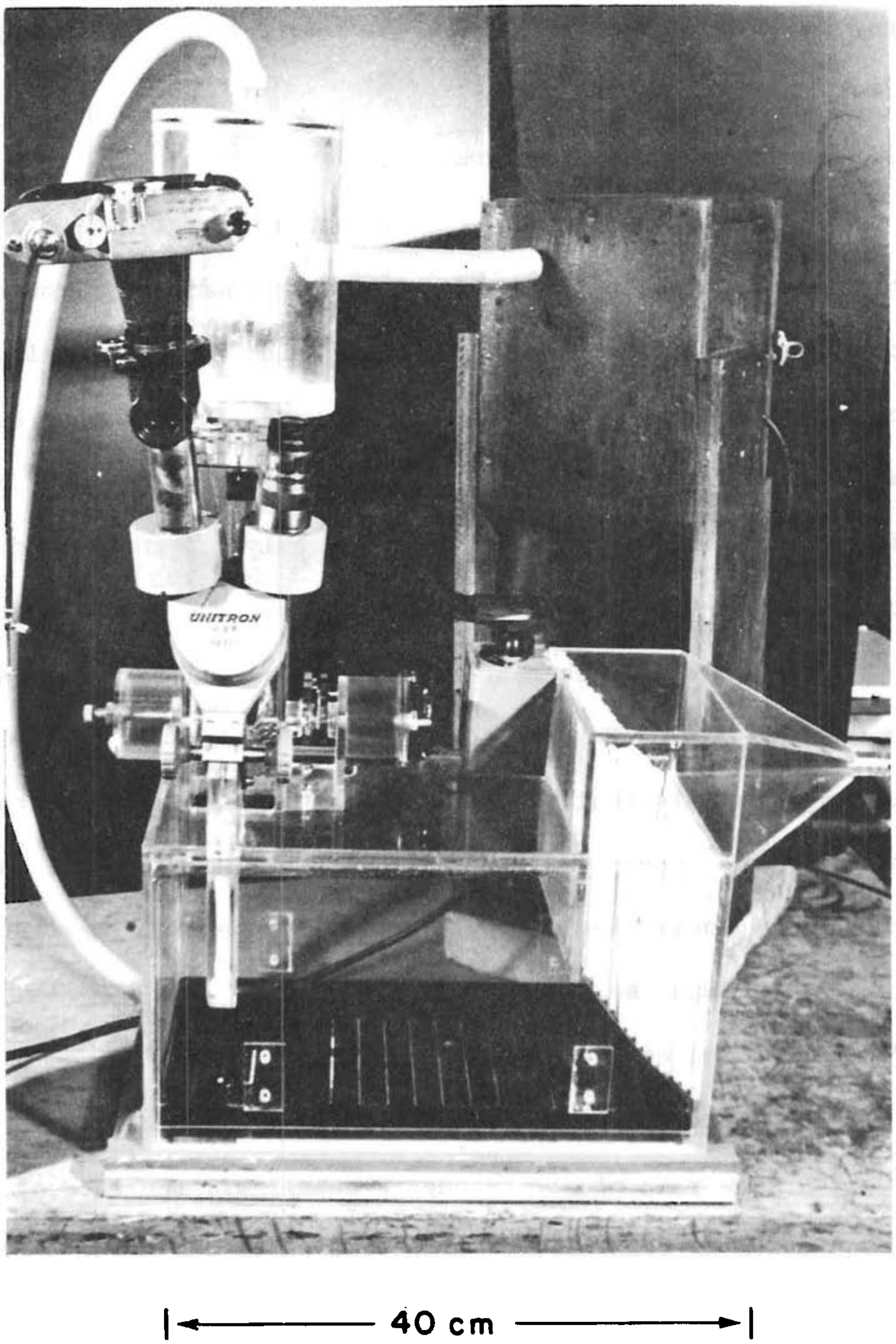

Figure 2-2. Photograph of chamber used in experiments.

placed below the tray to cool the sugar solution. To avoid air leakage, the chamber is placed on a thick soft rubber pad which is pasted on the aluminum plate.

2. Air flow through the chamber.

The chamber is connected to a suction pump by which the air flow is controlled. Since the air goes into the chamber only from the mixing cylinder, the impaction velocity of cloud water to the rotating bar can be controlled by the suction rate of the pump. The air goes out through a straw layer which is placed to produce a uniform flow. The air velocity at the exit estimated at approximately 2.5 cm sec^{-1} for the maximum impaction velocity of the experiments. The air velocity through the lower portion of the chamber is less than 1 cm sec^{-1} even at the maximum suction rate. The air flow pattern examined by injecting visible smoke reveals that the air from the pipe hits the bottom of the chamber and diffuses to fill the chamber. Therefore, it can be assumed that secondary ice particles, if any, are almost perfectly detected by the sugar solution.

3. Production of cloud water

Cloud water is generated by using a glass nebulizer. By changing the flow rate of air through a nebulizer, the rate of cloud water production is controlled. Distilled water was used. Under the same experimental condition, the growth rate of ice and the density of ice is repeatable. Therefore, it may be assumed that the production rate of cloud water was consistent.

4. Temperature measurements

The temperature of the air through the chamber is measured at 1 cm above the rotating bar. A thermocouple of copper and constantan with a diameter of .064 mm is used. Since the electromotive force of a thermocouple was measured by a millivoltmeter, the relationship between temperature and electromotive force of the circuit was obtained by using an accurate mercury thermometer.

D. Methods of Experiment

1. Procedures

a. The walls of the chamber are coated with glycerin, and then the air containing cloud water is sucked past the rotating bar so that an ice specimen starts riming on its surface. The rotation rate of the bar is three per minute.

b. After the diameter of the ice cylinder becomes at least 2.0 mm, the suction of the air is stopped in order to clean the inside wall of the pipe with a sponge wetted with glycerin. This is done to prevent the splintering of the ice accumulated on the wall.

c. A sugar solution tray which has been precooled is placed on the cold plate, and the chamber is placed back in position. The sugar solution is prepared following the description by Admirat (1962). The composition is as follows:

Water	Sugar	Sodium Silicate
100 gm	100 gm	200 gm

d. Again, cloud water is pulled into the chamber so that the ice specimen continues to grow by riming.

e. When secondary ice particles are produced during the growth of the ice, they are detected in the sugar solution.

f. The ice specimen on the rotating bar is observed through a microscope so that the growth rate of the ice specimen is measured.

to estimate the volume of the ice. Then the ice cylinder was immersed in silicon oil. The weight of the oil plus the ice cylinder were measured with a micro-balance.

The apparent density of the ice cylinder, ρ, was calculated by

$$\rho = m/v$$

Where m is the mass of an ice cylinder and V was the volume of the ice cylinder. From the equation

$$\ell n\rho = \ell n\ m - \ell n\ V \text{ or } \frac{d\rho}{\rho} = \frac{dm}{\rho} - \frac{dv}{v}$$

Therefore,

$$\left|\frac{\Delta\rho}{\rho}\right| = \left|\frac{\Delta m}{m}\right| + \left|\frac{\Delta v}{v}\right|$$

the accuracy of this method was considered as follows. The accuracy of the microbalance used was 1 mg. The weight of the ice was on the order of 10 to 30 mg depending on experimental conditions, so that $|\Delta m/m| \simeq 0.03 \sim 0.1$. $|\Delta v/v|$ is assumed to be 0.1. Therefore, $|\Delta\rho/\rho| \simeq 0.2$.

E. Results and Discussion

The results of all experiments with different conditions are summarized in Table 2-1. The experimental conditions are also written in the table. In this table the number of secondary ice particles produced per unit mass of ice grown by the riming process, dN/dm, is calculated as

$$\frac{dN}{dm} = \frac{N_1 - No}{\Delta m}$$

Little is known regarding mechanism e, frost growth on ice particles by contact with large drops.

Regarding mechanism f, accumulation of ice crystals or ice nuclei at the sampling level, one might expect to find a high concentration of ice crystals at the level where their fall velocities were just balanced by the updraft velocity of a cloud, providing the cloud were in a steady state. This is unlikely in cumulus clouds where a series of towers rise and then decay.

Mechanism g, seeding by ice particles from higher clouds, cannot be accepted as a general explanation for ice multiplication since many cases of ice multiplication have been observed in clouds where the skies above were completely cloudless (Mossop, 1969).

In recent years mechanism c, "splintering" when drops freeze in the riming growth of ice particles, has been strongly suggested by Mossop et al. (1969), Mossop (1970), Mossop et al. (1972) and Ono (1971). Their suggestions are based mainly on the circumferential evidence that large rimed ice particles proceed high concentration of ice particles. Laboratory studies should be conducted on this mechanism.

C. Implications from the Previous Studies

Each of the mechanisms described above can be a possible mechanisms of ice multiplication in a particular cloud and situation. Most of those suggested mechanisms cannot provide a satisfactory explanation for ice multiplication in cumulus clouds, where most of the observational emphasis has been placed in recent years.

Most of the previous studies consider only the microphysics of cloud particles. Little consideration has been given to the interactions between cloud particles and surrounding air, events which are

Chapter II

EXPERIMENTS ON SECONDARY ICE PARTICLES PRODUCTION DURING THE RIMING GROWTH OF ICE

A. Introduction

From the experiments of freezing of suspended water droplets, Johnson and Hallett (1968) concluded that the most important factors in the fragmentation of freezing drops are symmetry of heat transfer and effective conductivity. They concluded that while symmetry of heat transfer is a dominant factor in causing drop shatter, the symmetry is also linked with high heat conductivity. Therefore, it is possible that a high freezing rate may also increase the probability of shattering. Thus the freezing of a water droplet on an ice surface sometimes provides favorable condition for droplet shatter. The heat balance of a water droplet freezing on an ice surface was considered by Brownscombe and Hallett (1967). In the case of a water droplet freezing on a smooth surface of ice, the rate of heat flow away from the drop through the air is much smaller than that through the ice. According to Brownscombe and Hallett, even under strong convection (Re $\approx$100) the heat flow through the air is less than 10 percent of the heat flow through the ice, which indicates that even under conditions of extreme ventilation the drop will freeze much more rapidly from the contact surface of substrate ice than from the outside. This asymmetry of heat transfer is reduced when the drop freezes on an irregular surface so that the area of contact with the substrate ice is reduced. In this case, there is the possibility of a pressure build-up inside the drop followed by explosive shattering. Secondary ice particles may result from this process.

TABLE 2-1. The summary of riming experiments

Experimental condition

Ex. #	v(cm/sec)	$W(g/mc^3)$	T(°C)	n	$\rho(g/cm^3)$	dN/dm(1/mg)	$K \times 10^6$
(1)	238	.33	-7.2±.3	5	.25±.03	5.6±1.6	2.168± .666
(2)	238	.13	-7.1±.3	6	.24±.02	13.6±8.6	3.092±3.067
(3)	329	.28	-7.1±.3	6	.27±.01	3.3±2.3	4.451±1.923
(4)	329	.088	-7.1±.3	6	.26±.01	8.8±3.9	2.741±2.195
(5)	429	.25	-7.1±.3	6	.31±.01	1.8±1.1	6.367±4.336
(6)	429	.066	-7.3±.3	6	.29±.01	4.8±1.4	3.915±1.487

v : the ventilation velocity

W : the liquid water content of cloud

T : the temperature of air measured 1 cm above an ice cylinder

n : the number of experiments

ρ : the apparent density of an ice

dN/dm: the number of secondary ice particle per unit mass of ice

K : the number of accreted water droplets to produce one secondary ice particle where N_1 is the number of secondary ice particles during the riming experiment, No is the number of ice counted during control experiment conducted immediately after each riming experiment, and Δm is the estimated mass of ice grown for five minutes, which is the period of time spent in counting N_1 and No. The estimation of Δm is made from the measurement of an appraent density and the measurement of the diameter and length of the ice cylinder. (See Appendix I)

In the table the number of accreted water droplets to produce one secondary ice particle, K, is also given. K is calculated as

$$K = \frac{dm}{dN} \Big/ \frac{\pi}{6} \rho_m D_w^{\,3}$$

where ρ_w is the density, of water, and D_w is the mean diameter of cloud water droplets which are accreted on the rotating bar during the period of an experiment.

Analysis of the variance was conducted in order to examine if N_1 is statistically different from No for each experimental condition. The results of the analysis showed that for all experimental conditions, N_1 is statistically larger than No for a significance of $p < .05$.

The table shows that within the range of the experiments, the number of secondary ice particles is smaller than 10 per milligram of ice except for one experimental condition in which the average of dN/dm is 13.6 per milligram.

The table also shows that several million water droplets are necessary for the production of one secondary ice particle within the range of the experiments. It has been reported that one secondary ice particle per several 10^4 of droplets is produced (Johnson, 1972, Brownscombe and Goldsmith, 1972). In terms of dN/dm the result by

Brownscombe and Goldsmith (1972) is estimated as approximately 12 per milligram of ice. Therefore, present results, show lower production of ice particle than the previous studies in terms of dN/dm.

If grazing collisions were the cause of secondary ice particle production, the data should show larger values of dN/dm and smaller values of K when the ventilation velocity and liquid water content are increased. However, the results obtained show the opposite, namely large dN/dm and small K under the condition of lower ventilation velocity and smaller liquid water content.

Therefore, it is concluded that grazing collision is not a significant mechanism for secondary ice particle production at least within the range of present experiments. It may be inferred that even if there are phenomena related to a grazing collision, the drops leaving the ice remain liquid or are not frozen completely before reaching the sugar solution tray.

According to a study by Hobbs and Alkezweeny (1968), a water drop smaller than 50 microns in diameter does not shatter while being frozen in free fall. The maximum diameter of water droplets in the present study is about 20 microns. This implies that the secondary ice particles detected are not due to shatterings of freezing water droplets. The data tend to show that the lower the apparent density of ice, the higher the number of secondary ice particles. Therefore, the most likely mechanism of secondary ice particles for the present study is the mechanical fracturing of rimed ice by strong ventilation.

The results indicate that this mechanism would be effective only when ice particles grow in a cloud having a high concentration of cloud droplets. Simple calculations indicate that for $K = 10^4$ and 10^6

approximately 10 and 30 minutes are, respectively, required for the concentration to be multiplied by 10. In the calculations the cloud was assumed to have 500 cm^{-3} of cloud droplets with a mean volume diameter of 15 microns. (See Appendix II)

F. Conclusion

During the rimed growth of ice under the conditions where the ventilation velocities ranged from 2.3 to 4.3 m sec^{-1} and where the temperature was about -7C, the number of secondary ice particles are fewer than 10 per milligram of ice. In terms of secondary ice particles per collision number of water droplets, several 10^6 of water droplets were necessary for the production of one secondary ice particle. This leads to the conclusion that the secondary ice particle production during the growth of ice by the riming process is not an effective mechanism for ice multiplication.

Chapter III

EXPERIMENTS ON SECONDARY ICE PARTICLE PRODUCTION DURING THE EVAPORATION OF RIMED ICE

A. Introduction

It has been reported that ice whiskers appear on the surface of ice which is evaporating. According to the experiments by DeMichelli and Lincenblat (1967), ice whiskers commonly appear during the evaporation of ice under several conditions of subsaturation (relative humidities of 25, 50 and 80 percent with respect to ice at temperatures between -10°C and -22°C). Cross (1969) reported, from the observations of evaporating ice with a scanning electron microscope, that polycrystalline ice develops a fibrous surface during evaporation. Although these experiments were made in still air using ice formed by freezing bulk water, it is felt that the effect of subsaturated air on ice needs further study from the standpoint of ice multiplication.

Concerning the mechanical strength of ice it was reported by Latham (1963) that when air currents of a few cm sec^{-1} velocity are allowed to flow past frost deposited on a brass disc, small splinters are broken off the fragile dendritic crystals. Latham's results show that the number of splinters broken off is linearly proportional to the air velocity. For an air velocity of 2m sec^{-2} splinters were ejected from the frost specimen at the rate of 16 sec^{-1} cm^{-2}. Although it is not clear from his article what sizes of frost were exposed to airflow or the humidity of the airflow, it shows that ice exists which is mechanically fragile enough to be broken off by moderate velocity of airflow.

Circumstantial evidence, as described in Chapter I, indicates that before ice multiplication takes place, graupels are usually observed and their high concentration of ice crystals are observed at the edges of clouds where the mixing of subsaturated air of the environment and cloud air takes place.

From the above experimental results and the circumstantial evidence of field observations it can be implied that graupels which is formed by the riming process, may produce secondary ice particles by ventilation with subsaturated air. The purpose of this chapter is to report experimental results on the possible production of secondary ice particles during ventilation of rimed ice with subsaturated air. From preliminary experiments it was found that only the ice with lower apparent densities produces significant numbers of secondary ice particles during ventilation with subsaturated air. Therefore experiments were conducted mainly on the ice within these density ranges. The same experimental system was used for the following experiments with an addition of an apparatus to obtain the air having a desired relative humidity.

B. Procedures

1. Method of experiments

a. An ice specimen was formed on a rotating bar as described earlier. In order to make ice with low density, the cloud water was supplied with a slow velocity. The following impaction velocities and liquid water contents were used.

Apparent density (g/cm^3)	Impaction velocity (m/sec)	L.W.C. (g/m)
0.08 ± 0.02	.45	1.3
0.12 ± 0.02	.80	1.0
0.16 ± 0.02	1.20	0.7
0.22 ± 0.03	1.80	0.5
0.30 ± 0.02	4.30	0.3

The measurements of the apparent density were made by the methods described in the previous chapter.

b. While an ice specimen was being formed, the air was pulled through an ice layer and a heater so that subsaturated air with a constant temperature was produced. The detail of the ice layer will be described in the following section.

c. After an ice specimen grew to about 2.5 mm in mean diameter, the supply of cloud water was stopped. The chamber was cleaned in the same way as described in Chapter II.

d. By connecting an air hose from the subsaturated air source to the specimen chamber, subsaturated air flowed into the chamber so that the ice specimen was ventilated. Secondary ice particles produced, if any, were detected by observing the sugar solution.

2. Method for obtaining subsaturated air

In order to obtain subsaturated air, air from the cold room was forced through an ice layer which was made from packed snow. The construction of the ice layer is schematically shown in Figure 3-1. The snow was packed in a cylinder of one meter high and 20 cm in diameter. This snow-packed cylinder was immersed in a large can

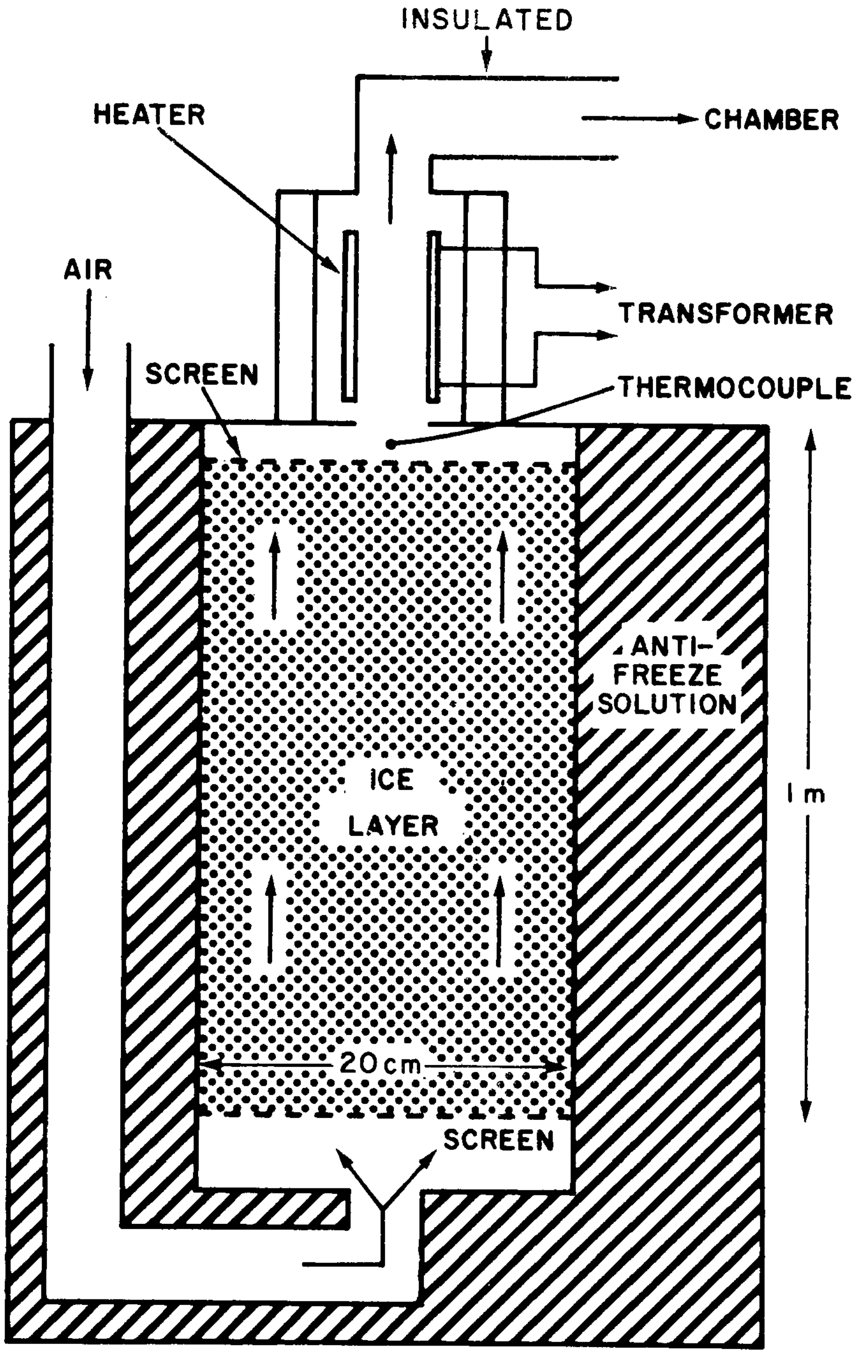

Figure 3-1. Schematic diagram of ice layer used for obtaining a desirable subsaturated air.

filled with antifreeze solution. To obtain the desired subsaturation the temperature of the ice layer was changed. To do this, the temperature of the cold room was kept controlled, so that the temperature of the ice layer reached the desired temperature. After the desired temperature was obtained, the temperature of the cold room was reset to -7°C. Because of the large heat capacity of the systems the temperature of the ice layer changes very slowly. If the temperature of the air entering the ice layer was kept slightly warmer than that of the ice layer, the temperature change of the air after flowing through the ice layer was only about 0.2°C per hour. On the other hand, the duration of the air flow into the chamber to ventilate the ice specimen was a maximum of 10 minutes, so that it can safely be assumed that the humidity of the air remained at a constant value during each experiment. After flowing through the ice layer, the air was warmed to approximately -7°C by flowing through a heater, and then supplied into the chamber through an insulated tube.

By measuring the temperature of the air above the ice layer and the temperature at 1 cm above the ice specimen, the subsaturation ratio of air was calculated. The humidity of the air which passed through the ice layer was determined. The dew point of the air was measured under similar conditions with experiments using a dew point hygrometer. The accuracy of the hygrometer was checked in air with known vapor pressures obtained above Li Cl solutions of different concentrations. The results of this examination are given in Figure 3-2.

In this figure the saturation vapor pressure with respect to ice, e_i, is plotted against the saturation vapor pressure with respect to

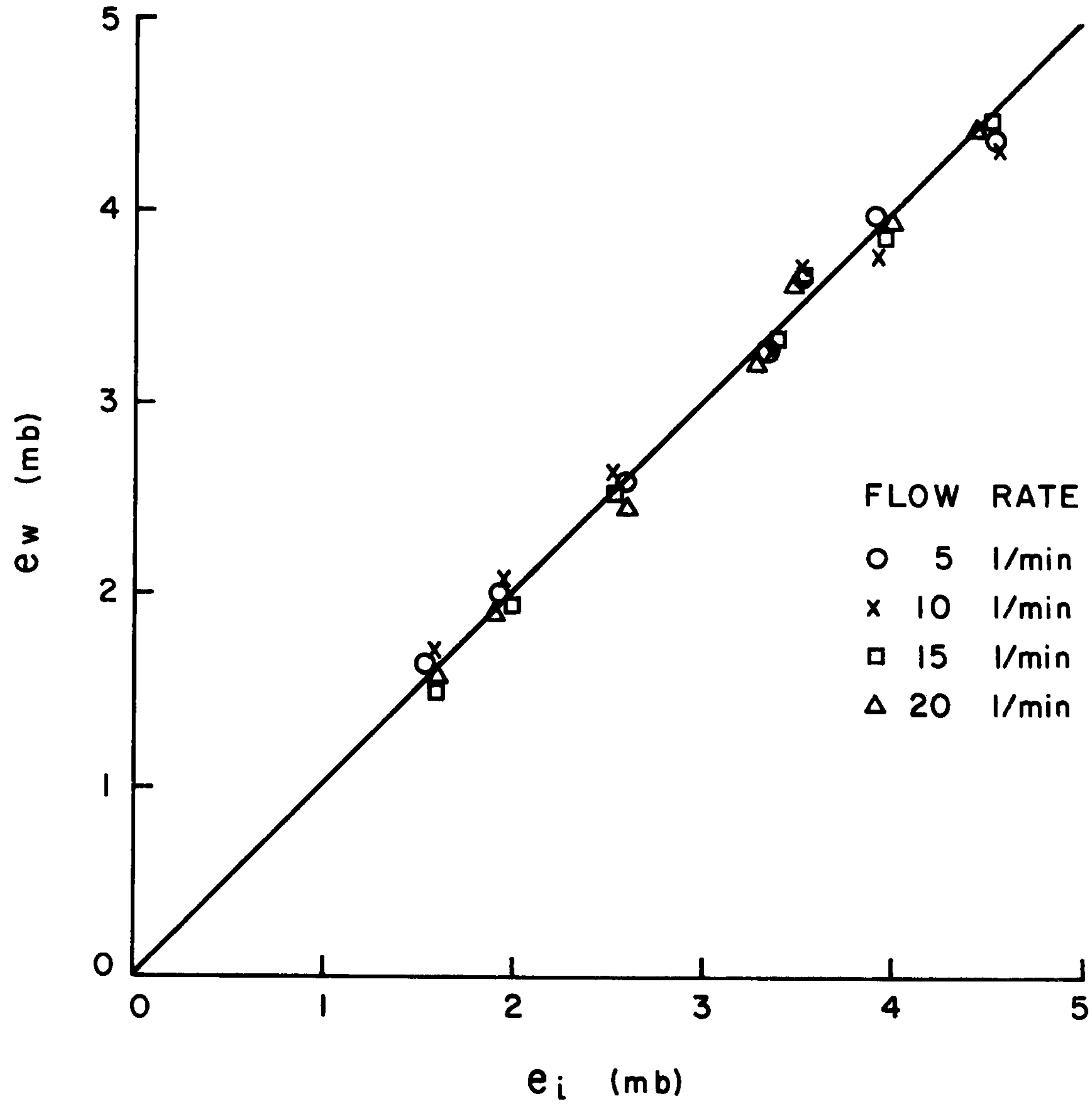

Figure 3-2. Results of the examination of the vapor pressure of air which passed through the ice layer. Here, e_i is the vapor pressure calculated from the temperature of ice layer; and e_w is the vapor pressure calculated from dew point measurement.

water, e_w. The former was obtained from the temperature measurement of the ice layer; the latter was obtained from the dew point measurement of the air. The figure shows that the vapor pressure of the air at the entrance to the chamber can be assumed equal to the saturation vapor pressure with respect to ice which was determined from the measurement of the temperature just above the ice layer. However, the result of a calibration of the dew point hygrometer showed that dew points measured by the instrument had a maximum error of ± .5°C. Therefore, the following consideration was made to estimate the error in the determination of subsaturation ratio. The error in measurement of temperature should be no greater than ± 0.2°C. (This includes the error in reading the mercury thermometer). The relationship between saturation vapor pressure with respect to ice and temperature is approximated by the Clausius - Clapeyron equation

$$\frac{de_s}{e_s} = \frac{L_s}{R_v} \frac{dT_i}{T_i^2} \qquad (3\text{-}1)$$

where e_s is the saturation vapor pressure, L_s is the latent heat of sublimation, R_v is the gas constant of water vapor, and T_i is the temperature of ice. The equation can be written as

$$\left| \frac{\Delta e_s}{e_s} \right| = \frac{L_s}{R_v} \left| \frac{\Delta T_i}{T_i^2} \right| \simeq 6.14 \times 10^3 \left| \frac{\Delta T_i}{T_i^2} \right|$$

Therefore, the error in determining the evaporation rate is

$$\left| \Delta \left(\frac{dm}{dt}\right) / \left(\frac{dm}{dt}\right) \right| = \left| \frac{\Delta \bar{\rho}}{\bar{\rho}} \right| + \left| \frac{\Delta \left(\frac{dv}{dt}\right)}{\frac{dv}{dt}} \right| = \pm 0.4 \qquad (3\text{-}3)$$

C. The Cause of Fluctuation in Data

The data obtained in the experiments showed considerable variation. This is considered to be caused by the following.

1. It was generally observed that 60 to 70 percent of the secondary ice particles fell into the section of sugar solution tray beneath a rotating bar. This implies that the air flow from the upper part of the chamber went to the bottom of a chamber before slowly leaving the exit as confirmed by an observation of the flow pattern of air in a chamber which was conducted by injecting visible smoke. Nevertheless, it is probable that a small fraction of secondary ice particles may be lost in the following ways.

a. The particles produced at a later time fall upon the section of the sugar solution tray at which the particle previously produced has grown large. This effect of overlapping can be large when large numbers of secondary ice particles are produced.

b. Although the volume of the lower portion of the chamber is far larger than the volume occupied by an air flow from the upper portion of the chamber, a small fraction of the secondary ice particles may be lost into walls of the chamber.

c. The chamber is designed in such a way that when the ventilation velocity is 2 m sec^{-1}, the velocity of air outgoing through the straw-filled exit is about 1 cm sec^{-1}. If we assume that the secondary ice particles have a density of 0.9 g cm^{-3} with a spherical shape and that the particles fall with a velocity given by the Stoke's law, the size of a particle with terminal velocity of 1 cm sec^{-1} is about 20 microns in diameter. Therefore, the secondary ice particles less than 20 microns in diameter can be carried to the exit and may exit with the outgoing air.

Although these three effects are considered to be minor, they give uncertainty to the data.

2. Because of a random nature of the accretion process, ice formed by the present method is not identical for each experiment, even though it is classified into different apparent densities based on the condition of formation. As will be seen later, ice which produces a large number of the secondary ice particles has a microscopically irregular shape. Since this irregular shape is one of the factors necessary for the production of the secondary ice particles, it may be inevitable that variations in the data occur.

3. In addition, as have been described, the errors in estimating the evaporation rate and the occasional fluctuation in ventilation velocity would contribute to the variation in the data.

D. Results and Discussions

1. Appearance of ice used.

The photographs of ice grown on a rotating bar are shown in Figure 3-3. These photographs were taken through a window of the chamber by using a camera with close-up ring. It can be seen that the lower the apparent density, the more feathery the appearance of the ice. The surface of the ice is not smooth but is protruded.

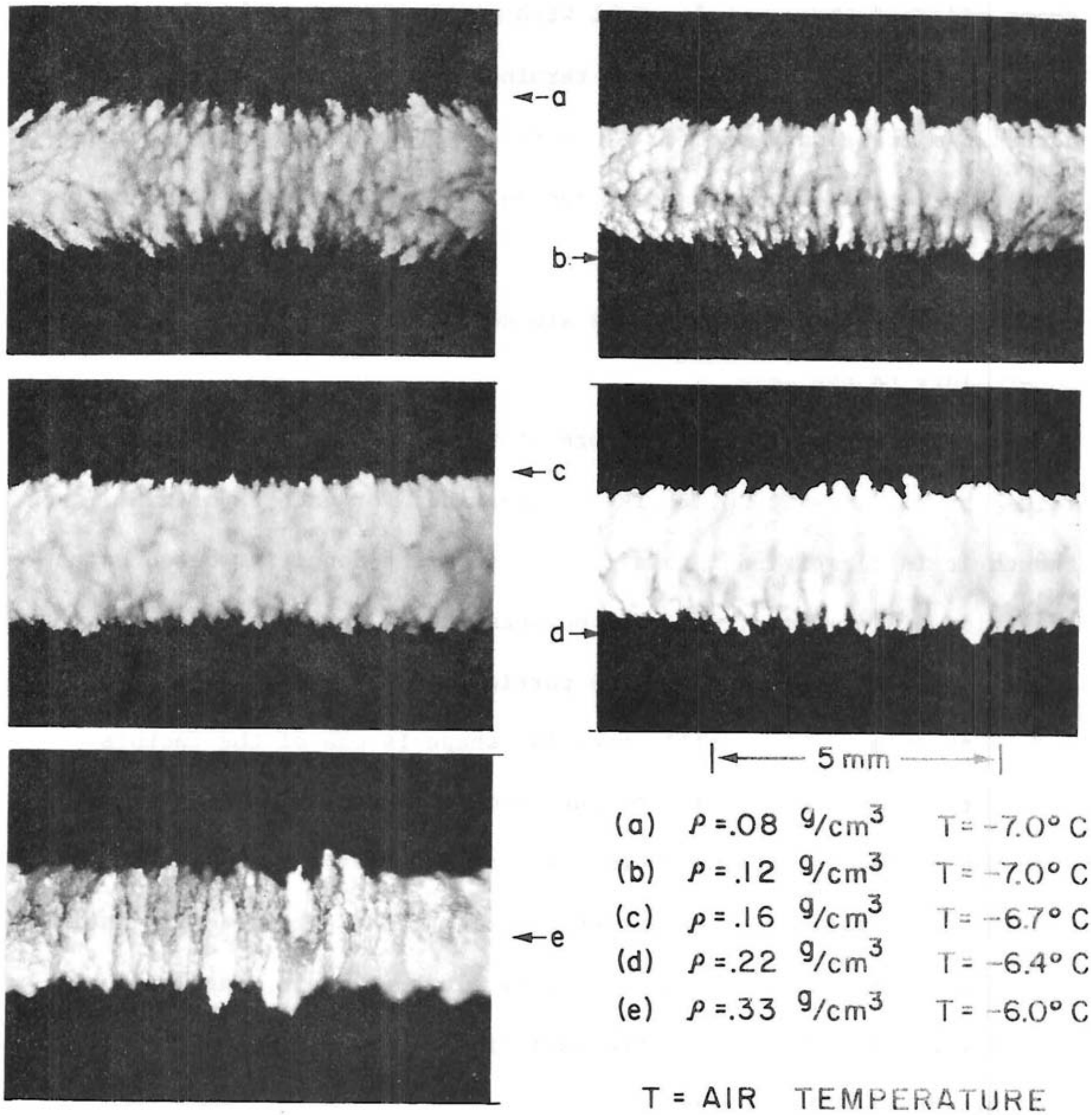

Figure 3-3. Photographs of ice cylinders grown on a rotating bar.

Microphotographs of part of the surface of these ice cylinders with different apparent density are shown in Figure 3-4. These photographs were taken with a microscope by immersing an ice cylinder into liquid hexane after the ice was grown on a rotating bar. It is seen that with the lower apparent density, the water droplets are the more lightly attached to each other; and there are many spaces between protrusions. The photograph of the ice cylinder of apparent density 0.33 g cm^{-3} shows a quite different character compared with the other photographs. This different appearance is probably caused by the larger impaction velocity than for those ice cylinders with lower apparent density. The water droplets are distorted and are packed more heavily in the case of high impaction velocity. It should be pointed out that the microphotographs of the ice cylinders of low apparent densities (< 0.22 g cm^{-3}) resemble lump graupel observed in the atmosphere (see Plate 138 of Magono and Lee, 1966).

The contribution of deposition growth to the formation of these ice is considered as follows. For ice with a cylindrical shape the rate of deposition of vapor per unit area is given by

$$\frac{1}{A}\frac{dm}{dt} = x\,\frac{D\Delta\rho}{d}\,(Sh) \qquad (3\text{-}4)$$

where x is the coefficient of surface roughness of the ice cylinder, D is the diffusivity of water vapor in air, $\Delta\rho$ is the difference between vapor density of air containing cloud water and that over ice, Sh is the Sherwood number, and d is the diameter of ice (Macklin, 1962). The equation (3-4) is derived from the similarity of vapor diffusion

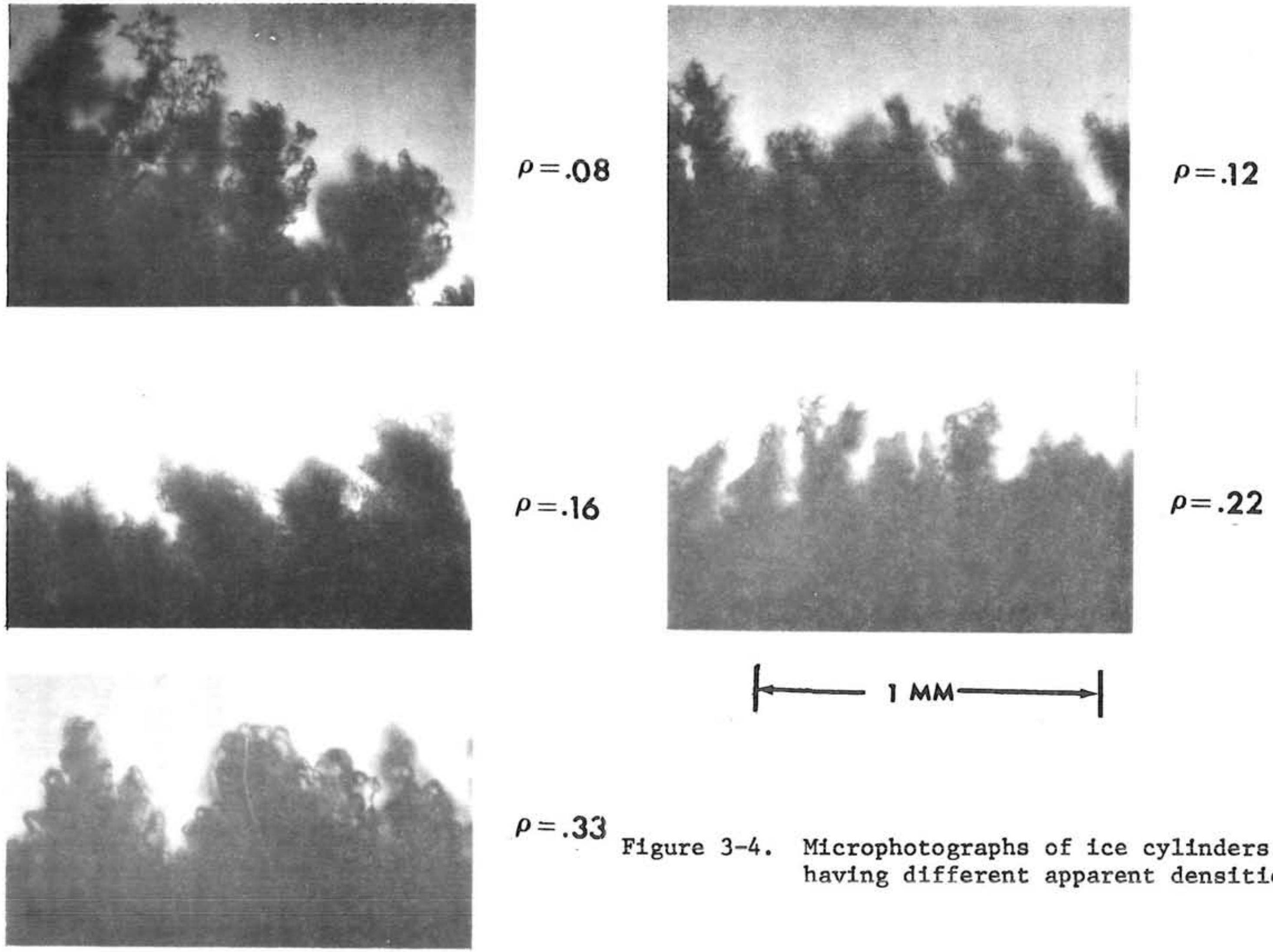

Figure 3-4. Microphotographs of ice cylinders having different apparent densities.

and heat transfer. Within the range of experiments the Sherwood number which expresses the effect of convection, can be written as

$$Sh = 0.615 Re^{.466} \tag{3-5}$$

where Re is the Reynolds number (Gebhart, 1961, Kreith, 1973).

$$Re = \frac{d \cdot v}{\nu} = \frac{\rho_a \cdot d \cdot v}{\eta} \tag{3-6}$$

where ν is the kinematic viscosity of air, d is the diameter of a cylinder, v is the impaction velocity of cloud water, ρ_a is the density of air, and η is the dynamic viscosity of air. The mean growth rate per unit area within the range of experiments is given by

$$\frac{1}{A}\frac{dm}{dt} \simeq .257 \times v^{.466} \left(\frac{d_o + d_1}{2}\right)^{-.534} \Delta\rho \tag{3-7}$$

Here, d_o is the initial diameter of a rotating bar (0.1 cm) and d_1 is the final diameter of the ice cylinder (0.25 cm). Within the range of the experiments the surface temperature of the growing ice is only several tenth degree warmer than that of the ventilating air containing cloud water. Therefore, the vapor pressure of the ventilating air is larger than the vapor pressure over the surface of an ice cylinder. Consequently, the ice cylinder grows simultaneously by the deposition and by the riming process. The mean growth rate by deposition is calculated for ice cylinders having different apparent densities. Since no data are available on x, it is assumed that x = 1. Since the surface of ice at the initial stage of the growth is smooth, the assumption of x = 1 should be reasonable, but x should become larger than 1 after the surface of ice becomes protruded. Therefore, the deposition growth rates can be larger than those given in Table 3-1.

On the other hand, the total growth rate (deposition growth plus accretion growth) for an ice cylinder to grow 2.5 mm in diameter is obtained from experiments by measuring the weight of the ice and the time necessary for an ice cylinder to grow to 2.5 mm. The mean total growth rate per unit area is expressed by

$$\frac{1}{A}\frac{dm}{dt}\bigg|_T = \frac{M}{t}/\{\pi(\frac{d_o+d_1}{2})\ \ell\} \qquad (3\text{-}8)$$

where M is the weight of ice, t is the time necessary for ice to grow to the diameter, d_1;d_o is the initial diameter of a bar; and ℓ is the length of ice. The values obtained by the equation (3-8) are also given in Table 3-1.

In the table the ratio of deposition growth rate to total growth rate is also given. It is seen that for the ice with lower apparent density, the growth due to deposition is considerably larger. This may be a partial reason for the appearance of ice with lower apparent density as shown in Figure 3-4. It should be noted, however, that since the value of x in the equation (3-7) is unknown, the ratios calculated are admittedly estimates.

2. Evaporation rate of ice

In order to obtain the production rate of secondary ice particles per unit mass of ice evaporating under the ventilated condition, the evaporation rate was measured for each experiment. Since it was known from preliminary experiments that only ice with a low apparent density produces secondary ice particles, the experiments were mainly conducted on ice with low apparent densities.

Table 3-1. The growth rate of an ice cylinder with different densities.

Apparent density (g/cm)	Calculated deposition growth rate$^{(A)}$ (g cm^{-2}sec^{-1})	Total growth rate$^{(B)}$ (g cm^{-2}sec^{-1})	A/B
0.08	4.28×10^{-7}	2.19×10^{-6}	.20
0.21	5.55×10^{-7}	4.10×10^{-6}	.13
0.16	7.15×10^{-7}	4.84×10^{-6}	.15
0.22	6.02×10^{-7}	1.00×10^{-5}	.06
0.30	6.95×10^{-7}	2.21×10^{-5}	.03

Figure 3-6, a ~ d show the evaporation rate of ice with the apparent densities 0.08, 0.12, 0.16 and 0.22 g cm^{-3}, respectively. The evaporation rates of ice are plotted as a function of saturation ratio with respect to ice. These data were obtained under a condition of ventilation velocity 2 m sec^{-1}. Although the data are variable, these figures clearly show that the evaporation rate increases with decreasing saturation ratio. From a comparison among the figures, it is seen that there is no difference in the evaporation rate as a function of ice density within the range of the apparent density of ice used in the experiments.

In the case of d = 0.23 cm, v = 2 m sec^{-1}, and ℓ = 1.0 cm, which is an average condition of the experiments, the total evaporation rate is from equation (3-4) given by

$$\frac{dm}{dt} \approx 2.89 \cdot 10^2 \; x\Delta\rho \; [g \cdot min^{-1}] \qquad (3\text{-}9)$$

The evaporation rate for x = 1 calculated from this equation is plotted in Figure 3-5, a ~ d. It is seen that the evaporation rates obtained in the experiments were greater than the calculated values. This discrepancy becomes greater at lower saturation ratios. This may be explained by the fact that the ice used in the experiments had a larger surface area exposed to the air flow than an ice cylinder with a smooth surface because the ice used in the experiments had protruded surfaces. It can be seen from the figures that if the value of x is assumed to be 3, the evaporation rates calculated by (3-9) coincide with the experimental values of dm/dt. However, it should also be pointed out that if the saturation ratio is lower, the mass decrease of ice is not only caused by the evaporation process but also by the production of

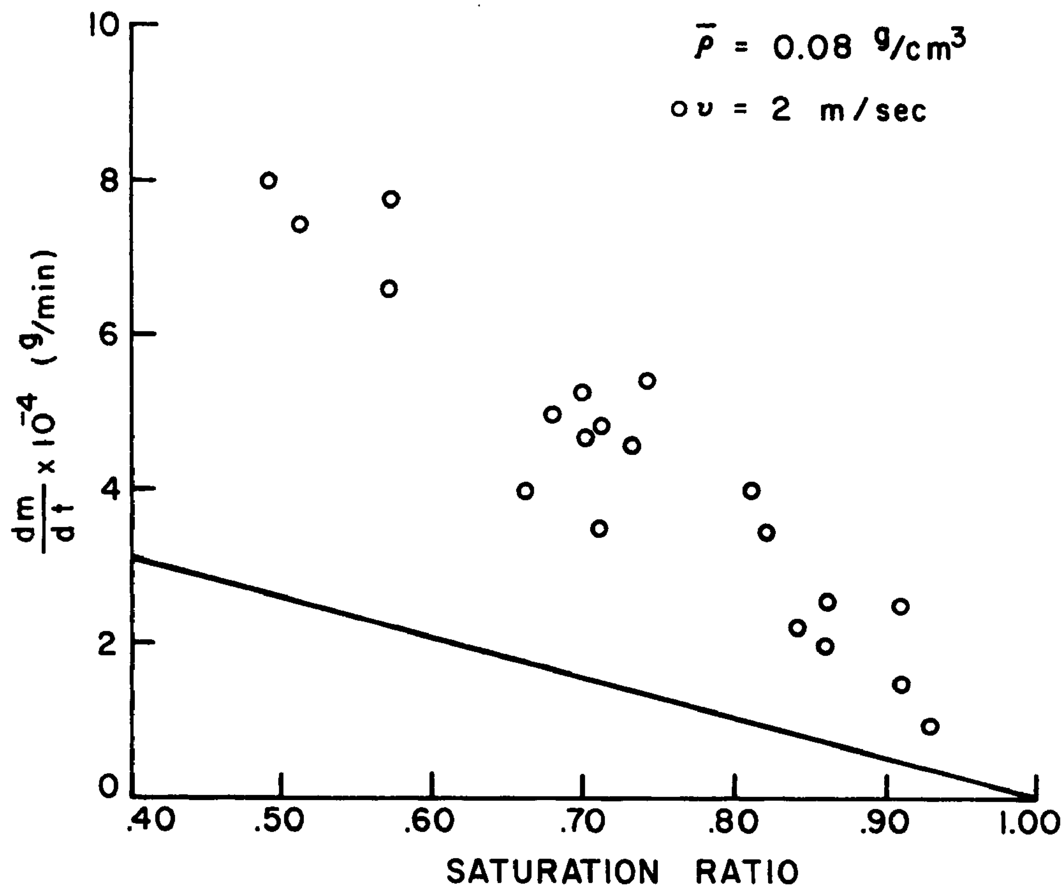

Figure 3-5a. Evaporation rate of ice as a function of saturation ratio. ρ = 0.08 g/cm^3.

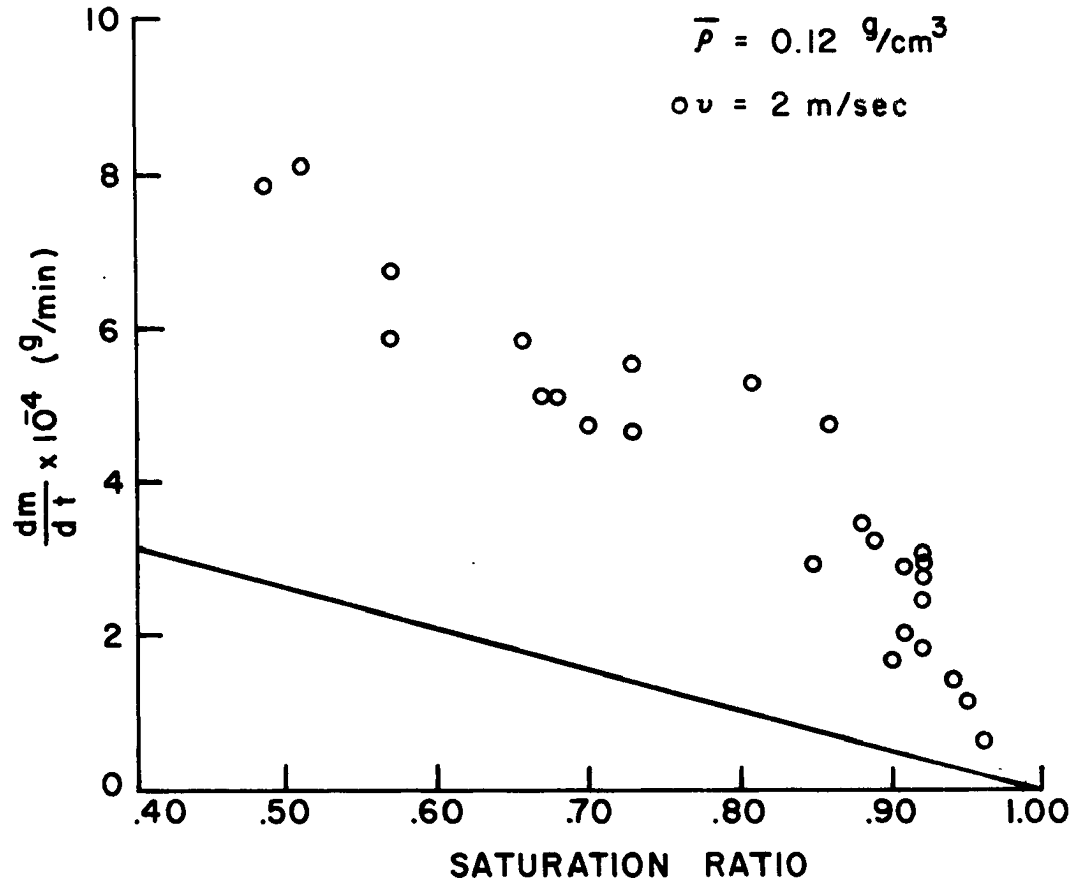

Figure 3-5b. Evaporation rate of ice as a function of saturation ratio. $\rho = 0.12$ g/cm^3.

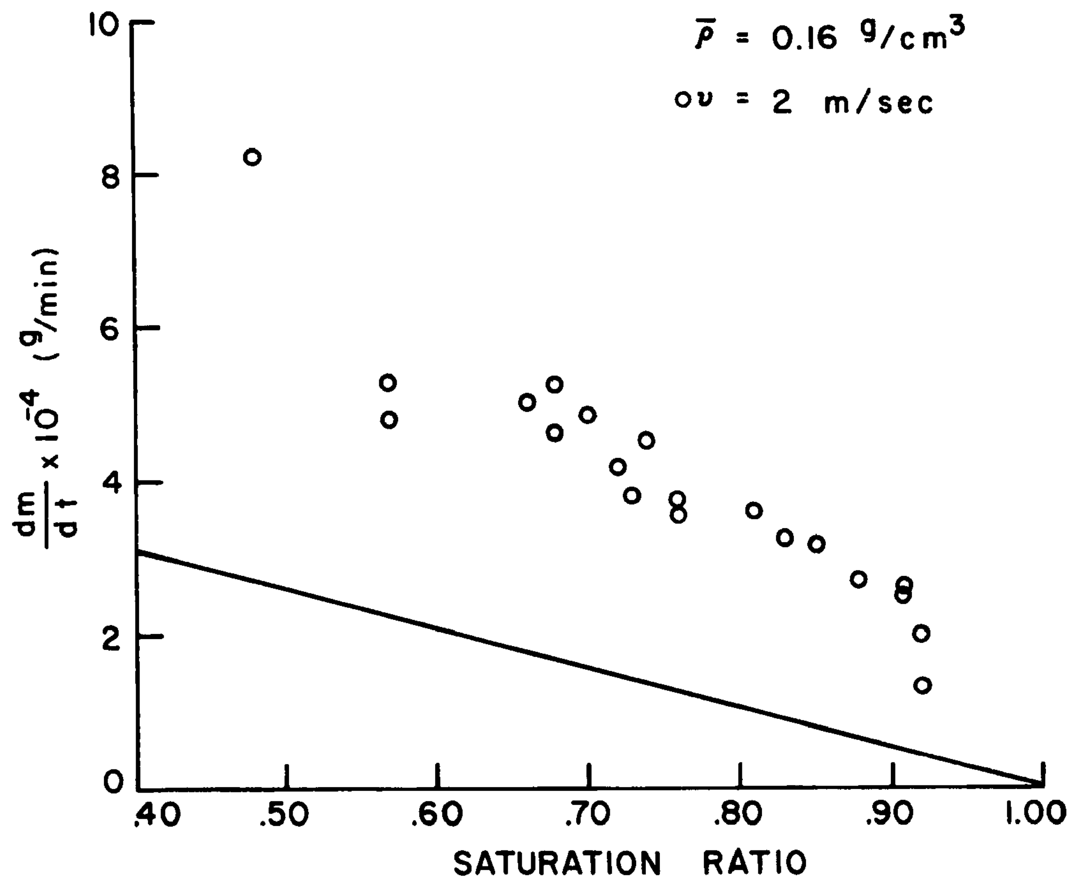

Figure 3-5c. Evaporation rate of ice as a function of saturation ratio. ρ = 0.16 g/cm^3.

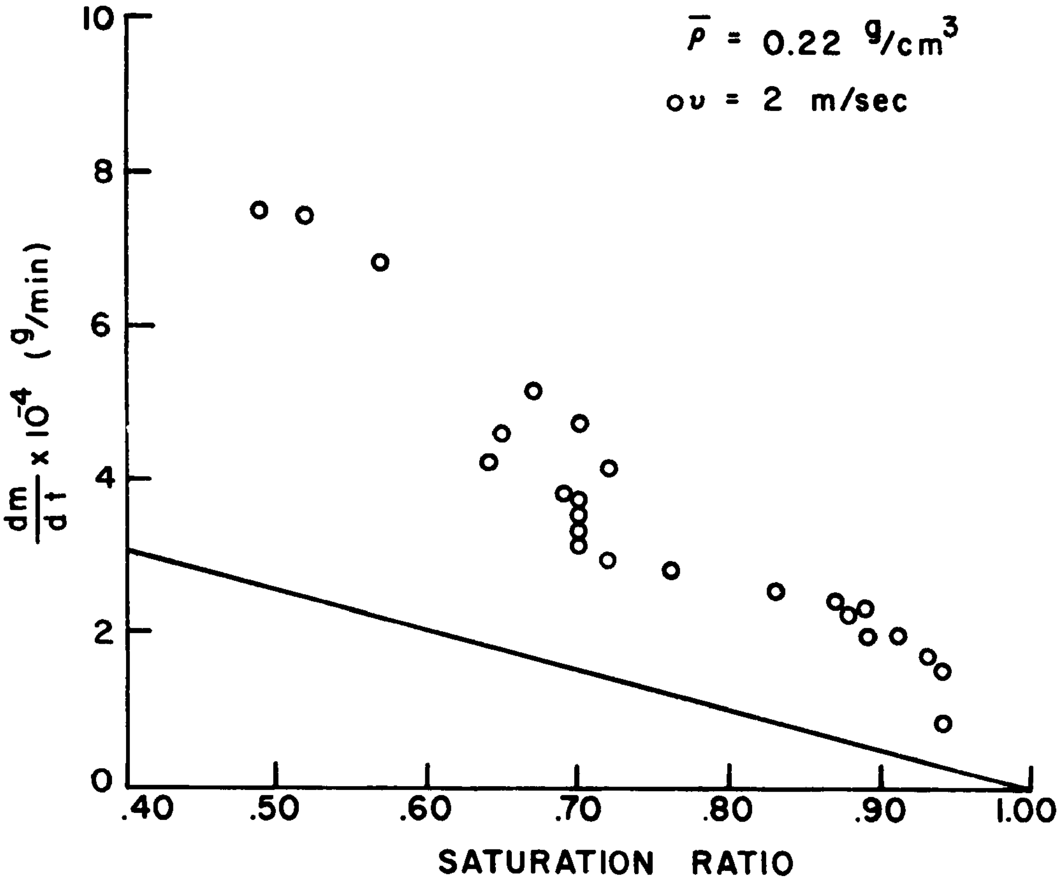

Figure 3-5d. Evaporation rate of ice as a function of saturation ratio. $\rho = 0.22$ g/cm^3.

secondary ice particles due to ventilation. The mechanism of the production of secondary ice particles will be described later.

3. Secondary ice production rate as a function of saturation ratio and evaporation rate

Figure 3-6, a ~ d show the secondary ice production rate per unit area, $\frac{1}{A}\frac{dN}{dt}$, as a function of saturation ratio with respect to ice with an apparent density of 0.08 and 0.12, 0.16 and 0.22 g cm^{-3}, respectively. All of the experiments were made under the ventilation velocity of 2 m sec^{-2}. Since the surface area of ice changes with time by the evaporation of ice, the mean surface area is used to calculate $\frac{1}{A}\frac{dN}{dt}$ assuming that the shape of ice is perfectly cylindrical.

From these figures it is clear that the rate of secondary ice particle production increases with decreasing saturation ratio, at least to the saturation ratio of 0.6. If a saturation ratio decreases further, the rate of secondary ice particle production tends to decrease. This is probably due to the complete evaporation of secondary ice particles with smaller size before reaching the sugar solution tray. It should also be pointed out that ice with a lower apparent density produces larger numbers of secondary ice particles. In a series of these experiments, the number of background ice nuclei was checked twice a day by sucking subsaturated air through the sytem without an ice specimen. The number of background ice nuclei and also splinters and fragments from the chamber walls at a ventilation velocity of 2 m sec^{-1} was always less than 1 per minute. Therefore, the effect of ice nuclei in the air and ice particles from the ice layer can be neglected.

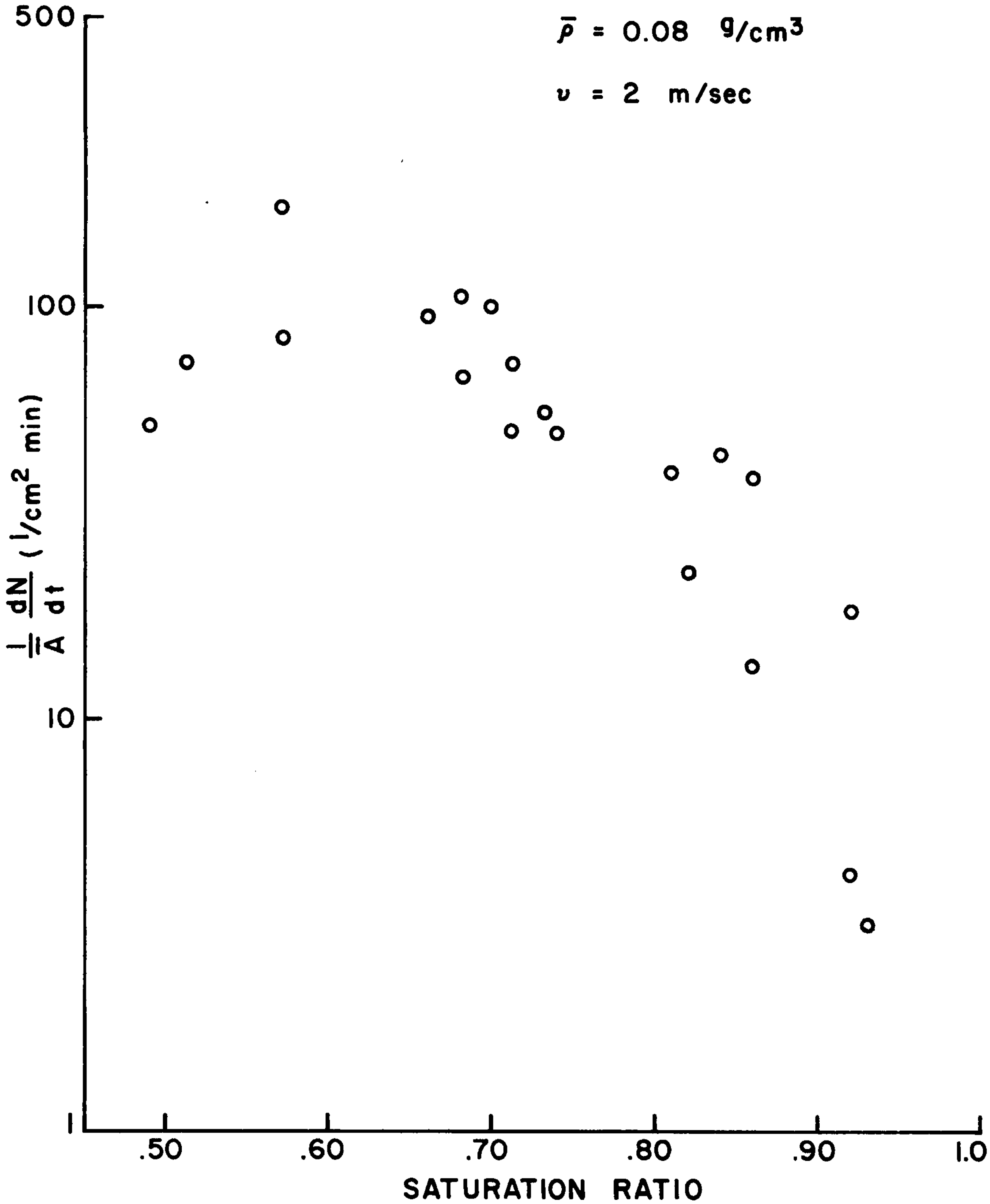

Figure 3-6a. Secondary ice particle production rate as a function of saturation ratio. $\rho = 0.08$ g/cm^3.

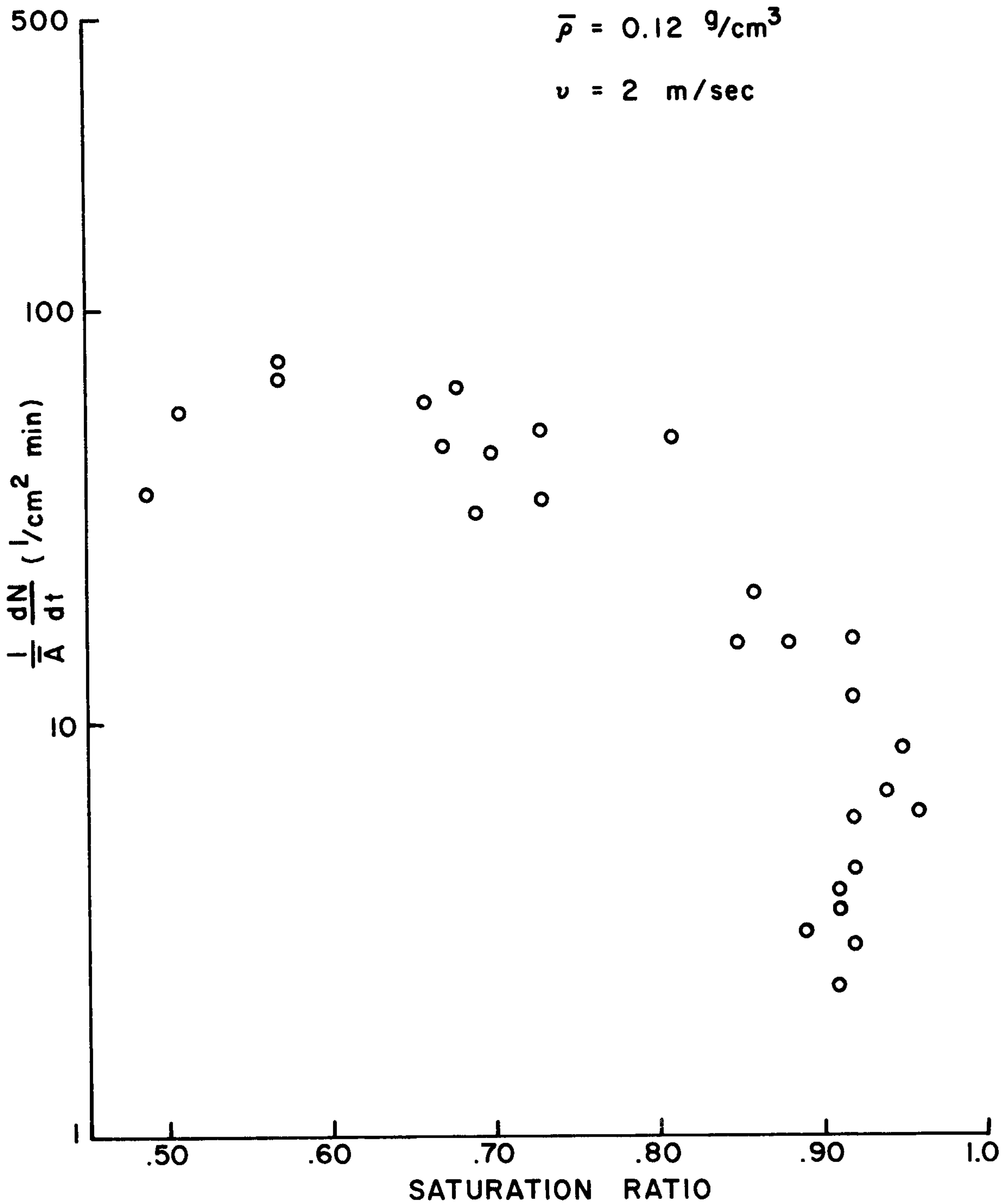

Figure 3-6b. Secondary ice particle production rate as a function of saturation ratio. $\rho = 0.12$ g/cm^3.

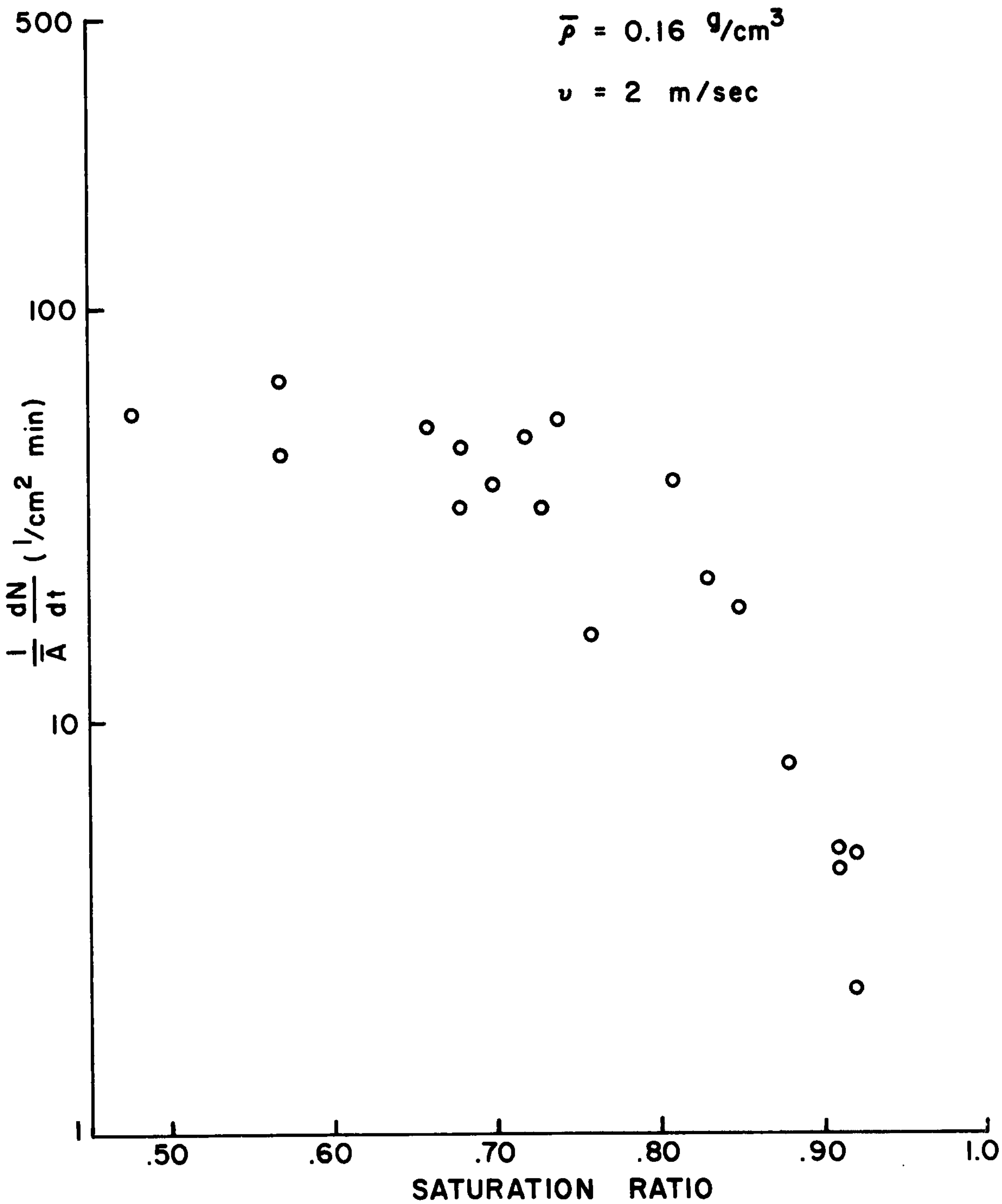

Figure 3-6c. Secondary ice particle production rate as a function of saturation ratio. $\rho = 0.16$ g/cm^3.

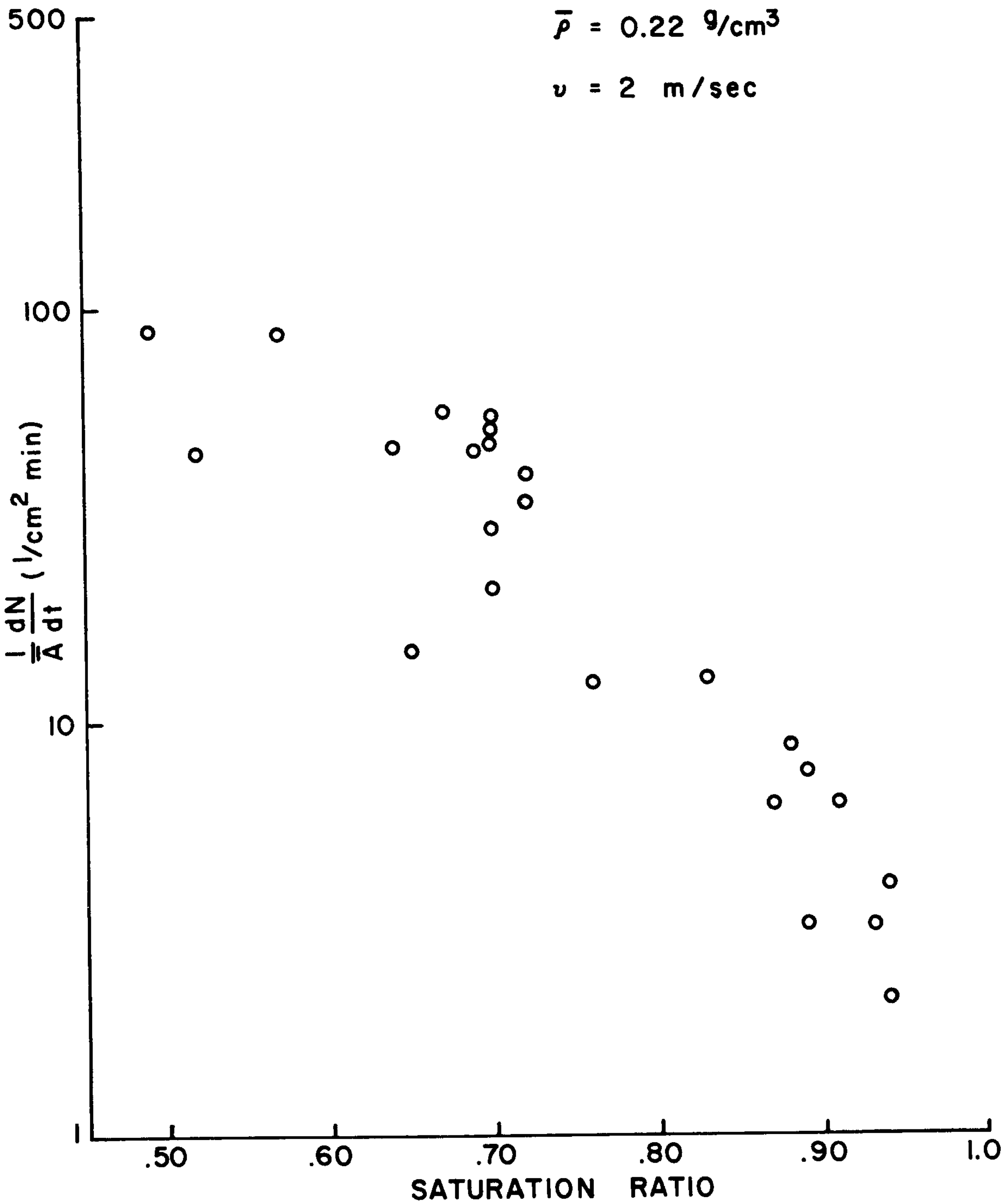

Figure 3-6d. Secondary ice particle production rate as a function of saturation ratio. ρ = 0.22 g/cm^3.

It is interesting to compare these results with Latham's (1963) experiments. By ventilating frost ice formed on a brass disc by deposition, he obtained 16 cm^{-2} sec^{-1} when the ventilation velocity was 2 m/sec^{-1} (saturation ratio of the air was not reported in the paper). Latham's value is about one order of magnitude larger than the present results. The frost ice in his experiment may have been mechanically more fragile than the ice formed by the riming process in this work.

Figures 3-7, a ~ d show the secondary ice production rate as a function of the evaporation rate for ice of apparent densities of 0.08, 0.12, 0.16 and 0.22 g/cm^3, respectively. Although, there is considerable scatter in the data, it is seen that the secondary ice production rate, dN/dt, increases with increasing evaporation rate.

The secondary ice production rate per unit mass of evaporating ice, dN/dm, was calculated by using the data for Figures 3-5, a ~ d and Figures 3-7, a ~ d. The secondary ice production per unit mass of evaporating ice is shown in Figures 3-8, a ~ d.

The comparison of Figures 3-8, a ~ d indicates that dN/dm is also larger for lower apparent densities of ice. The maximum number of secondary ice particles per unit mass is as high as 2 x 10^5 per gram of ice for the ice of apparent density 0.08 g/cm^3. dN/dm becomes a maximum when the subsaturation ratio is around .65 or .75. When the subsaturation ratio of air is high, dN/dm becomes small.

4. Effect of ventilation velocity

From the results shown in the previous section, it is clear that the lower the apparent density, the larger the magnitude of dN/dm and that the maximum of dN/dm is obtained when an ice cylinder is

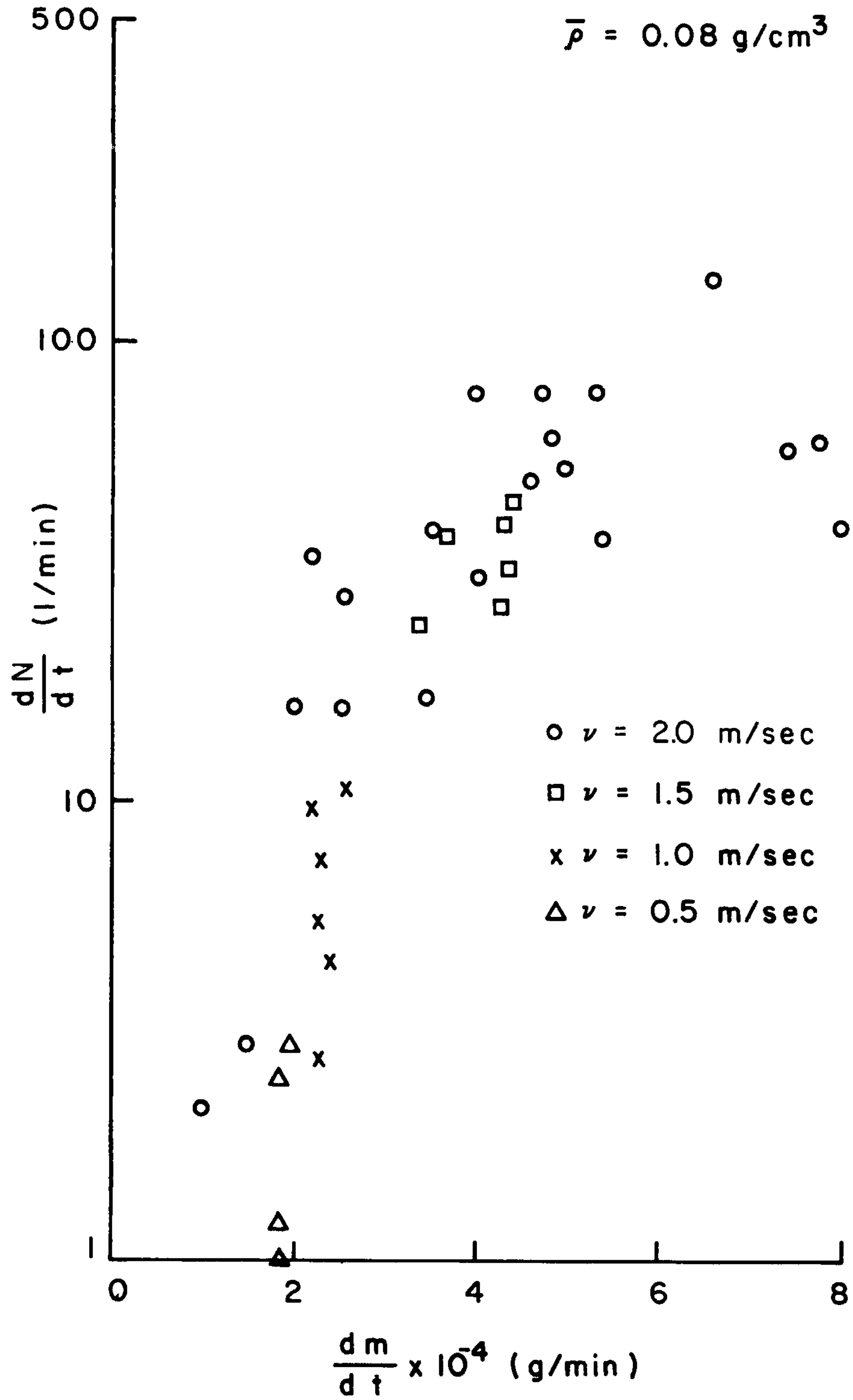

Figure 3-7a. Secondary ice particle production rate as a function of evaporation rate. ρ = 0.08 g/cm^3.

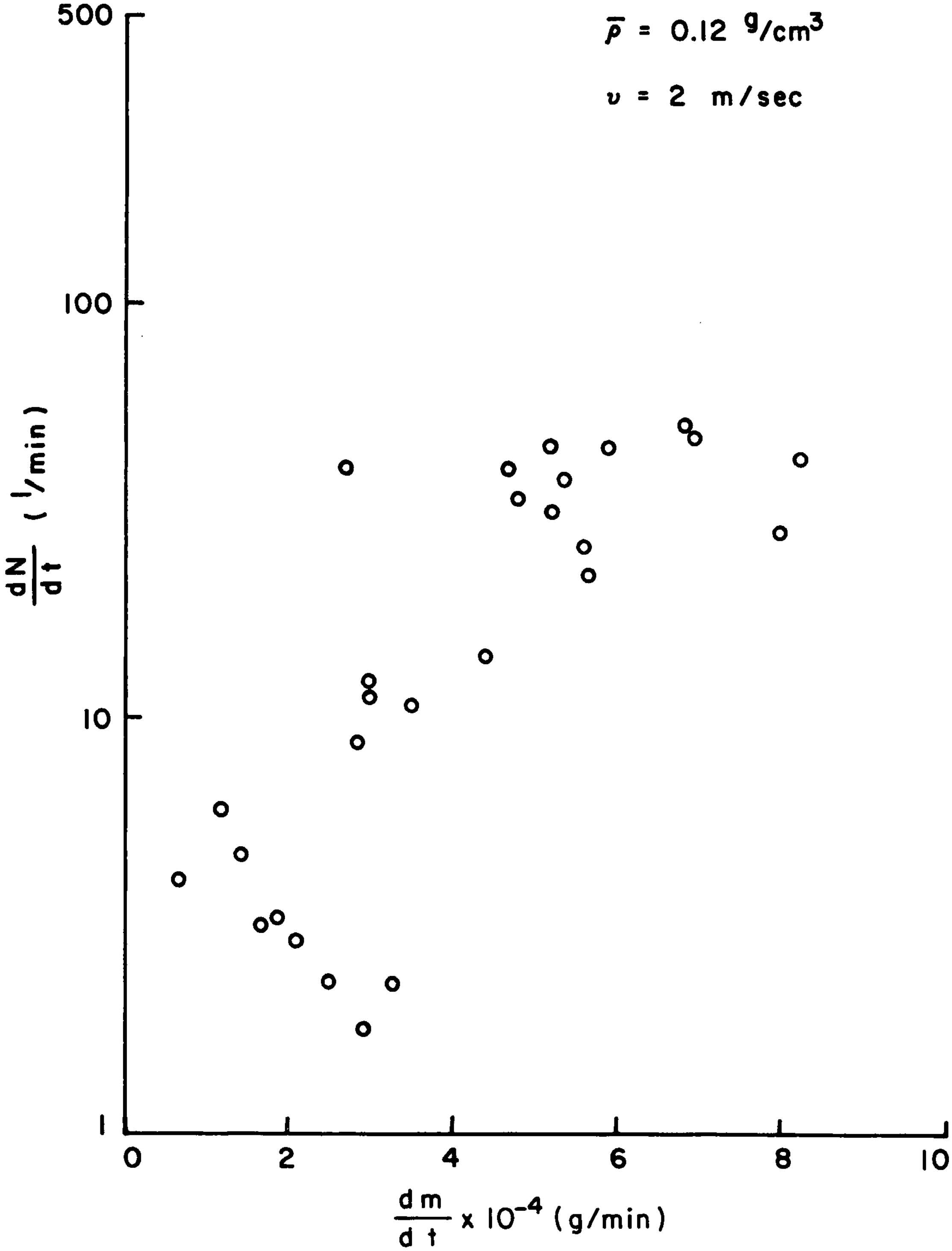

Figure 3-7b. Secondary ice particle production rate as a function of evaporation rate. $\rho = 0.12$ g/cm^3.

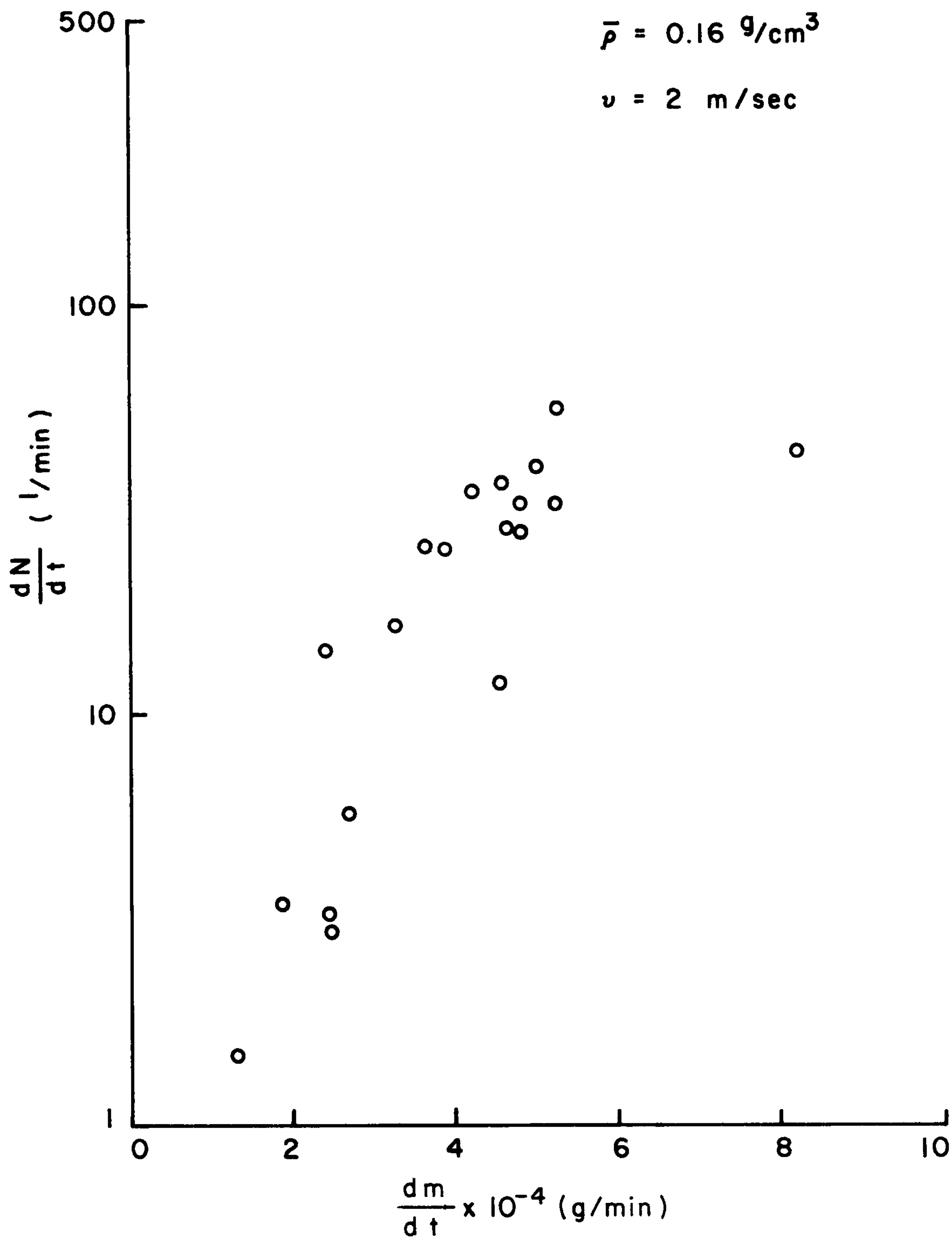

Figure 3-7c. Secondary ice particle production rate as a function of evaporation rate. ρ = 0.16 g/cm^3.

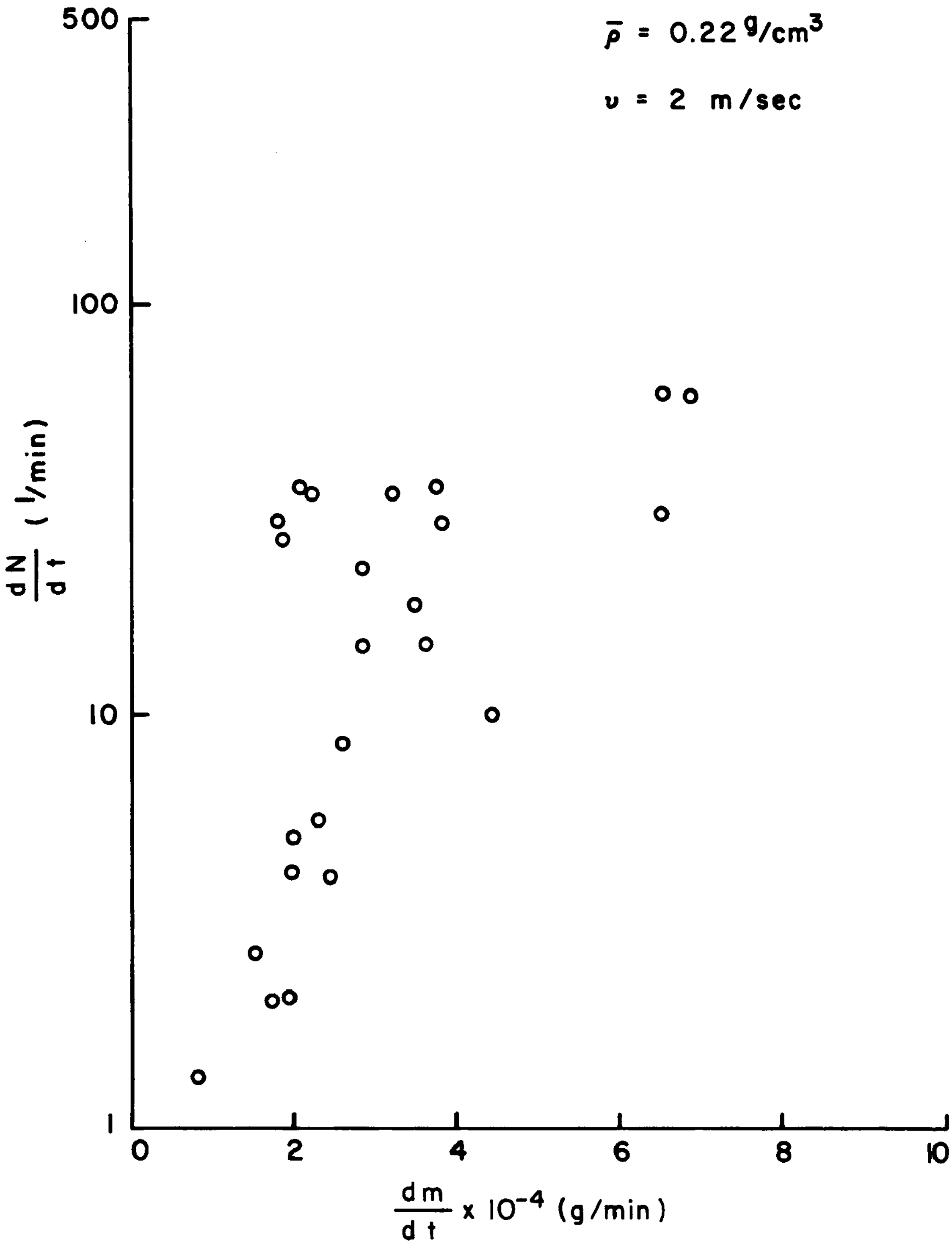

Figure 3-7d. Secondary ice particle production rate as a function of evaporation rate. $\rho = 0.22$ g/cm^3.

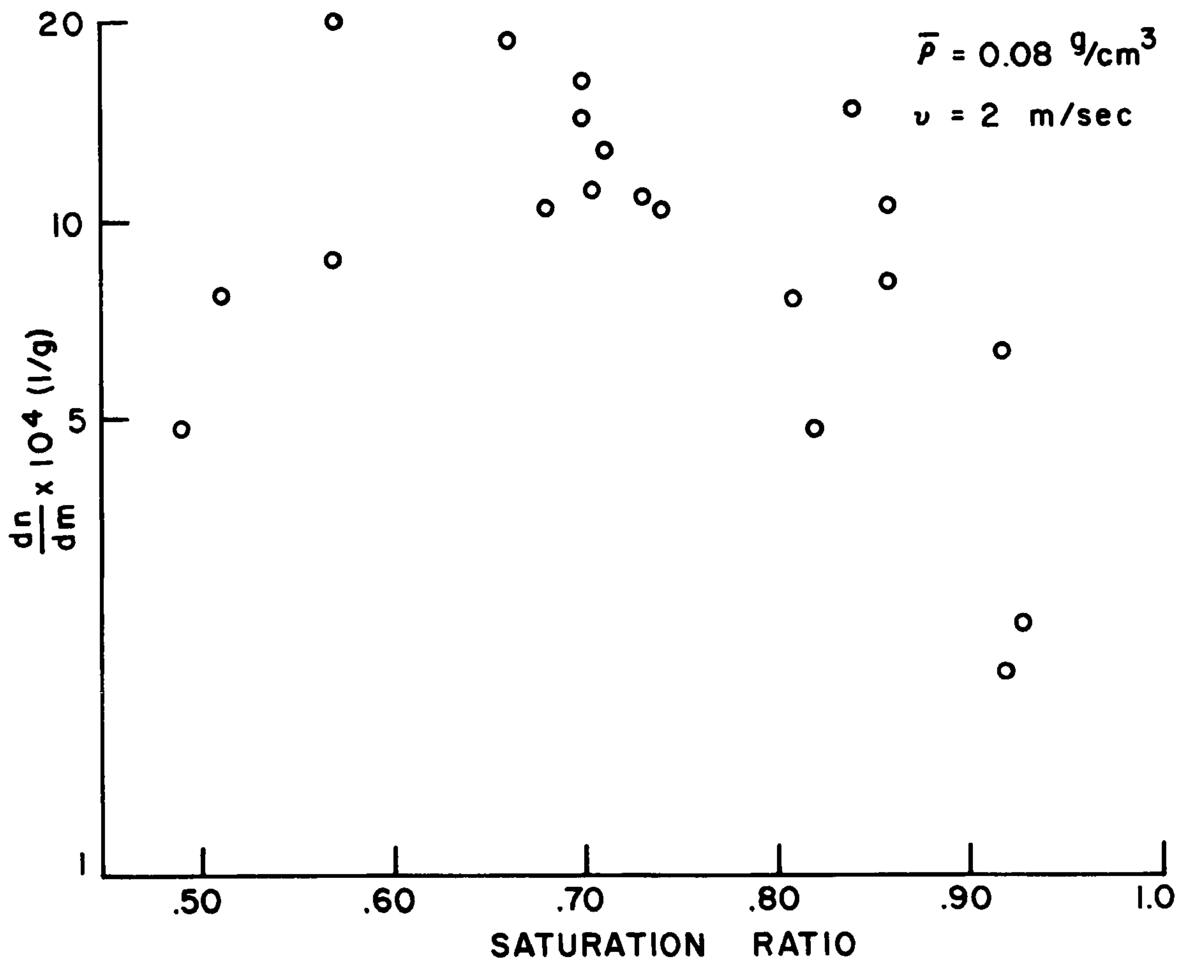

Figure 3-8a. Secondary ice particle production per unit mass of evaporating ice as a function of saturation ratio. $\rho = 0.08$ g/cm^3.

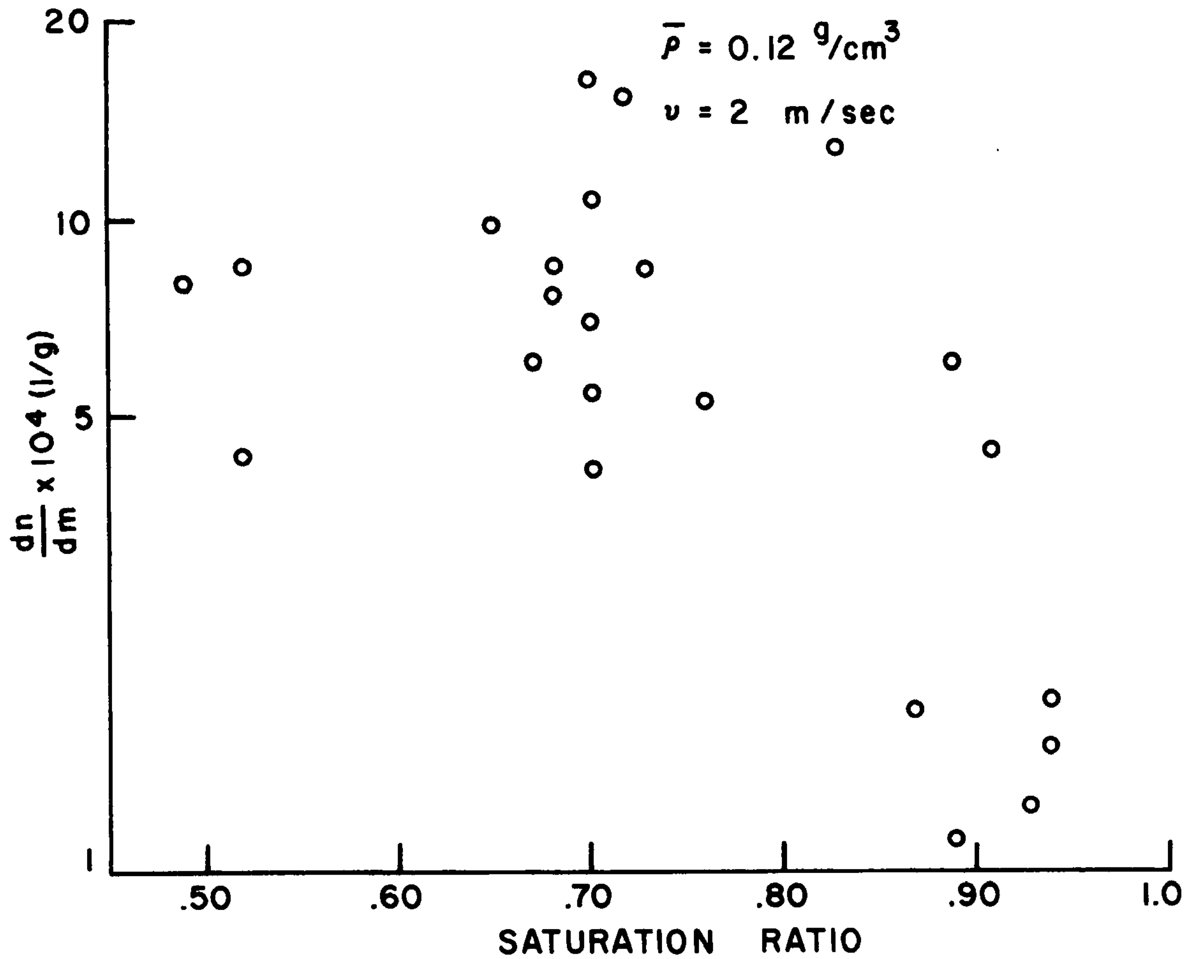

Figure 3-8b. Secondary ice particle production per unit mass of evaporating ice as a function of saturation ratio. $\rho = 0.12$ g/cm^3.

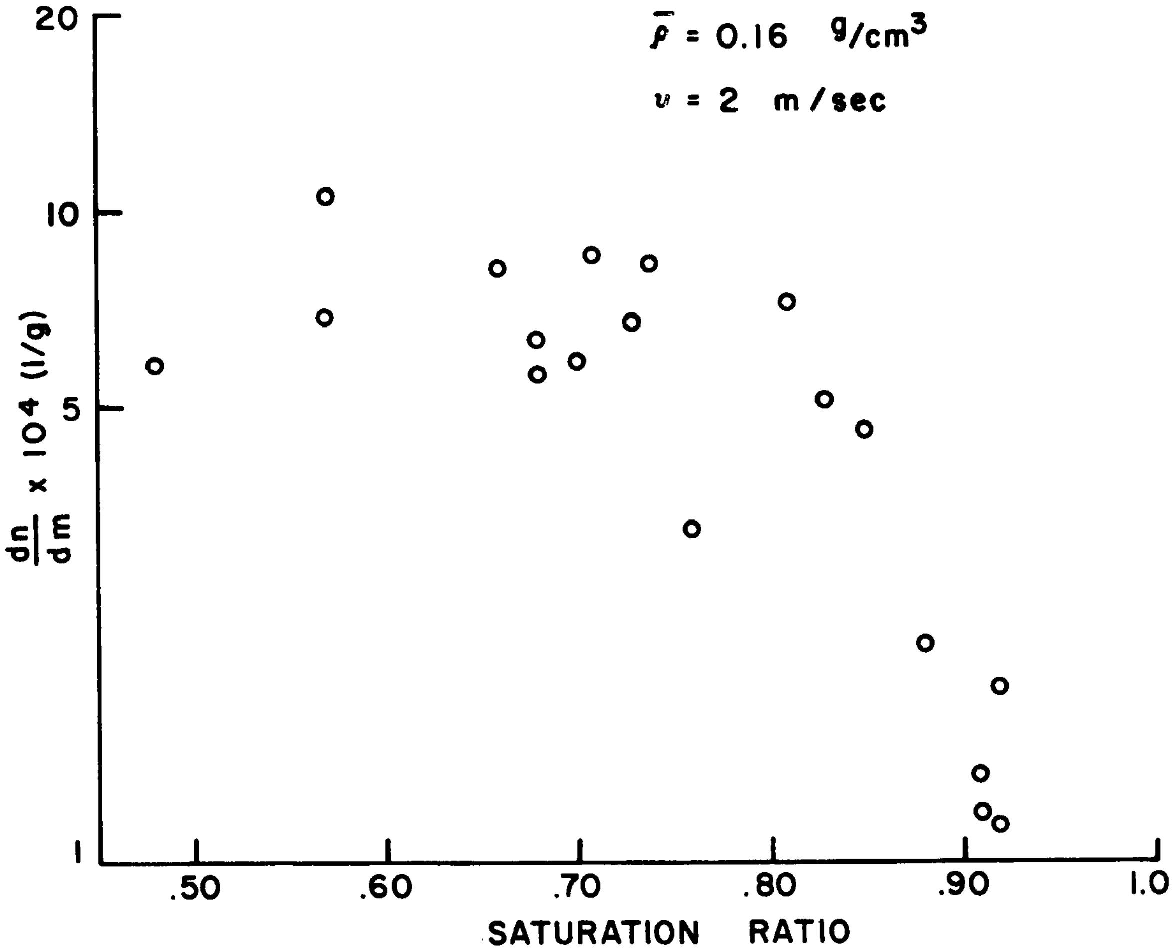

Figure 3-8c. Secondary ice particle production per unit mass of evaporating ice as a function of saturation ratio. $\rho = 0.16$ g/cm^3.

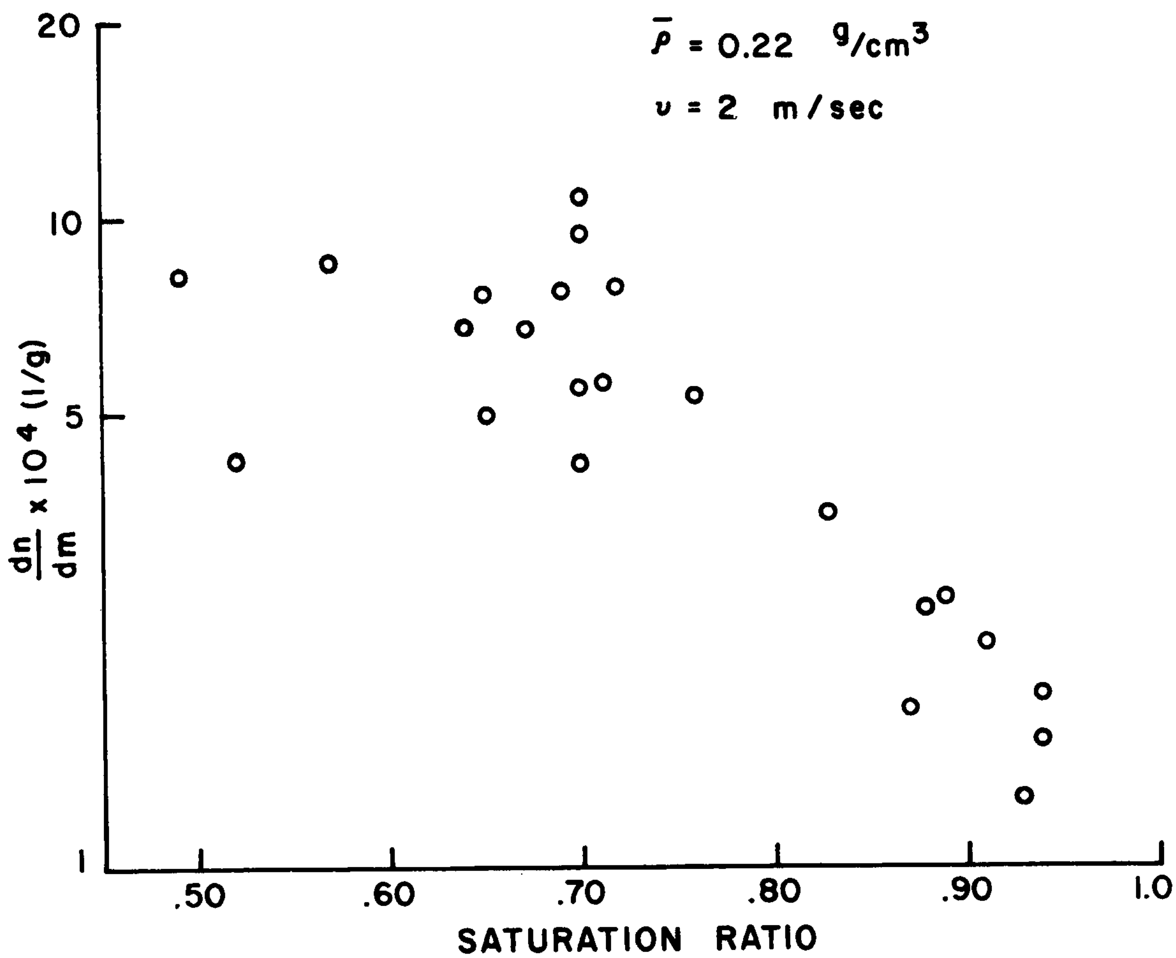

Figure 3-8d. Secondary ice particle production per unit mass of evaporating ice as a function of saturation ratio. ρ = 0.22 g/cm^3.

ventilated with the air at .65 or .75 of the saturation ratio with respect to ice. Therefore, in order to examine the effect of ventilation velocity on secondary ice production rate, ice with an apparent density of 0.08 g/cm^3 was chosen for examination under several ventilation velocities. The results are given in Figure 3-9.

The figure shows that ventilation velocity is a dominant factor in the production of secondary ice particles. The secondary ice production rate increases with increasing ventilation velocity within the range of the experiments. In order to examine this, dN/dt obtained at ventilation velocities of 0.5, 1.0, and 1.5 m/sec, are plotted as a function of dm/dt in Figure 3-7a (page 56). This figure clearly indicates that dN/dt is smaller ventilation velocities even when dm/dt is of the similar magnitude.

5. The effect of the apparent densities of ice

Using the data obtained for a ventilation velocity of 2 m/sec and subsaturation ratio of air between 0.65 and 0.75, the variation in secondary particle production as a function of ice density has been determined and is shown in Figure 3-10. This figure shows that the secondary ice production rate is nearly constant to densities up to .22 g cm^{-3} and then decreases drastically for ice with high apparent density. The reason for this decrease is attributed to the physical characteristics of the ice having high apparent density. As it is seen in Figure 3-4, the appearance of the ice having apparent density 0.33 gm cm^{-3} is quite different from those of the ice having lower apparent densities. In the case of the ice of apparent density 0.33 gm cm^{-3}, the water droplets are packed more heavily, and therefore

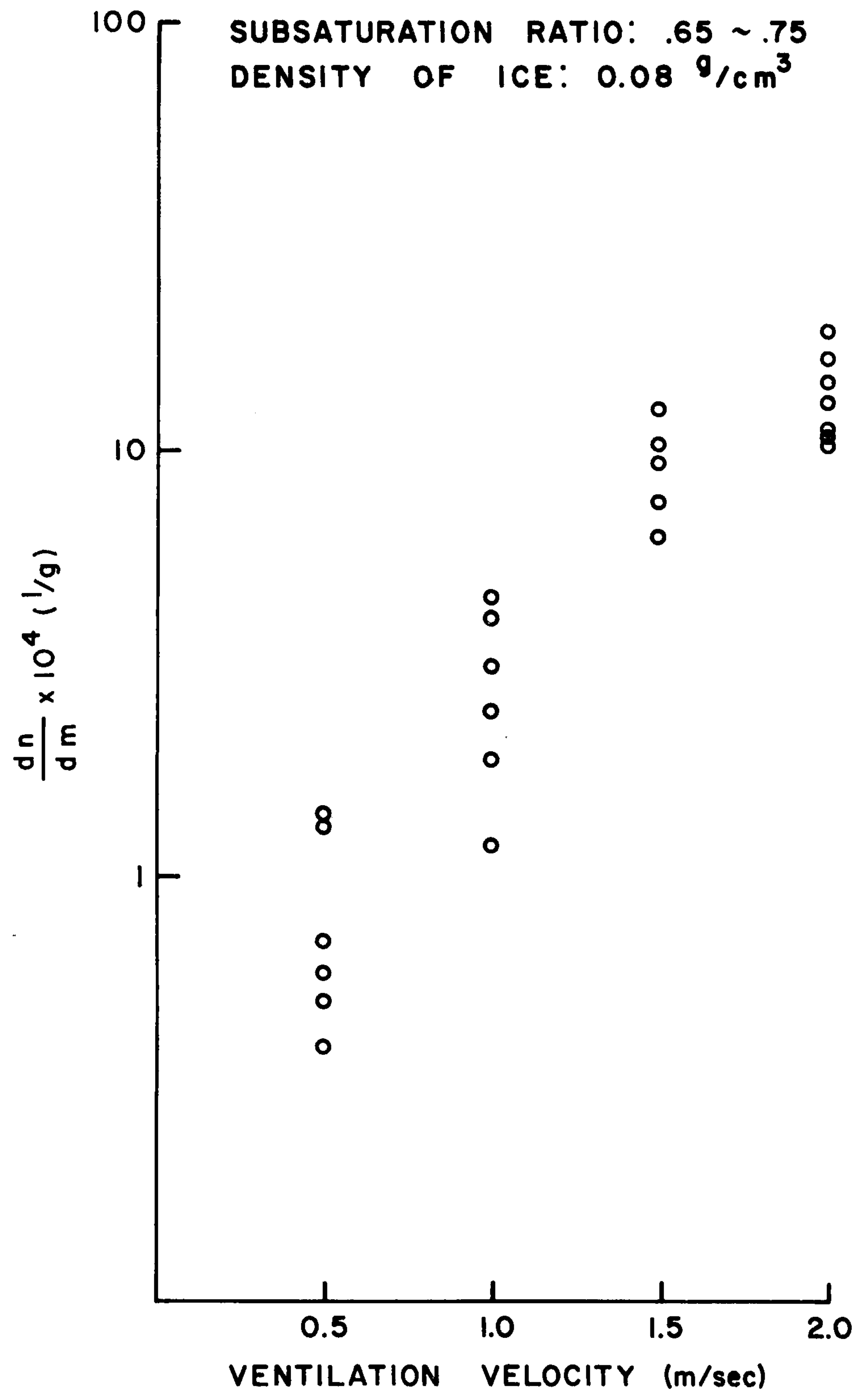

Figure 3-9. Secondary ice particle production per unit mass of evaporating ice as a function of ventilation velocity.

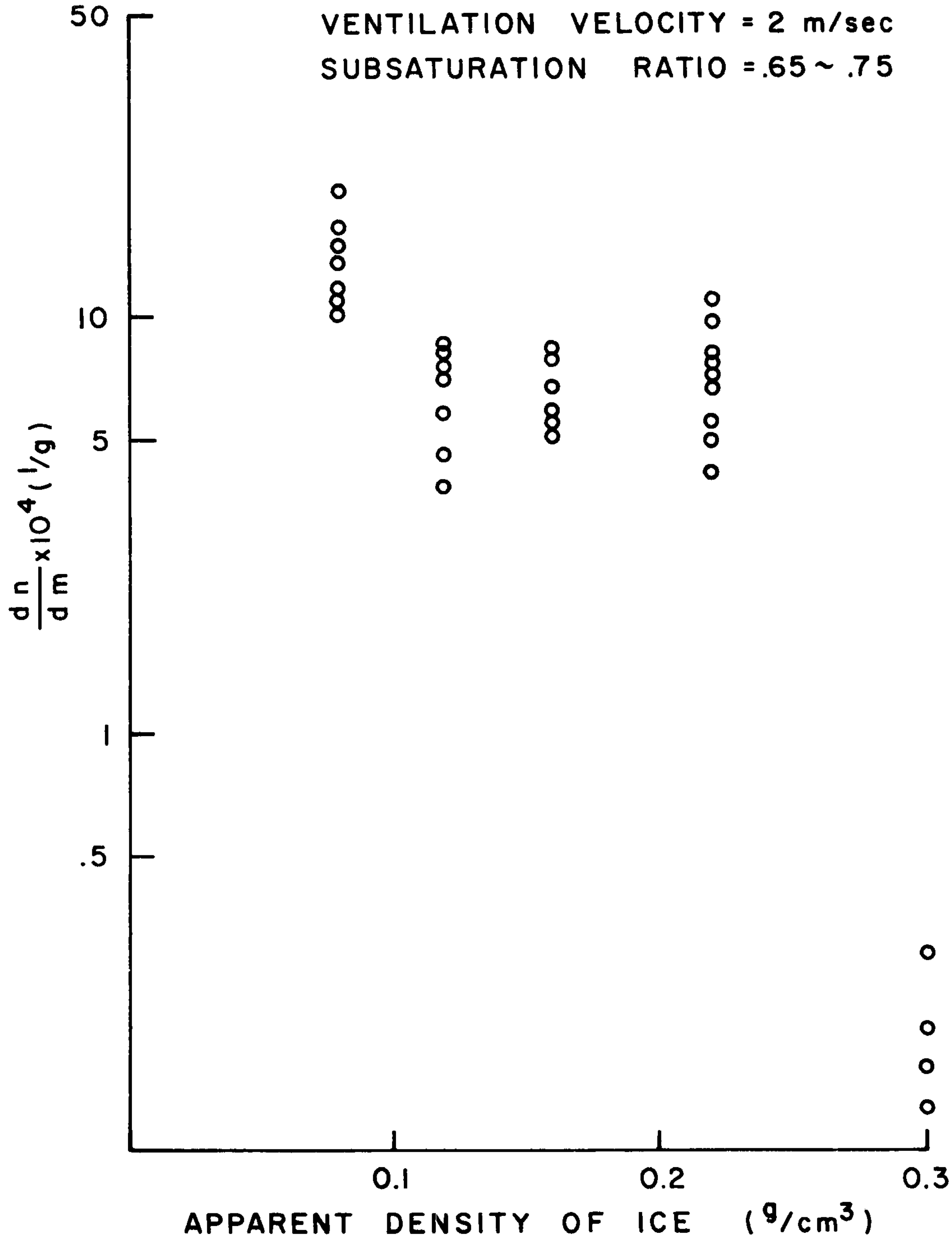

Figure 3-10. Secondary ice particle production per unit mass of evaporating ice as a function of apparent density.

the ice appears to be more mechanically stronger. The smaller permeability of air through the ice may be also one of the reasons for this decrease.

6. The size distribution of secondary ice particles

In order to obtain the size distribution of secondary ice particles, slide glasses coated with silicone oil were placed at the bottom of the chamber. To obtain sufficient numbers of secondary ice particles in a small area of the slide glass so that the size distribution and shape could be studied, several ice specimens with apparent density of 0.08 g/cm^3 were ventilated at 2 m/sec with air of subsaturation ratio between .65 and .75.

Figure 3-11 is a photograph taken under the microscope. These ice particles are irregular in shape.

The size distribution obtained from these microphotographs is shown in Figure 3-12. In this figure the diameter, D, is defined as the length of the average of maximum and minimum dimensions of a particle. In the same figure the curve of accumulated percent is also drawn, which shows that 50 percent of the particles are smaller than 10 microns. It can be seen from the microphotographs that the smallest particle is about 5 microns in diameter and the largest is about 60 microns. However, it is possible that there are particles smaller than 5 microns because the smallest size that can be identified on the photograph is about 5 microns. By assuming that particles are spherical the mean volume diameter of these secondary ice particles was calculated to be about 16 microns. However, the size distribution shown in Figure 3-12 should be regarded as a crude one with the following reasons: The distance from the ice cylinder to the bottom

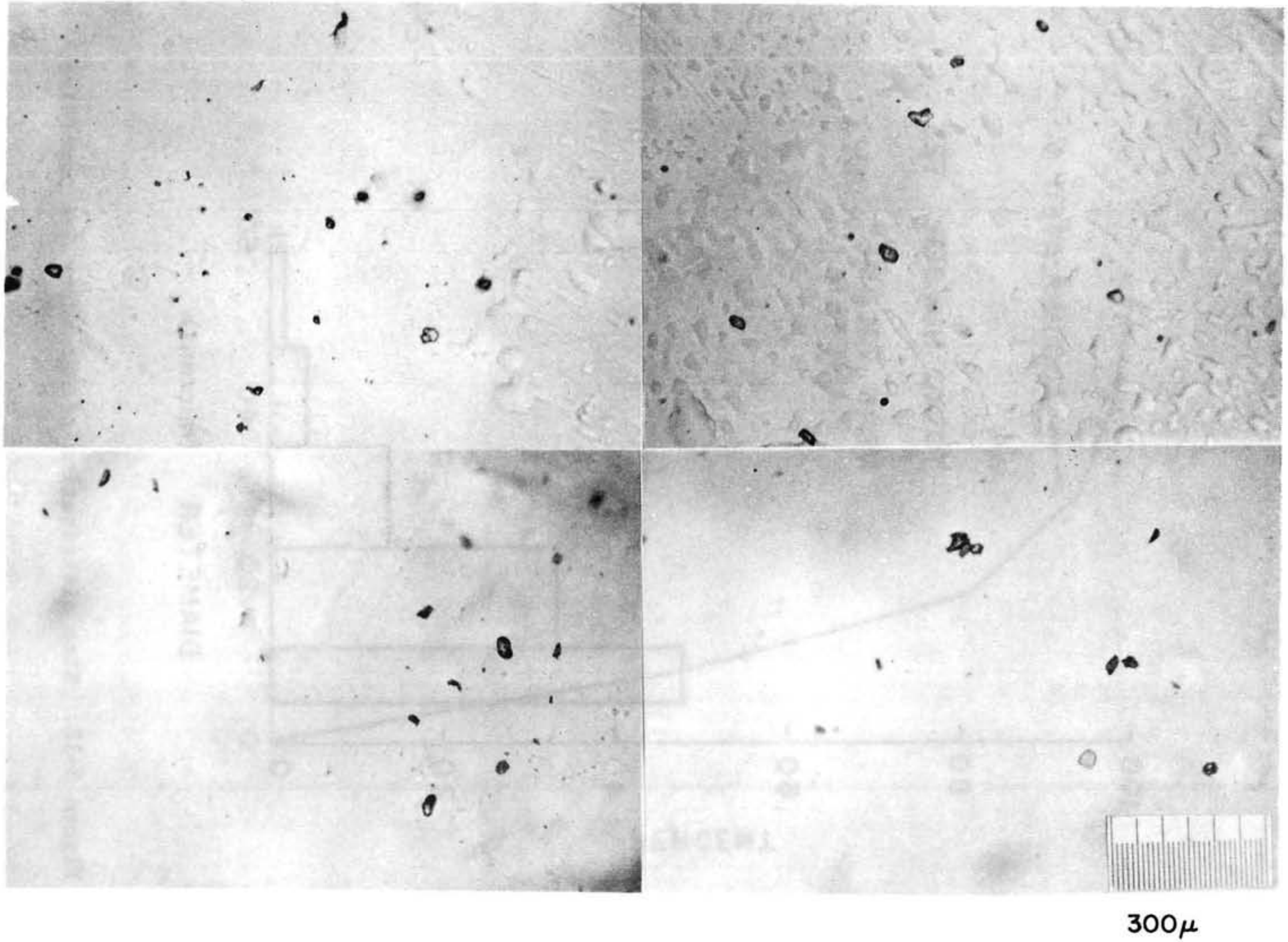

Figure 3-11. Microphotographs of secondary ice particles.

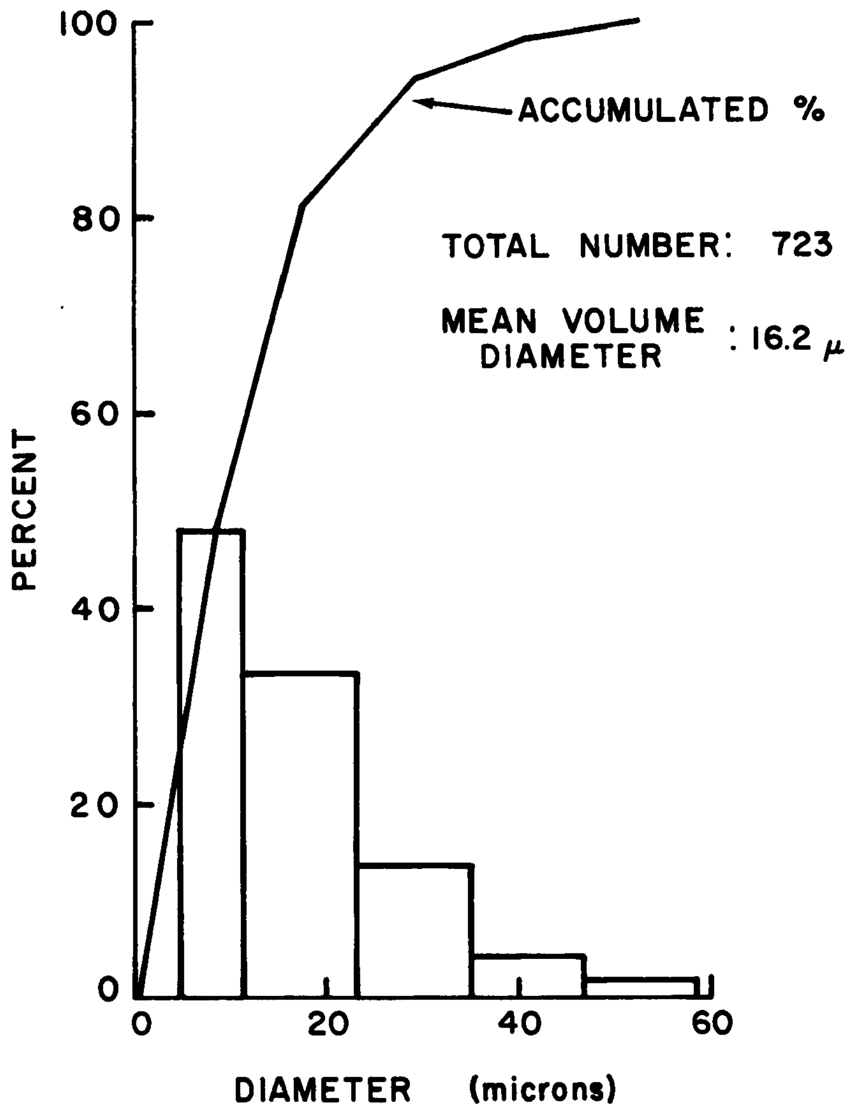

Figure 3-12. Size distribution of secondary ice particles.

of a chamber is 27 cm. Although the air flow from the upper part of the chamber goes to the bottom of a chamber before diffusing into the lower part of a chamber, the air stream expands after passing the ice cylinder. It may be a reasonable assumption that secondary ice particles reach to the bottom at 0.5 seconds after they are produced. Using the diffusion-growth equation of a spherical ice, the decrease in the diameter of an ice particle due to the exposure to subsaturated air for 0.5 sec is calculated. The results are shown in Figure 3-13. In the figure, the final diameter, D_f, is drawn as a function of the initial diameter, D_i. Here, D_f is the diameter of an ice particle after it has been exposed to subsaturated air for 0.5 sec. Saturation ratio of the air is taken as a parameter. The average saturation ratio of the air was 0.7 with respect to ice when the particles were collected. Using Figure 3-13, it can be estimated that secondary ice particles initially smaller than 7 microns cannot reach to the bottom of a chamber and that the particle initially smaller than 8.7 microns could not be observed.

Although it is impossible to make a quantitative estimate, it can be inferred that the size distribution shown in Figure 3-12 gives smaller fraction at the range of small diameter than that actually produced at the surface of ice. It may be also inferred that the numbers of secondary ice particles counted in the present study are the number smaller than those actually produced at the surface of ice.

7. The mechanism of secondary ice production

It has been shown that ice which produces secondary ice particles has a featherly appearance and that the surface of such ice is protruded. Using a microscope it was observed that under the

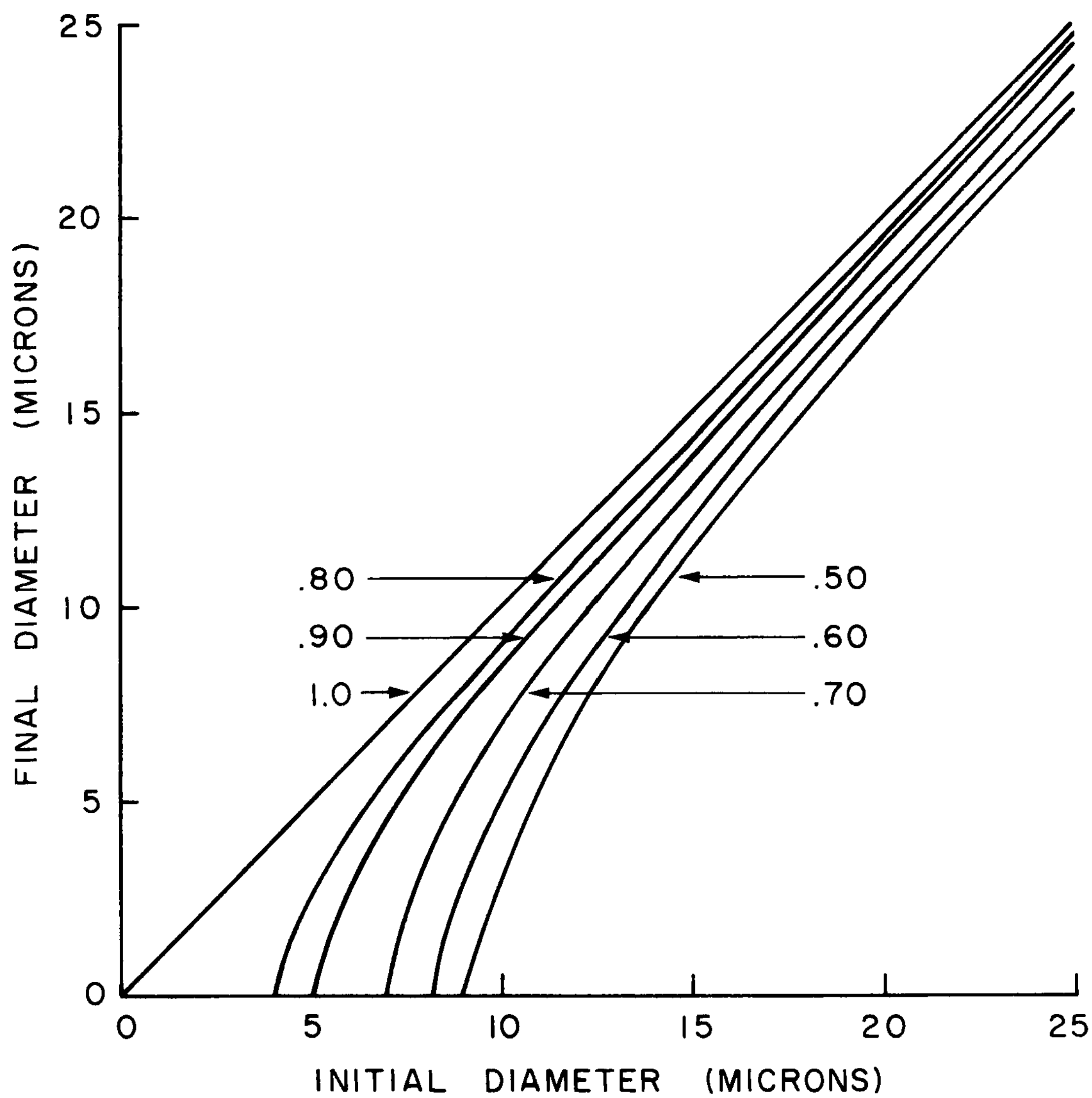

Figure 3-13. Final diameter of an ice particle as a function of an initial diameter after the exposure to sub-saturated air for 0.5 sec. Saturation ratio of the air is taken as a parameter.

conditions of ventilation with subsaturated air, the protruded parts become thin by evaporation and are blown off. It was also generally observed that after the protruded parts disappear as a result of exposure to subsaturated air flow, the secondary ice production rate from ice becomes smaller. To demonstrate this time dependence, the accumulative number of secondary ice particles with time are plotted in Figure 3-14. Four cases with different ventilation velocities are shown. For the ventilation velocities of 1.5 m/sec and 2 m/sec large fraction of secondary ice particles are produced within 2 minutes after the exposure to subsaturated air. On the other hand, for smaller ventilation velocities the number increases slowly with time. This can be explained by the following. The drag force per unit area exerted on the ice by ventilation is expressed by

$$\frac{F_D}{A} = \frac{1}{2} Z C_D \rho_a v^2$$

where C_D is the coefficient of fractional drag, v is the ventilation velocity, Z is the roughness coefficient and ρ_a is the density of air. Ice has more protruded parts on its surface and consequently a larger value of Z at the beginning stage than after it has been ventilated by subsaturated air. Therefore, ice receives a stronger drag force at the beginning stage of the exposure to subsaturated air than after it becomes smaller and smoother due to evaporation.

From the above considerations, the following conditions must be simultaneously present for ice to produce a large number of secondary ice particles.

a. Ice must be lightly packed and the surface of the ice must be protruded. The protrusions are essential features of ice which is formed by riming process.

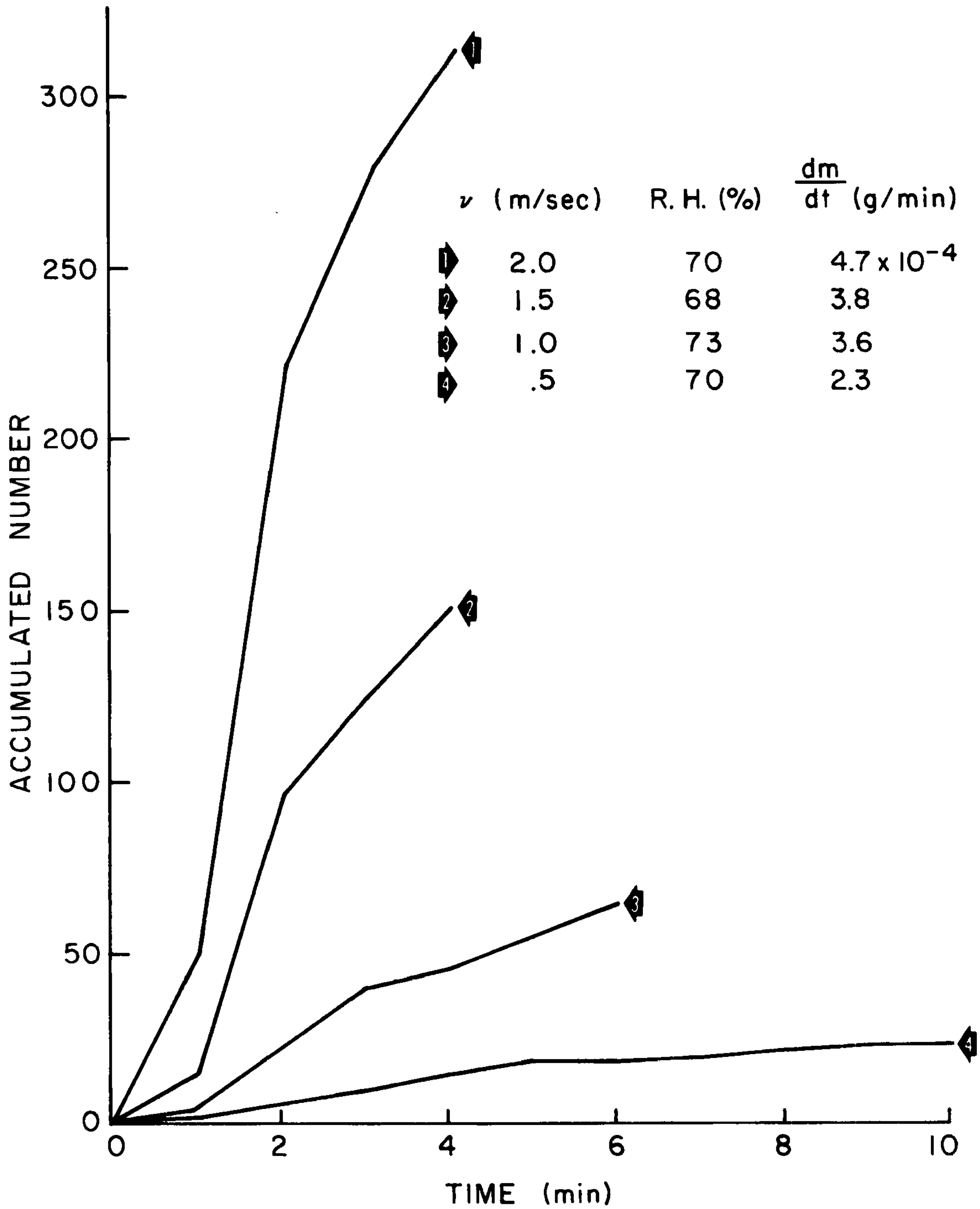

Figure 3-14. Accumulative number of secondary ice particles as a function of time. (For ice $\rho = 0.08$ gm cm^{-3})

b. Ice must be evaporated under the condition of ventilation with velocity larger than 1.5 m sec^{-1}.

c. The saturation ratio of air must be lower than .8 (with respect to ice).

E. Chapter Summary and Conclusion

1. Summary

The effects of ventilation by subsaturated air on ice specimens formed by the accretion process were reported as a possible mechanism of ice multiplication, in this chapter. The following findings should be emphasized.

a. The appearance of ice which produces a large number of the secondary ice particles is feathery. Microscopic examination shows that the surface parts of such ice are similar to those found on lump graupel observed in the atmosphere.

b. Under similar condition of ventilation velocity and saturation ratio of the ventilation air, ice specimens with a lower apparent density tend to produce a larger number of the secondary ice particles. For an ice specimen with the apparent density $\bar{\rho} = 0.08$ g/cm^3, a number of the secondary ice particles as high as 2×10^5 per gram of evaporating ice were observed. This occurred when the ice formed on a rotating bar was ventilated with velocity of 2 m sec^{-1}. The saturation ratio of air was 0.66 with respect to ice. With an increase of apparent density, the number of the secondary ice particles per unit mass was observed to decrease.

c. Under the condition of a constant ventilation velocity (2 m sec^{-1}), the production rate of secondary ice particles increases with decreasing saturation ratio of air at least to the saturation ratio of 0.6. If a subsaturation decreases further, the rate tends to decrease.

d. The secondary ice production rate decreases with decreasing ventilation velocity under the similar condition of sub-saturation ratio of the air.

e. It was also found that the secondary ice production rate increases with increasing evaporation rate of ice under a constant ventilation velocity. However, the comparisons of the data for the similar magnitude of evaporation rate show that the secondary ice production rate decreases with decreasing ventilation velocity.

f. From the above findings it was concluded that the mechanical break-up of protruded parts on the surface of ice specimen being evaporated due to ventilation is responsible for the secondary ice particle production. It should be emphasized that preferred combinations of ventilation velocity, subsaturation ratio of air and apparent density of ice are required for ice to produce a large number of the secondary ice particles. Within the range of the present experiment the combination of ventilation velocity, 2 m sec^{-1}, subsaturation ratio, 0.65 ~ 0.75, and apparent density, 0.08 g cm^{-3} was the one which produced the largest number of the secondary ice particles.

g. The shapes of secondary ice particles were irregular and the equivalent mean volume diameter was about 16 microns.

2. Conclusion

The purposes of the experiments were first to examine a possible role of the interaction of ice formed by the riming process and subsaturated air on ice multiplication and second to study the physical mechanism responsible for secondary ice particle production due to the interaction.

It was found that ice with a low apparent density formed by riming process produced a large number of secondary ice particles when it was ventilated with subsaturated air. The production rate of secondary ice particles by this process is one or two orders of magnitude greater than that from ice while it is growing by the riming process.

It was found that a mechanical break-up due to ventilation of protruded parts on the surface of ice is responsible for the production of a large number of secondary ice particles.

Chapter IV

GRAUPEL PARTICLES IN THE ATMOSPHERE

A. Introduction

In the previous chapters the experiments on secondary ice particle production by the riming process and evaporating process of ice were described. It was found that the production rates of secondary ice particles from evaporating ice were one or two orders of magnitude greater than those from growing ice by the riming process and produced up to 2×10^5 secondary ice particles per gram of evaporated ice. This chapter considers whether physical conditions necessary for the production of secondary ice particles by this process exist in the atmosphere. According to the experiments in Chapter III, it was concluded that the physical mechanism responsible for the production of a large number of secondary ice particles is the mechanical break-up of the surface parts of rimed ice with a low apparent density while the ice is being evaporated. The combination of the drag force due to ventilation and fast evaporation of the ice due to the exposure to subsaturated air was considered to cause the mechanical break-up.

In the atmosphere some of the graupel particles which are formed by the riming process of ice crystals or frozen droplets seem to have similar physical characteristics to the rimed ice used in the experiments. An initial step in evaluating the likelihood that similar secondary ice production occurs in the atmosphere involves; (1) an evaluation of the probable occurrence of apparent rimed ice densities as low as those used in the laboratory experiments, (2) comparison between drag forces acting on ice used in the laboratory, (3) the evaporation rate of graupel particles, and (4) the possibility of the presence of subsaturated air in and around cumulus clouds.

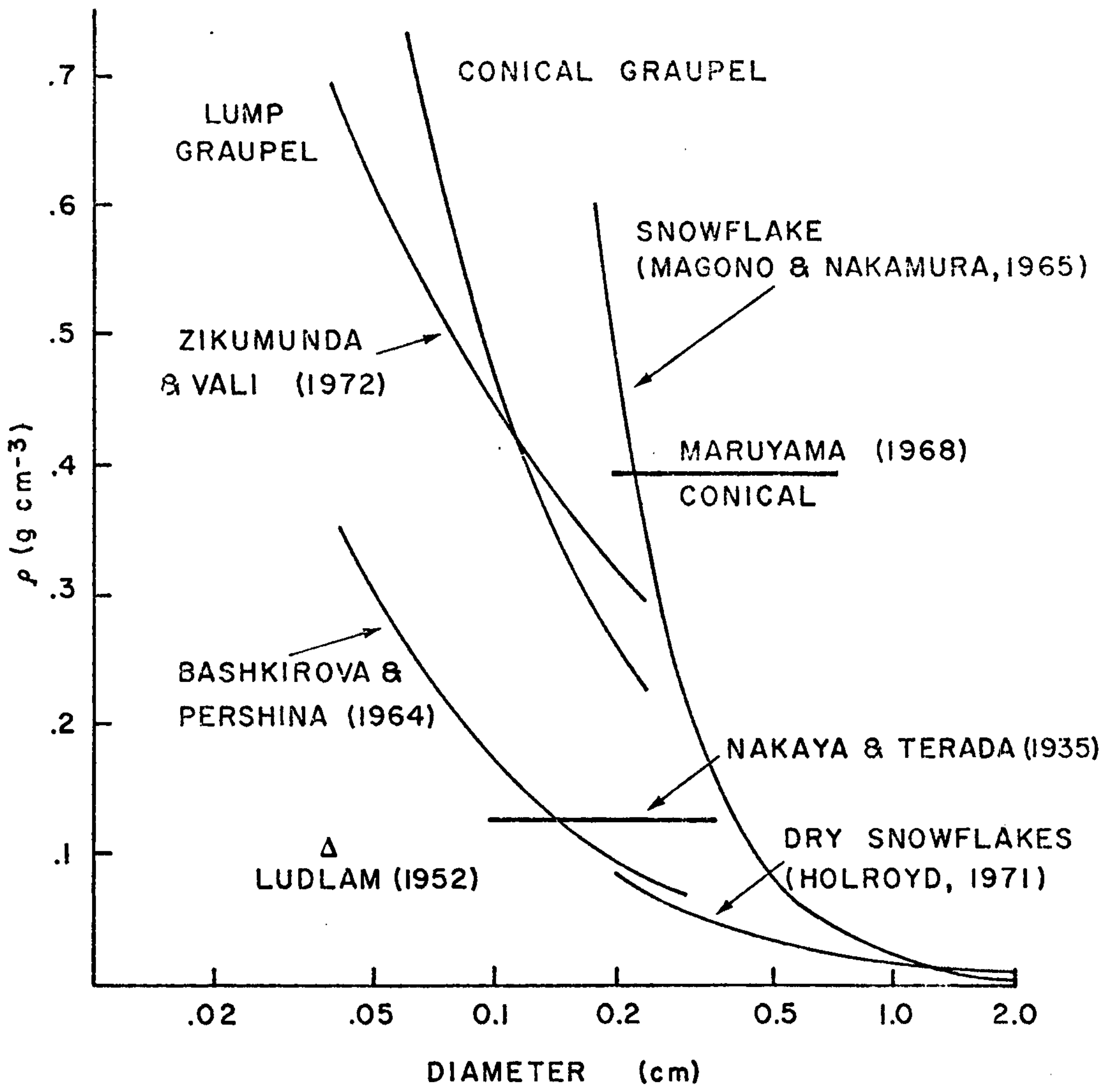

Figure 4-1. Densities of graupel particles as a function of their diameters, compiled from literatures.

B. Density of graupel

1. Observational results in field

Measurements of the density of the graupel have been reported by several authors (Nakaya and Terada, 1935, Bashkirova and Pershiana, 1964, Maruyama, 1968, and Zikmunda and Vali, 1972). All the measurements were conducted in the wintertime on the ground by measuring the equivalent diameter of a graupel particle and its mass. In Figure 4-1 the density of the graupel as a function of the equivalent average diameter obtained by these authors is summarized. The densities of graupel vary considerably, suggesting that graupel densities change in response to variations of cloud temperatures, cloud drop size distributions and liquid water contents. The large variation in the density may also be caused by different methods of measurements. Nevertheless, the figure shows that the density of graupel can be as low as 0.1 g cm^{-3}. Furthermore, it should be noted that the examination of an individual sample obtained by Nakaya and Terada showed density of graupel as low as 0.04 g cm^{-3}.

For comparison, the average density of snowflakes obtained by Magono and Nakamura (1965) is also cited in the figure. Their data include both dry and partially melted snowflakes. The snowflake density data of these authors were reanalyzed with all the wet snowflake data eliminated by Holroyd (1971). The result is also cited in the figure showing that the density of dry snowflakes is less than 0.1 g cm^{-3}.

2. Calculation of the density of graupel

In order to understand the effects of various physical factors on the density of a graupel, the density of a graupel is calculated as a function of its size. Although the assumptions below are far from the conditions in a real cloud, some useful implications can be drawn from the calculation. The following are the assumptions made:

a. The graupel particles grow only by the riming process from frozen water droplets with an initial diameter of 100 microns.

b. The shape of the graupel particles is spherical throughout their growth.

c. Liquid water in the cloud accretion zone is constant (three cases, L.W.C.=0.5, 1.0, and 2.0 gm^{-3} are considered.)

d. The cloud droplets are homogenous (three cases, the median volume r=5, 10, and 15 microns are considered.)

e. The temperature of the cloud accretion zone is constant (two cases, Ta=-5 and -10°C are considered)

f. The density of rimed ice as a function of a parameter $(-rv_o/Ts)$

$$\rho = 0.11\left(-\frac{rv_o}{Ts}\right)^{0.76} \qquad g\ cm^{-3} \qquad (4\text{-}1)$$

is used (Macklin, 1962). Here, ρ is the density of ice in g cm^{-3}, r is the median volume radius of cloud water droplets in microns, v_o is the impaction velocity of cloud water to a graupel particle in m sec^{-1}, and Ts is the average surface temperature of a growing graupel in C.

g. The fall velocity of a graupel is expressed by

$$v = 286d^{0.44}, \text{ d in cm}$$

This is an approximate equation based on those obtained for graupels by Zikumunda and Vali (1972) (see Figure 4-2).

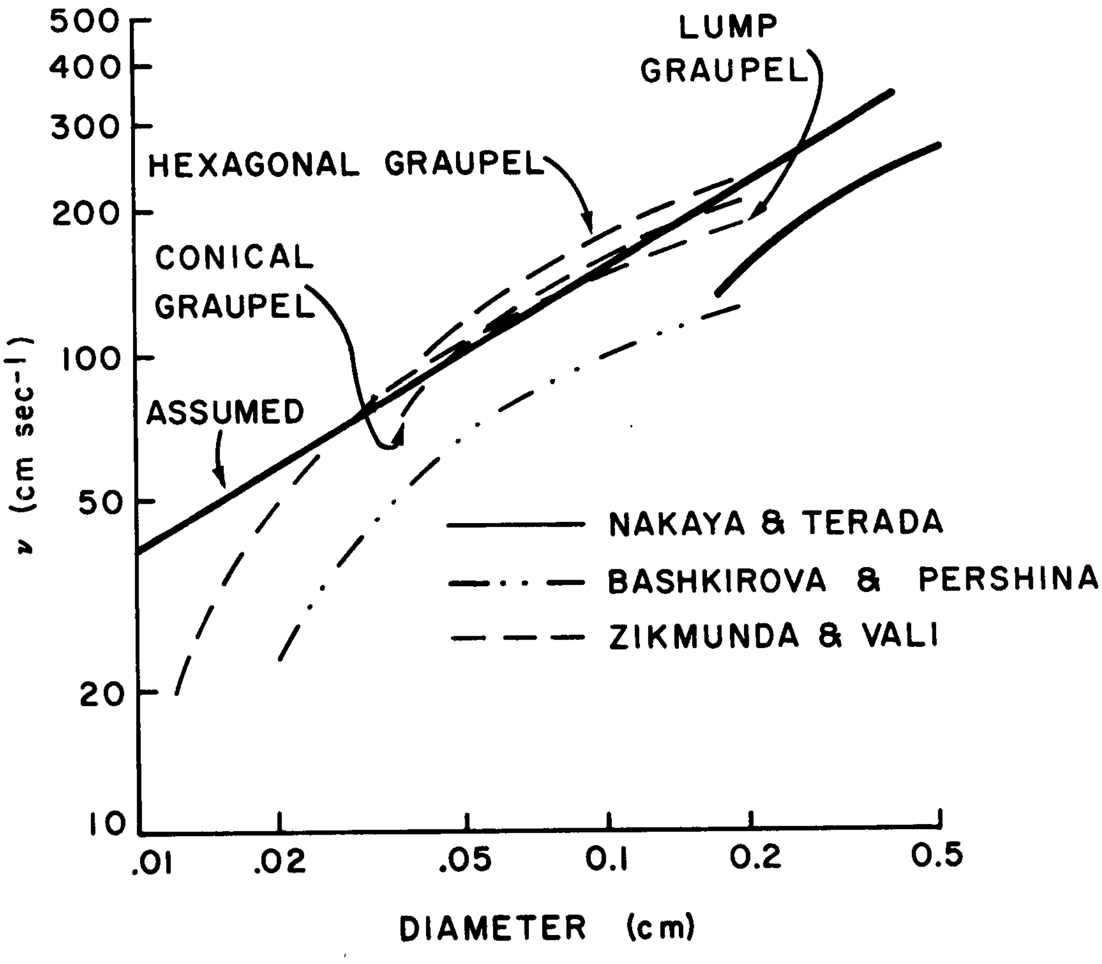

Figure 4-2. Terminal velocities of graupel particles as a function of their diameters.

The average surface temperature, T_s, of a growing graupel particle is calculated by the heat balance equation (Mason, 1971).

$$E R^2 V_o W\{L_f + Cw\ (Ta-Tm) + Ci\ (Tm-Ts)\}$$
$$= 2\pi Rx(2 + 0.54\ Re^{1/2})\{(k\ (Ts-Ta) + Lv\ K\Delta\rho v)\} \qquad (4\text{-}3)$$

Where:

E = the collection efficiency

R = radius of a graupel particle

V_o = impaction velocity

W = liquid water content of a cloud

L_f = latent heat of fusion

Lv = latent heat of vaporization

Cw = specific heat of water

Ci = specific heat of ice

Ta = temperature of an environment

Tm = melting temperature of ice

Ts = temperature of the surface of a graupel particle

x = roughness coefficient of the surface of a graupel

Re = the Reynolds number

k heat conductivity of the air

K diffusivity of water vapor

ρv the difference of vapor density between the surface of a growing graupel particle and the environment.

The collection efficiency, E, defined by Langmuir and Blodgett (1946) was used.

The average density of a graupel particle with diameter, D, is obtained by

$$\bar{\rho} = \frac{\int_0^D \rho D^2 dD}{\int_0^D D^2 dD} \tag{4-4}$$

The results of the calculations are shown in Figure 4-3, a ~ f. Several implications can be drawn from these figures. The lower the temperature of the cloud, the lower the density of the graupel. The accretion of larger cloud water droplets produces a higher density graupel. A graupel particle grown in a cloud with lower liquid water content has a lower density than one grown in a cloud with a high liquid water content. The figures show that at the initial stage of its growth, the density of a graupel particle is low. This results from the small velocity of a small particle. As riming proceeds, the impaction velocities of water droplets increase, and the temperature of the surface of a graupel particle becomes warmer, so that rimed water drops spread more before freezing. Consequently, the average density of a graupel increases with the increasing diameter. Although graupel particles observed in the atmosphere are generally formed by the riming of ice crystals, the calculations imply that riming on a frozen water droplet also produces a low density graupel.

From both the observational results and the calculations it can be concluded that graupel particles of a density lower than 0.2 g cm^{-3} are commonly present in the atmosphere and that densities lower than 0.1 gm cm^{-3} should not be unusual. However, the following fact should be reminded: In the atmosphere graupel tend to fall in a constant

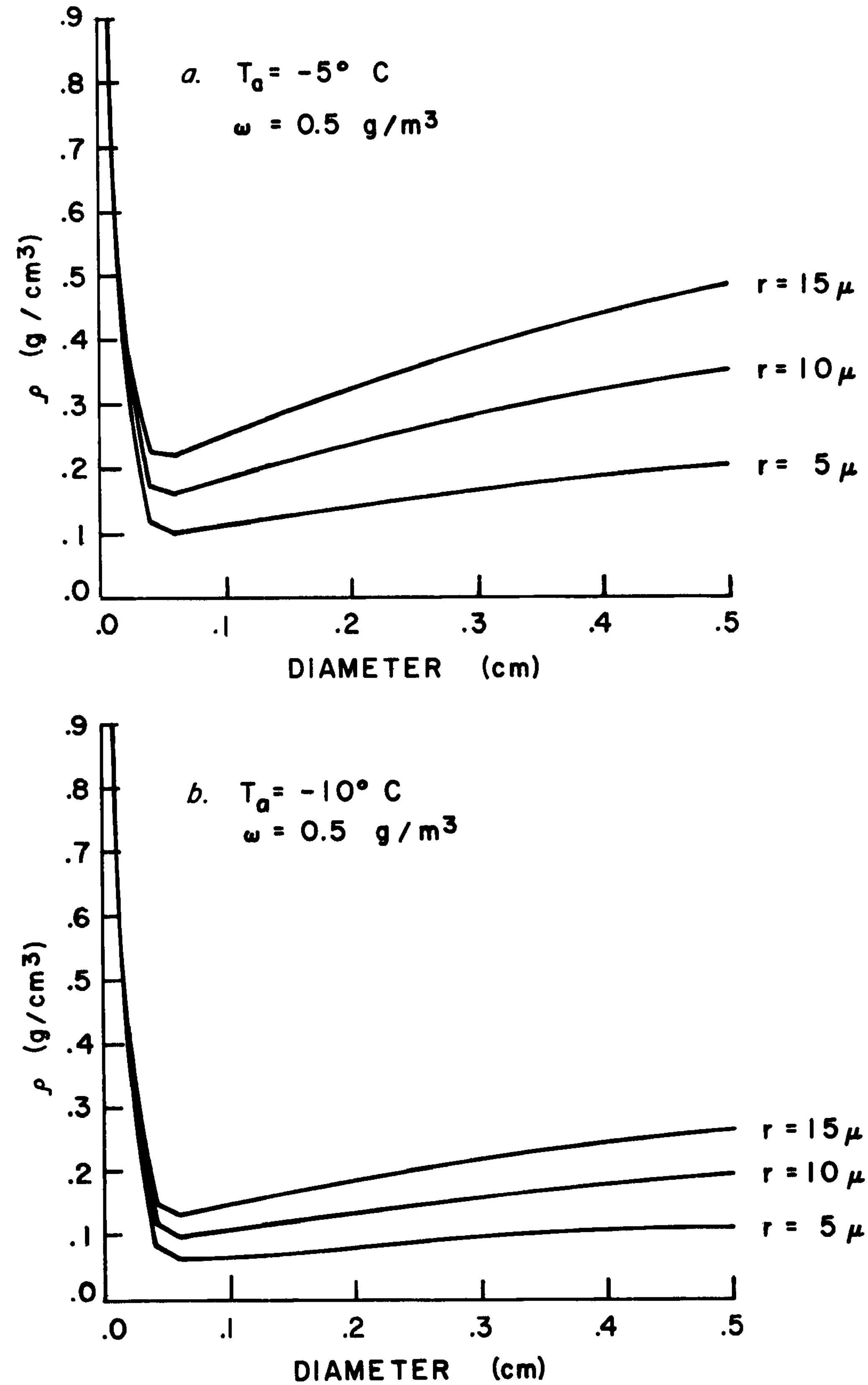

Figure 4-3a,b. Calculated densities of graupel particles as a function of their diameters. w = 0.5 g/m^3.

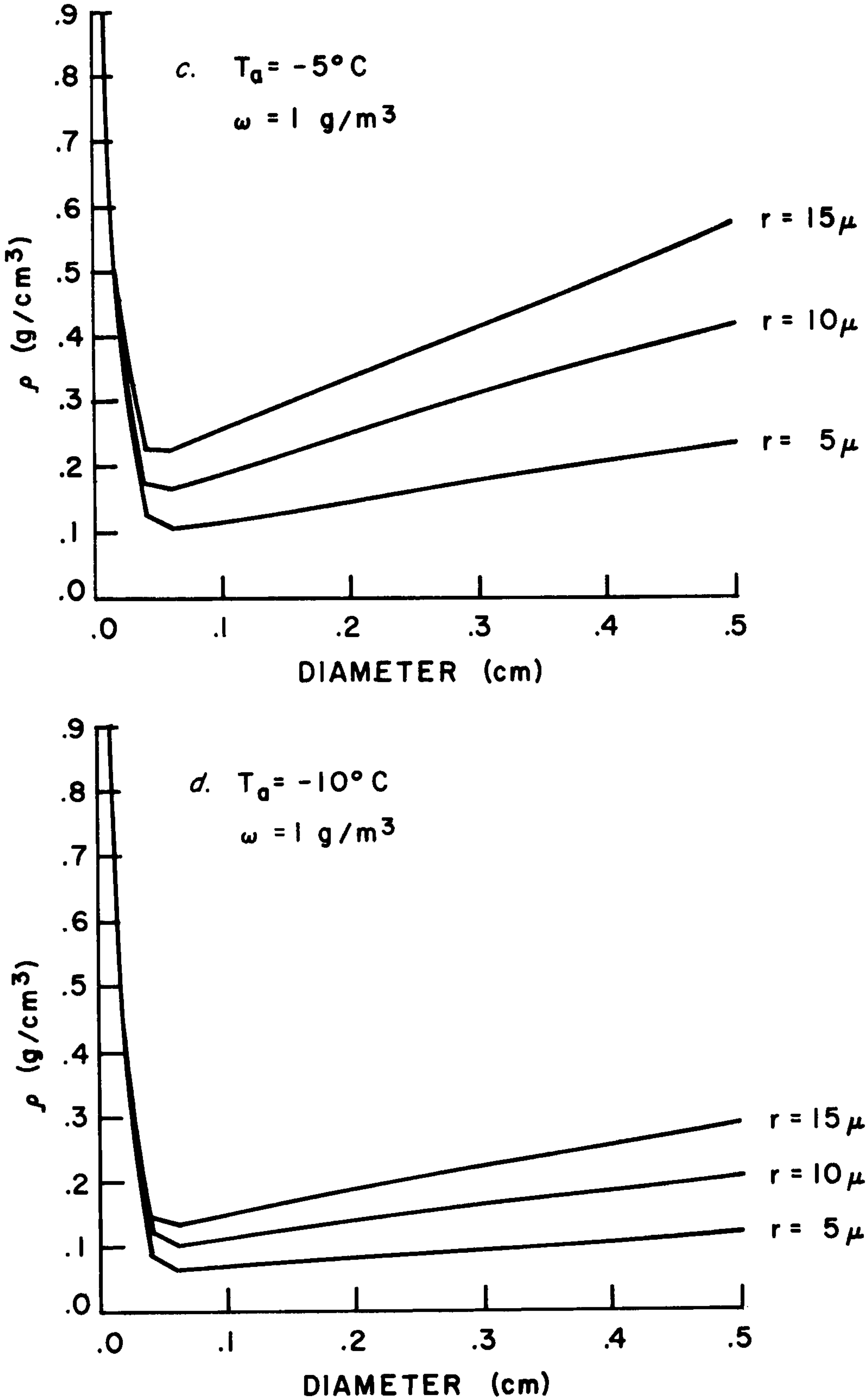

Figure 4-3c,d. Calculated densities of graupel particles as a function of their diameters. w = 1.0 g/m^3.

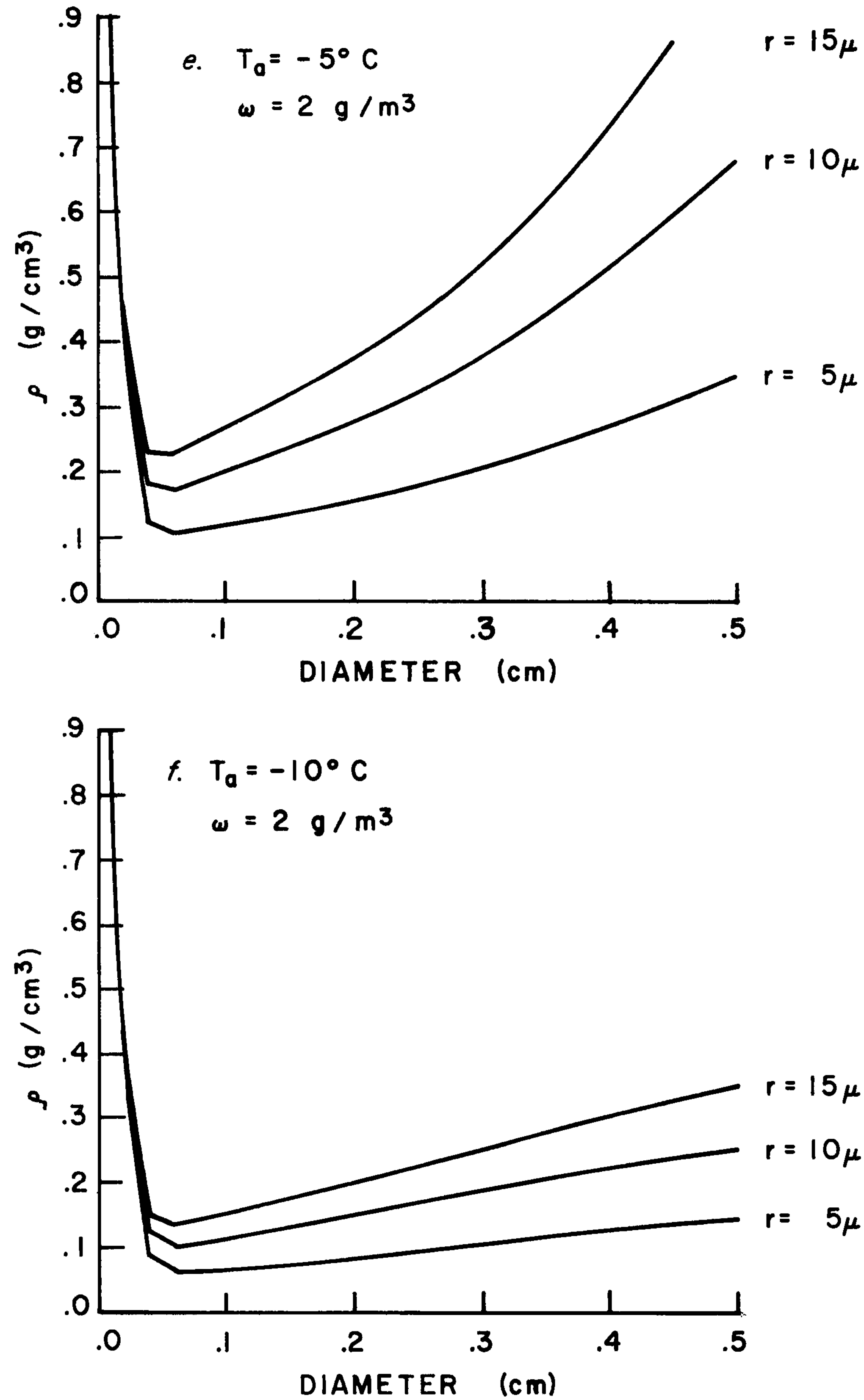

Figure 4-3e,f. Calculated densities of graupel particles as a function of their diameters. w = 2.0 g/m^3.

orientation. Consequently the density of the portion which is faced toward the falling direction becomes larger than that of the portion faced the opposite direction. This is due to the higher collection efficiency of the portion which is faced toward the falling direction. the non-uniformity in the density have been observed on conical graupel by Arenberg (1941), Maruyama (1968) and Knight and Knight (1973). On the other hand, the rimed ice used in the present study was formed under the condition such that all the surface were uniformly exposed to the stream of cloud water. Therefore the density of ice should be more uniform. This difference in the physical characteristics of ice may yield different result in the occurrences of secondary ice particles through the evaporation process of ice.

C. Drag Force

It was shown in the previous chapter that the drag force acting on an ice specimen was one of the important factors for the production of secondary ice particles while the ice specimen are ventilated with subsaturated air.

The drag force per unit area acting on a body is generally expressed by

$$\frac{F_D}{A} = \frac{1}{2} ZC_D \rho_a v^2 \qquad (4\text{-}5)$$

Where Z is the roughness coefficient, C_D is the drag coefficient ρ_a is the density of air, and v is the ventilation velocity. The comparison of the drag force per unit area on an ice specimen in the experiments and on natural graupel particles will now be considered.

1. Ice cylinder

Using the C_D-Re relationship for a cylinder given by Goldstein (1965) the drag forces per unit area on an ice cylinder in the experiments are estimated to be 23.6, 14.3, 6.6, and 1.7 dynes cm^{-2} for ventilation velocities of 2.0, 1.5, 1.0 and .5 m sec^{-1}, respectively. It is assumed that Z is equal to 1. These values are for a temperature of -7°C and a pressure of 850 mb. The values of C_D used for the calculations are for a cylinder with a smooth surface in an infinite flow. The surfaces of the ice cylinders in the experiments were not smooth but protruded. Therefore, the surface roughness coefficient, Z, should be larger than 1. On the other hand, if the ratio of length to diameter of a cylinder is finite (in the experiments, $\ell/d \simeq 4$), C_D becomes smaller. Therefore, it is assumed here that these opposite effects offset each other.

2. Graupel

For graupel the C_D-Re relationships were obtained by Zikmunda and Vali (1972). The relationships were given by the following equations:

$$C_D = 98.41\ Re^{-.77}, \text{ for lump graupel} \quad (4\text{-}6)$$

$$C_D = 73.35\ Re^{-.73}, \text{ for conical graupel} \quad (4\text{-}7)$$

The terminal velocities given in Figure 4-2 are used to calculate the drag force per unit area of a graupel. It is assumed that graupel particles observed by Nakaya and Terada, and Bashkirova and Pershina were of the lump type. The calculations are made for a temperature of -7°C and a pressure of 850 mb.

The results are given in Figure 4-4. It is clear that over a wide range of size, the drag force per unit area on a graupel is similar in magnitude with that on an ice cylinder used in the experiments. Although the above considerations are based on crude approximations, it may be inferred that graupel particles in free fall receive a similar drag force per unit area as that effective in production of secondary ice particles from an ice specimen used in the experiments.

D. Evaporation Rate

Another important factor in the production of the numerous secondary ice particles from an ice specimen was the large evaporation rate of the ice specimen. In order to compare the results of the experiments, the evaporation rate per unit area of graupel particles will be considered here.

1. Ice Cylinder

For an ice cylinder the evaporation rate per unit area is given by the equation (3-9). It has been shown in Figure 3-5 that the experimental results of the evaporation rate, which were obtained under a condition of ventilation velocity of 2m sec^{-1}, were about three times greater than those calculated for an ice cylinder with a smooth surface. Therefore, within the range of experiments, the coefficient of the surface roughness, x, should be written as 3. For a comparison of the evaporation rate it is convenient to use the quantity

$$y = x\,\frac{(0.615Re^{.466})}{d} \qquad (4\text{-}8)$$

which is dependent on the dimension of an ice specimen and ventilation

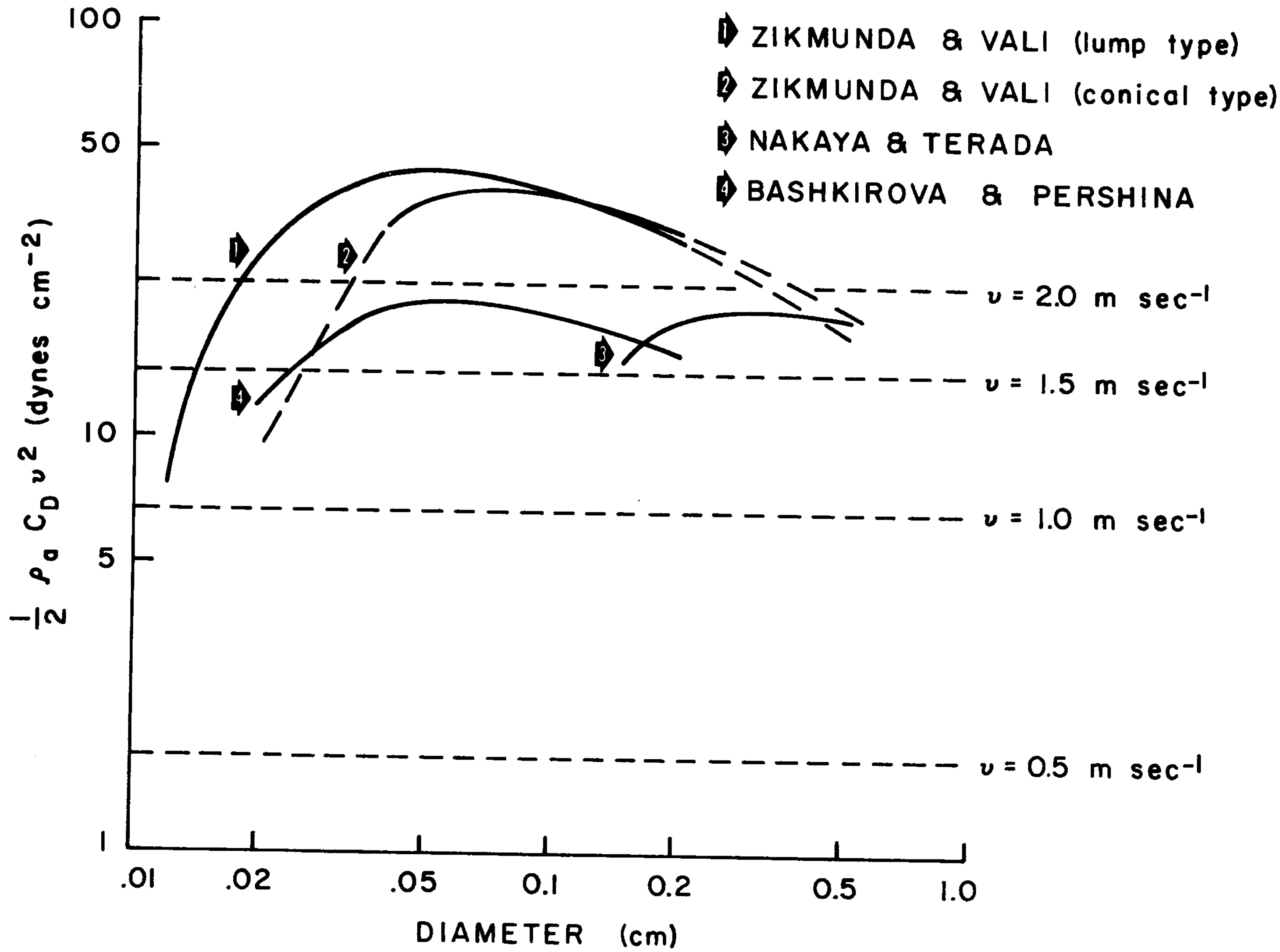

Figure 4-4. Drag forces per unit area acting on graupel particles as a function of the diameters of graupel particles.

intensity. For an ice specimen in the experiment this quantity is calculated as 109 cm^{-1} and 96 cm^{-1} for ventilation velocities of 2.0 and 1.5 m sec^{-1}, respectively.

2. Graupel

Assuming that a graupel is spherical, an equation similar to equation (4-8) can be written (Mason, 1971).

$$y = x \left(\frac{2 + 0.54Re^{1/2}}{d}\right) \tag{4-9}$$

The fall velocities for graupel obtained by Nakaya and Terada (1935), Bashkirova and Pershira (1964), and Zikmunda and Vali (1972) are used for the calculation of this quantity, assuming that graupel have smooth surfaces (x=1). The results are given in Figure 4-5. It is seen that the evaporation rate per unit area for graupel particles decreases with increasing size and that even under the assumption of x=1, the value of y is larger than that for the ice cylinder for particles smaller than 800 microns. The surface of a graupel, especially one of low density, is by no means smooth but protruded. Therefore, the coefficient of surface roughness should be larger than 1 and could be as large as 3. So, it can be concluded that if graupels are present in a similar degree of subsaturation; they are evaporated with a rate per unit area similar to those in the experiments.

E. Presence of Subsaturated Air in and Around Clouds

In the previous section it was implied that graupel particles in natural clouds may produce secondary ice particles if they are ventilated with subsaturated air. Therefore, the structure of clouds should be reviewed briefly with special attention to evaluate the possibilities of the presence of subsaturated air in and around clouds.

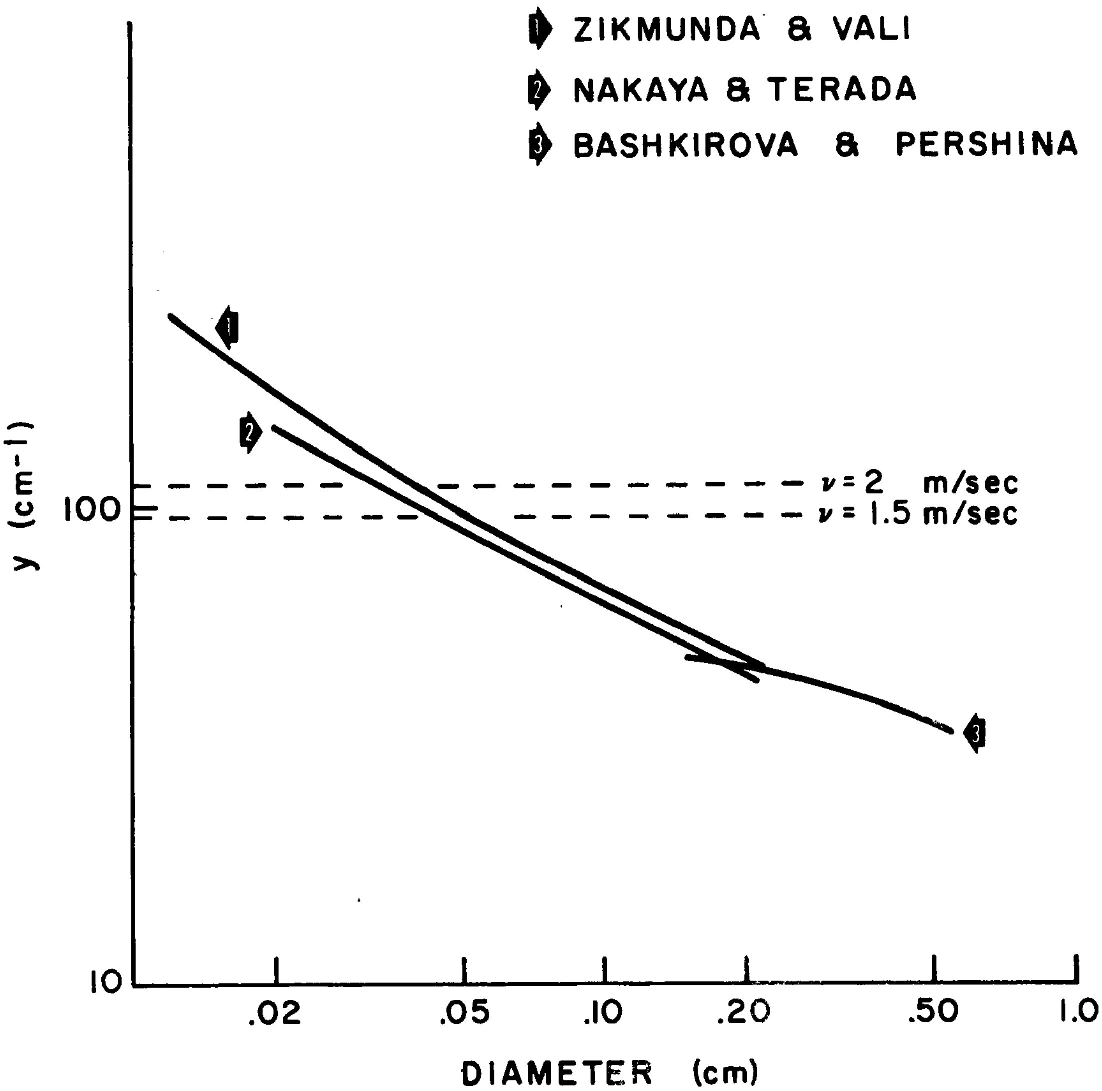

Figure 4-5. A factor proportional to the evaporation rate of graupel particles.

Fluctuations of various properties (temperature, L.W.C., and air speed) with respect to time and space within clouds, especially of cumulus clouds, are well known. The predominant horizontal scales of these fluctuations for hurricane clouds, revealing two peaks in cloud properties centered most frequently around 2.5 and 5 to 6 cycles a mile, have been examined by Ackerman (1967). More rapid fluctuations in visibility were reported by Weickmann and aufm Kampe (1953). Visibility in a cumulus cloud varies largely over distances of a few meters.

The measurements of liquid water content indicate that cloud processes are far from adiabatic, and a dominating role is played by the admixture of dry air from outside the cloud (Squires, 1958, Warner, 1955, and 1970). Squires reported that out of nearly a thousand samples of water droplets taken in cumuli, about eight percent of them did not have any water droplets; more than half of these were isolated. Cloud droplets were found about 200 m away from each side of the region of where no liquid water was found. From the study of size distribution of cloud droplets Warner (1970) found that bimodel size distributions of cloud water droplets are not unusual. Warner suggested that the development of a bimodel distribution is found not only around the edge of a cloud but also inside the cloud. Warner's explanation for this bimodel size distribution is as follows: If a parcel of cloudy air, containing drops whose size distribution has only a single mode, is mixed with subsaturated environmental air, all the drops will decrease in size. Subsequent mixing of this parcel with some of the original cloud will result in the development of a bimodel drop-size distribution in the mixture. Records of cloud traverse in his report show that low or null liquid water content is generally in downdraft regions, sometimes of considerable horizontal extent (three to four hundred meters). These observational results show that a cumulus cloud contains pockets of subsaturated air.

Apart from the results of microphysical observations in clouds there is additional evidences to support the fact that considerable mixings take place in and out of the clouds and that subsaturated air exists in the clouds. It is well known that the lapse-rate of temperature in a cumulus cloud is steeper than the wet adiababic. Stommel determined the fractional amount of the entrainment, level by level. The results of his calculation indicate that in the trade wind clouds studied the amount of entrainment frequently corresponded with a doubling of the mass flux of the rising air in 1 km ascent. Malkus (1954) made improved calculations of entrainment for a trade wind cumulus cloud by using the data which were obtained by an airplane observation through a cloud. In her paper she distinguished gross entrainment and dynamic entrainment. Gross entrainment was defined as the total amount of environmental air mixed with cloud air, while dynamic entrainment was defined as the difference between gross entrainment and detrainment. The former corresponds to the entrainment defined by Stommel, and the latter was originally introduced by Austin and Fleisher (1948). Gross entrainment calculated by Malkus was consistent with the results obtained by Stommel. Comparisons of the amount of gross entrainment and dynamic entrainment indicated that gross entrainment greatly exceeded dynamic entrainment at the top of a cloud where the wind shear was large and where the cloud had a pronounced backslant. This indicates a strong mixing process at the level of a cloud top. Calculations by both Stommel (1947) and Malkus (1952) were based on the concept that the entrainment is due to turbulent lateral mixing. There are other possible mechanisms which explain the presence of subsaturated air in clouds: The dry air may not have moved far from its original position having mixed in situ with the saturated, cloudy air rising from below. This model is closely related to the bubble theory of convection developed by Scorer and Ludlan (1953), according to which the growth of a cumulus is the result of the arrival at condensation level of a succession of buoyant bubbles, each of which is steadily eroded as it rises. If other bubbles follow the same path through the air, they will penetrate further because the ambient air has been moistened by the predecessors; by this process a cumulus builds up in steps. Another mechanism was proposed by Squires (1958). According to Squires, the dry air may originate from the region just above the growing cloud top, entering the cloud as downdrafts and mixing vertically with the updraft. In other words, a parcel of dry air which enters the top of a growing cloud by turbulent diffusion will be cooled by the evaporation of liquid water and may subside into the cloud.

It has not been confirmed at the present time which of the three mechanisms above is the most dominant one for entrainment. However, the implication that subsaturated air exists frequently in the clouds with respect to time and space should be emphasized here.

There are several reports of direct observation of relative humidity in clouds (Cunningham, 1958, Cunningham and Glase, 1965, and Simpson and Woodley, 1969). All the records of relative humidity obtained in horizontal transverse flights show considerable fluctuations, indicating the presence of subsaturated air in and around clouds. It may be inferred that cumulus clouds are nonuniform in structure with respect to space and time and that there are always portions in which the air is subsaturated such is the case on the edges of a cloud and even inside a cloud.

Contrary to cumulus clouds, which are characterized by considerable mixing with environmental air and, consequently, by nonuniform structure with respect to time and space, layer type clouds such as stratiform clouds and stratocumulus are usually characterized by vertical velocities of low magnitude and by little mixing with environmental air except at the top of clouds. This makes the inside structure more uniform than that of a cumulus cloud.

F. Chapter Summary

The purpose of this chapter was to examine whether physical conditions which are necessary for the production of secondary ice particles by the evaporation of ice exist in the atmosphere. Since a graupel particle seems to have similar characteristics as those of the rimed ice which were used in the experiments, considerations were made on a graupel particle with respect to its density, the drag force acting on it, and its evaporation rate. In addition, literatures on the studies of cumulus clouds were briefly reviewed with special attention to the presence of subsaturated air in the clouds.

Although the density of a graupel in the atmosphere is highly variable, a graupel with a density lower than 0.2 g cm^{-3} is not unusual. The calculations of the density of hypothetical graupel, based on simple assumptions, show that if a graupel does not continue to grow to a few millimeters, it could be as low as 0.2 g cm^{-3} even under the conditions of a cloud temperature of -5°C, a liquid water content of 2 g m^{-3}, and a mean cloud droplet diameter of 30 microns. If these physical parameters are lower than the above values, it is likely that a graupel particle will grow with a density lower than 0.2 g cm^{-3}.

The results of the calculations show that the drag forces per unit area acting on graupel particles are similar in magnitude to the drag force per unit area acting on an ice cylinder which is effective in the production of secondary ice particles.

The evaporation rates per unit area of graupel particles in free fall are, over a wide range of size, possibly as large as those obtained in the experiments if the particles are exposed to subsaturated air.

The presence of subsaturated air, which is the necessary condition for low-density rimed ice to produce numerous secondary ice particles, is frequently observed in cumulus clouds at all stages of their growth and decay.

From the above results it can be concluded that physical conditions which are necessary for the production of secondary ice particles by the evaporation of ice exist commonly in the atmosphere.

Chapter V

IMPLICATIONS OF THE EXPERIMENTAL RESULTS TO THE ATMOSPHERE

In the previous chapter the physical conditions necessary for the production of secondary ice particles by the evaporation process of ice exist in the atmosphere were considered. It was concluded that the conditions commonly existed in cumulus clouds.

It seems likely from the previous considerations that secondary ice particles could occur when graupel particles with low densities encounter subsaturated air in and around a cloud. If the secondary ice particles produced are then incorporated into saturated regions of the cloud, they would cause substantial changes in the cloud characteristics. In this chapter a simple calculation is made by using the data obtained from the experiments in Chapter III to consider the likelihood that secondary ice particle production by evaporation of ice is actually a mechanism for ice multiplication in clouds.

Calculation is based on the following concept. When a graupel particle encounters subsaturated air in or around a cloud, it will evaporate and produce secondary ice particles. When there is a mixing associated with the subsaturated air, a fraction of the secondary ice particles may be incorporated into the saturated air by the turbulent mixing before the particles evaporate completely and, consequently, multiply the ice particle concentration in the saturated region.

The results of direct observation of relative humidity in and around cumulus clouds (Cunningham, 1958, Cunningham and Glase, 1965, and Simpson and Woodley, 1969) showed that relative humidity in clouds could grow into the environments where relative humidity were smaller than 50 percent. Furthermore, it was shown that the gradients of relative humidity from saturated regions of a cloud to subsaturated regions have large variation. Therefore, ice multiplication due to the secondary ice particle production from evaporating graupel in the air having different relative humidities will be considered. Although the model is simple, some useful conclusion can be reached.

A. Model and Procedure of Calculations

The following are the assumptions made for the calculations.

1. It is assumed that a spherical graupel particle with a density of .15 gm cm^{-3} encounters a subsaturated air. This can typically occur when a graupel particle is carried by turbulent motion from inside of a saturated cloud into an adjacent dry environment.

2. In the subsaturated air, the graupel particle evaporates and produces secondary ice particles in a manner similar to that observed in the laboratory. The subsaturated air, in which secondary ice particles are produced, is then mixed by turbulent motion with cloud air saturated with respect to water. The humidity of mixed air becomes saturated with respect to ice after a certain time, T. The time T depends on many factors, for instance, the ratio of mass flux of saturated air to that of subsaturated air.

3. The fall velocity of the graupel particle follows the curves given by Nakaya and Terada (1935) for the diameter of a graupel particle larger than 2 mm and by Bashkirova and Pershina (1964) for that smaller than 2 mm (See Figure 4-2).

4. The secondary ice particle production rate per unit mass of an evaporated graupel is given in Figure 5-1 which is composed from Figure 3-8, a through d.

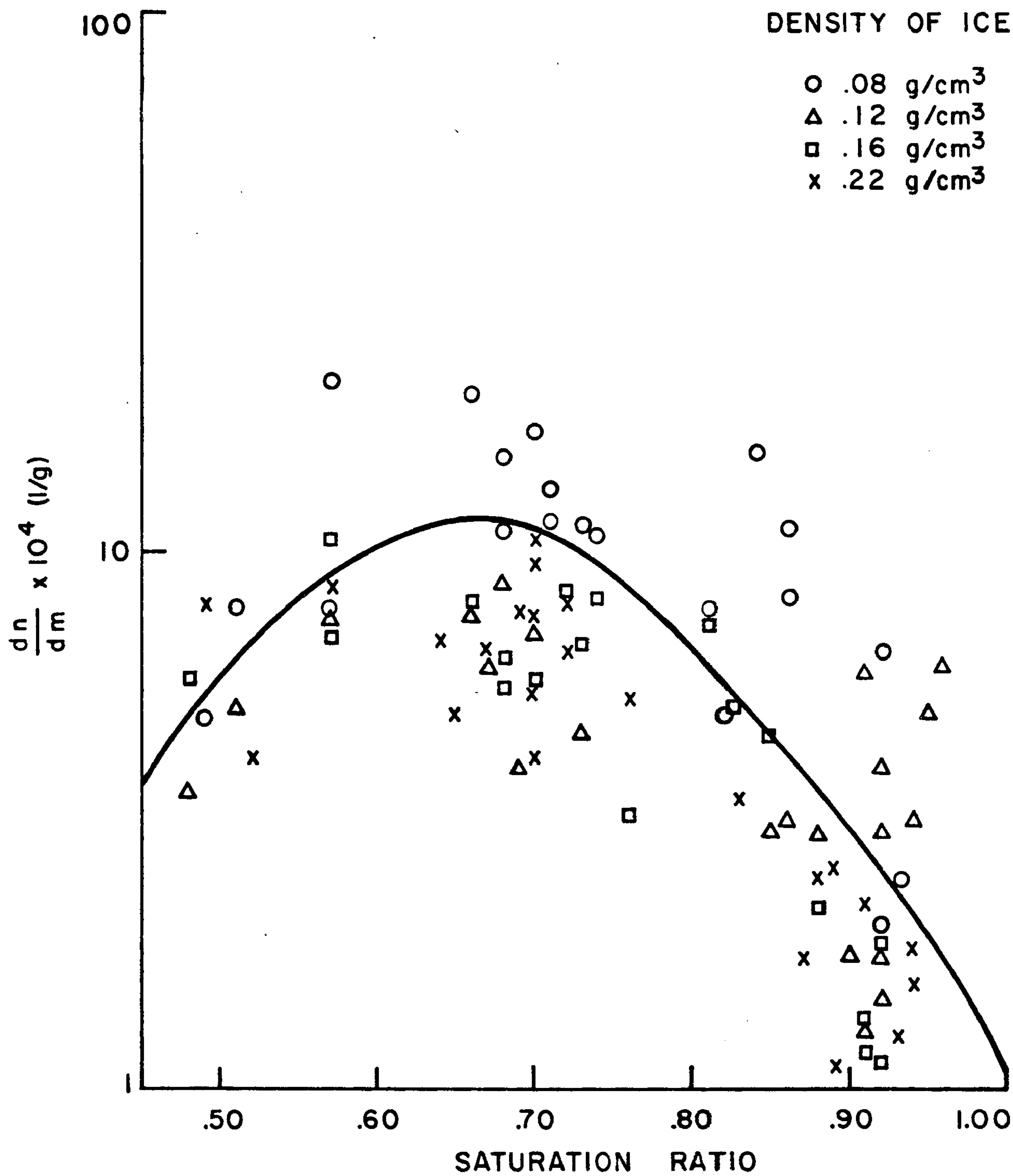

Figure 5-1. Secondary ice particle production per unit mass of exaporating ice as a function of subsaturation ratio compiled from Figure 3-8, a through d.

5. The size distribution of secondary ice particles is given in Figure 3-12 regardless of the relative humidity of air. Since the particles are small, the density of the secondary ice particles is assumed to be 0.9 gm cm^{-3}.

6. The evaporation rate of a graupel particle is given by

$$\frac{dm}{dt} = X \frac{2\pi D(S-1)}{A+B} (1 + 0.27 \ Re^{1/2}) \tag{5-1}$$

Here, D is the diameter of the graupel particle, S is the saturation ratio, Re is the Reynolds number, and A and B are coefficients (See, for instance, Byers, 1965). X is a roughness factor. Since the experimental results in Chapter III showed that the evaporation rate of rimed ice with protruded surface is about three times larger than that of ice with smooth surface, X is assumed to be three.

From equation (5-1), the mass of a graupel evaporated within the time Δt is written as

$$\Delta m = \rho_i \frac{\pi}{6} (D_n^3 - D_{n-1}^3) \tag{5-2}$$

where

$$D_n = (D_{n-1}^2 + \frac{X}{\rho_i} \frac{8(S-1)}{A+B}(1 + 0.27 \ Re^{1/2})\Delta t)^{1/2} \tag{5-3}$$

7. The saturation ratio, S, changes with time from the initial value So to the ice saturation Si. It is assumed that the change of saturation ratio proceeds as

$$S = So + \frac{Si - So}{T} \ t_n \tag{5-4}$$

where S is the saturation ratio of air at the time, t_n. Therefore, the secondary ice particles produced at the time, t_n, spend the time, $T - t_n$, in the subsaturated condition. The number of secondary ice particles produced at the time, t_n, is given by

$$\Delta N_n = - \frac{\pi \rho_i}{6} [\frac{dN}{dm}] (D_n^3 - D_{n-1}^3) \tag{5-5}$$

The time, t(d), within which a secondary ice particle of the diameter, d, evaporates completely in the air of the subsaturation ration, S, is given by:

$$t(d) = - \rho \frac{A+B}{8(S-1)} \int_o^d d(D^2) \tag{5-6}$$

where ρ is the density of the secondary ice particles. Therefore if the time for a secondary particle with diameter d is

$$t(d) > T - t_n$$

the particle will survive and will be incorporated into the cloud.

The number of secondary ice particles produced at time t_n, which becomes effective for ice multiplication is, therefore, given by,

$$N_n = P_n(d) x \Delta N_n \tag{5-7}$$

where $P_n(d)$ is the percentage of secondary ice particles produced at H_n which has a diameter larger than d. Therefore, the total number of secondary ice particles effective for ice multiplication is given by:

$$N = \sum_{n-1} N_n . \tag{5-8}$$

B. Results and Discussion

1. Results of calculation

The calculations were made for the initial diameters of graupel between 2.0 mm and 5.0 mm. Initial saturation ratio of the air, So, is varied from .40 to .80 with respect to ice. The time, T, in which the saturation ratio of the air changes from So to the ice saturation, Si, varies from 2 sec to 30 sec.

The effect of the time, T, is shown in Figure 5-2, a and b. In the figure, the effective number of ice particles per graupel particle which are incorporated into the cloud are plotted as a function of the time, T. The initial values of saturation ratio, So, are taken as a constant. Figure 5-2, a and b, are for a graupel particle having the initial diamter .5 cm and .35 cm, respectively. It can be seen that the smaller the saturation ratio So, the greater the effective number N. This is because the mass evaporated is larger when So is smaller and also due to the assumption that secondary ice particles have a size distribution independent of the subsaturation of the air. It is also seen that the effective number, N, increases with T at smaller values of T and then at still longer times decreases with the increase of T. The longer the time T the greater the total number of secondary ice particles produced but the greater the loss of secondary ice particles due to evaporation.

In Figure 5-3, the effective number, N, is plotted as a function of the initial diameter of graupel for the time T = 10 sec. The saturation ratio, So, is taken as a constant. It is natural that N increase with the increase of the diameter.

Suppose that the saturation ratio of dry air is .60 with respect to ice, that by turbulent motion, a graupel particle having the diameter .5 cm encounters the dry air, and that this dry air is mixed into a cloud, changing its saturation ratio from .6 to 1.0 in 10 sec. In this case it can be seen from Figure 5-3 that the concentration of ice particles in the region where the turbulent mixing has taken place becomes about four times greater than that before the mixing. If the same graupel particle experiences similar process a few times in a few

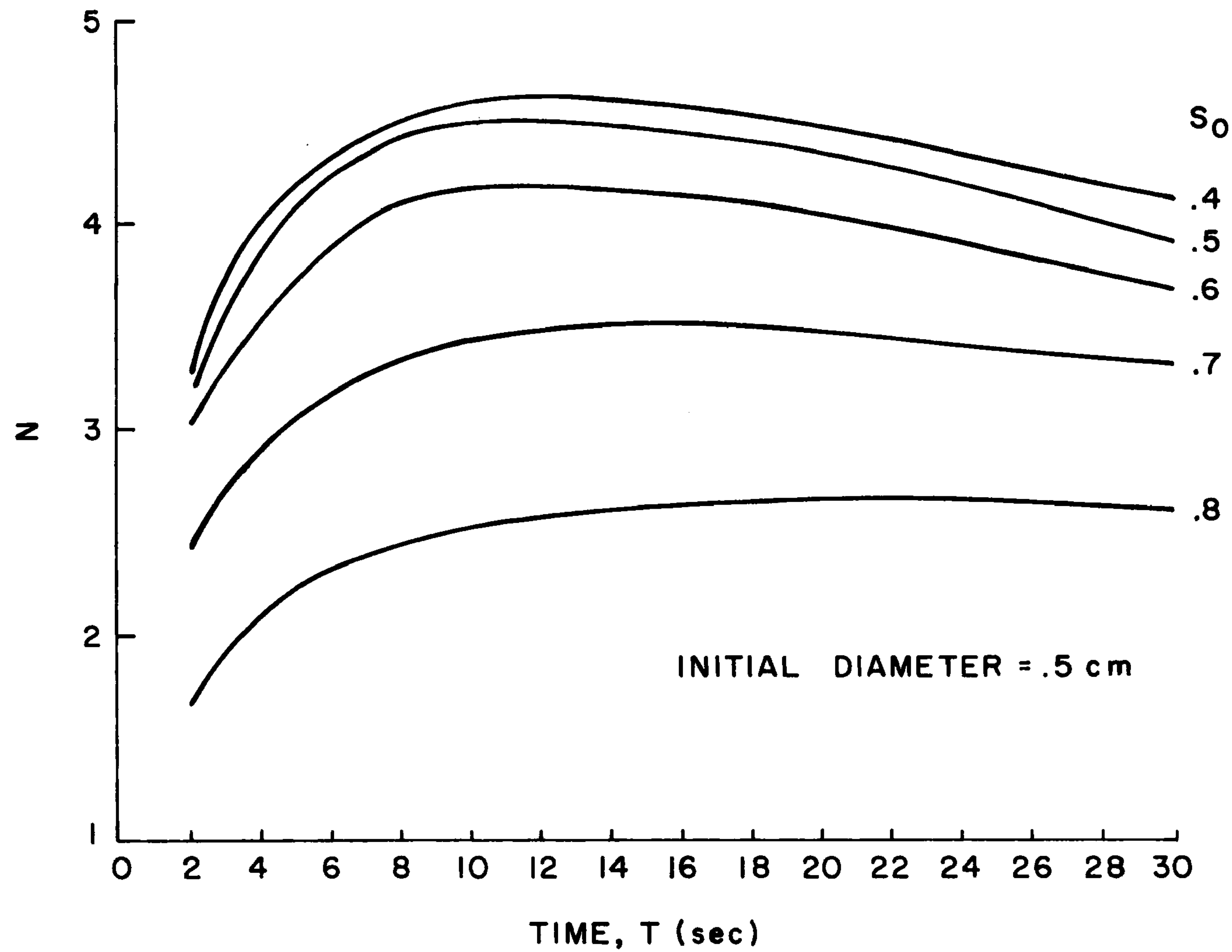

Figure 5-2a. Effective number N of secondary ice particles as a function of the mixing time T (for initial diameter of a graupel = .5 cm). So is taken as a constant.

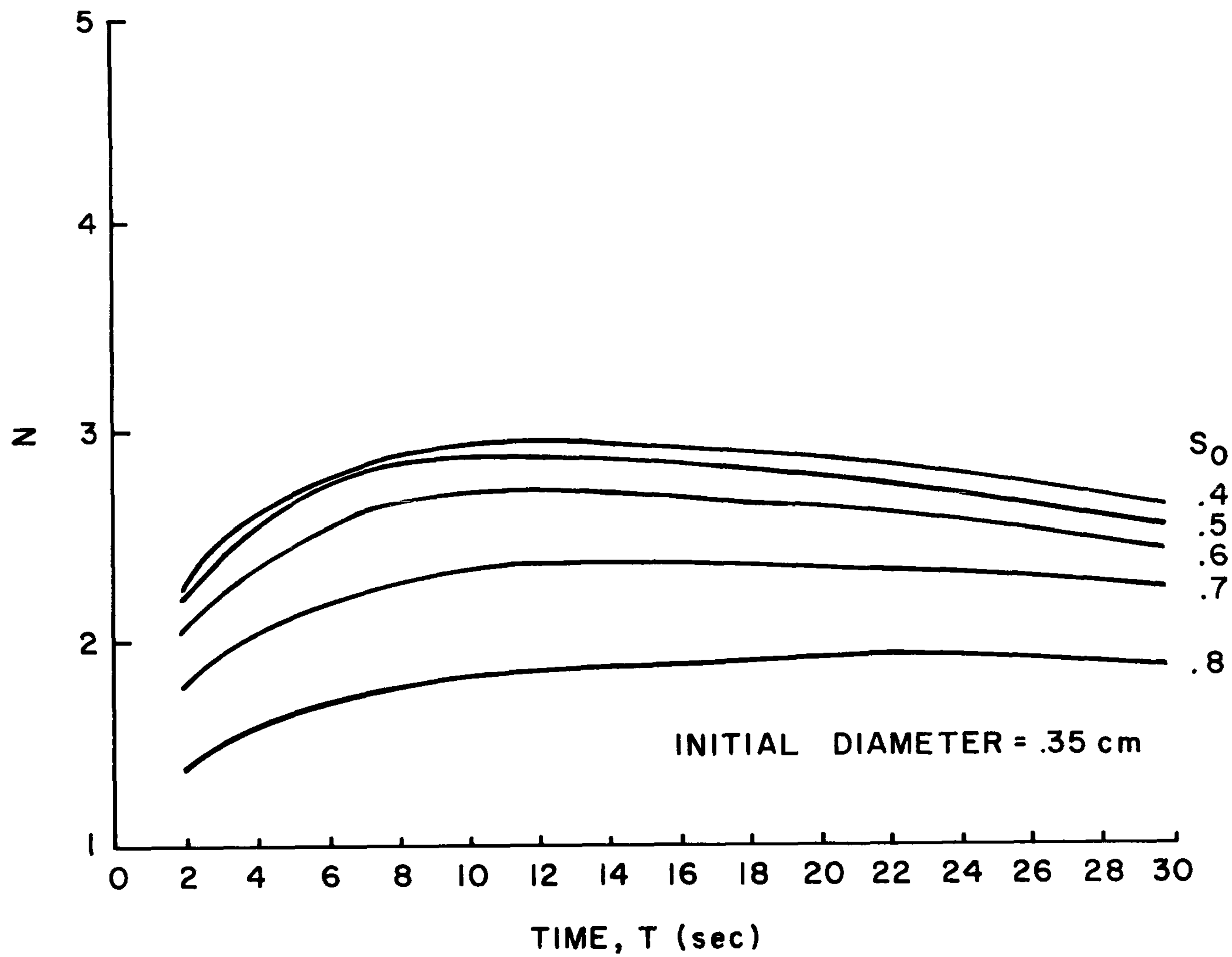

Figure 5-2b. Effective number N of secondary ice particles as a function of the mixing time T (for initial diameter of a graupel = .35 cm). So is taken as a constant.

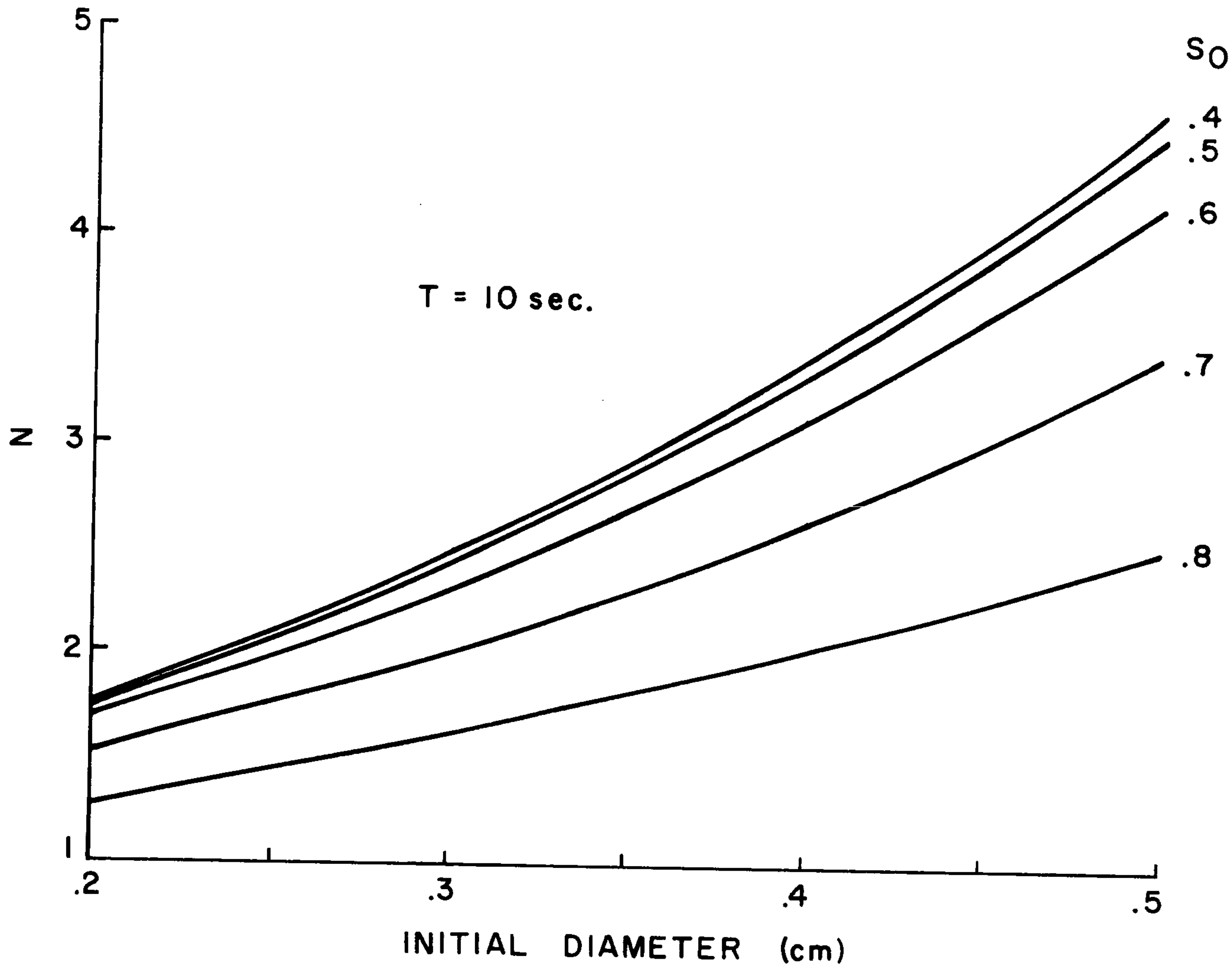

Figure 5-3. Effective number N of secondary ice particles as a function of initial diameter. The saturation ratio So is taken as a constant (for T - 1o sec).

minutes, the concentration of ice particles in the cloud could increase with the rate of several per minute.

From the above consideration, in order for ice multiplication to take place by the process of evaporation of graupel particles, the following can be inferred:

1) A cloud grown in drier environment has a better chance of ice multiplication.
2) The subsaturated air, with which graupel particles encounter, must be incorporated rather quickly into a cloud. Therefore, the region where strong mixing process between saturated air and subsaturated air is taking place is required if ice multiplication occurs by this process.

2. Significance of the Process in Clouds.

As has been reviewed in the previous chapter, cumulus clouds grow by entraining a considerable amount of environmental air. For instance, Stommel's (1947) calculation indicates that the amount of outside air entrained frequently corresponds with a doubling of the mass flux of the rising air in a 1 km ascent. It is probable that by this entrainment process a fraction of the secondary ice particles produced in the environment where the air is subsaturated can be incorporated into the cloud, resulting in ice multiplication in a cloud.

According to Squires (1958), the dry air may originate from the region just above the growing cloud top, entering the cloud as downdrafts and mixing vertically with the updraft. If graupel particles, which are carried to the top of the cloud by updraft, are incorporated with this penetrative downdraft, secondary particles could be produced in the downdraft. As a consequence, ice multiplication would take place in the region where the vertical mixing takes place.

3. Effect of Preactivation.

In the above discussion it was assumed that secondary ice particles are composed of pure water substance. However, in clouds, graupel particles are formed by the riming of cloud water droplets. Each cloud water droplet should contain a condensation nucleus or some other impurity collected by the scavenging process after a water droplet is formed. Therefore, most secondary ice particles produced from a graupel particle should also retain such impurities. If an impurity is an insoluble particle, such as a soil particle, the particle may retain a sub-microscopic film or a patch of ice on the surface of the particle or may retain embryos of ice in small cavities and capillaries even after the microscopic ice is completely evaporated (Mason, 1971). Roberts and Hallett (1968) reported that naturally occurring soil particles, such as kaolinite, gypsum, calcite, montmorillonite, bentonite, vaterite, albite and glacier debris, upon on which crystals
which ice has once grown and subsequently evaporated, can retain adsorbed ice
can grow again if the particles are exposed to saturated air. This property is destroyed within a few minutes by exposure to temperatures above −5°C or by exposure to relative humidities below about 30 percent with respect to ice. Therefore, it is inferred that some secondary ice particles produced from an evaporating graupel particle may be reactivated by this mechanism even after the microscopic ice is completely evaporated.

If this mechanism of preactivation is incorporated with the mechanism of the secondary ice particle production from an evaporating graupel, the latter becomes even more effective for ice multiplication. For instance, a graupel particle of 3 mm diameter having an apparent density of .15 g cm^{-3} has a possiblity for the production of 1.8×10^2

secondary ice particles, if it encounters the air whose relative humidity with respect to ice is 70 percent; and it is kept in the air until its diameter becomes 2 mm. Since the surface of a graupel having a low apparent density is not smooth but protruded, the time required for this evaporation process could be no longer than 4 ~ 5 minutes. Suppose that the initial concentration of graupel particles is 1 per liter in the subsaturated air, and that while the evaporation of graupel particles is taking place, one part of the sub-saturated air is incorporated with 9 parts of the cloud air; the former contains the secondary ice particles either as ice particles or as preactivated ice nuclei and the latter contains neither ice particles nor ice nuclei. In this case, the concentration of ice particles in the cloud after the mixing is enhanced from initially 1 per liter to 18 per liter within 3 or 4 minutes. Therefore, if the effect of preactivation nuclei is taken into the consideration, the mechanism of secondary ice particle production can be more effective for ice multiplication.

C. Chapter Conclusion

It seems proper to conclude that the multiplication rate of ice particles of at least several per minute can be explained by the mechanism of secondary ice particle production from evaporating graupels. It is interesting to note the observations by Mossop et al. (1970) and Koening (1963). Mossop et al. reported that the multiplication rate of ice particles in a cumulus cloud was approximately 1 $min.^{-1}$. On the other hand, Koenig observed an extremely large multiplication rate of approximately 1×10^{2} $min.^{-1}$. The multiplication rate such as reported by Mossop et al. can be well explained by the present mechanism.

Chapter VI

SUMMARY AND CONCLUSION

The purpose of this study was to examine the roles of the riming process on ice multiplication in clouds. Experiments were conducted in a cold room to examine secondary ice particle production from rimed ice.

The purpose of the first series of experiments was to study the secondary ice particle production from ice during its growth by the riming process. The experiments were conducted using cloud water droplets with a size distribution of 3 to 20 microns in diameter. Ice was formed by ventilating a rotating bar with cloud water at velocities of 2.4 to 4.3 m sec^{-1}. Temperature of the air was kept between -7.1 and -7.3°C. It was inferred that the detachment of pieces of ice from the surface structure of growing ice due to strong ventilation was responsible for the secondary ice particle production. The number of secondary ice particles during the growth of ice were fewer than 10 per milligram of ice. In terms of the collision number of water droplets, several "10^6" water droplets were necessary for the production of one secondary ice particle. Calculations indicate that at this rate approximately 30 minutes are required for the concentration of ice particles to be multiplied by 10. In the calculations a cloud having the concentration of 500 cm^{-3} of cloud droplets with a mean volume diameter of 15 microns was assumed. This leads to the conclusion that secondary ice particle production during the riming growth of ice is not a significant process for ice multiplication in clouds.

The second series of experiments were designed to study the secondary ice particle production due to the evaporation process of ice which had been formed by the riming process. In these experiments, ice specimens were formed in a similar manner to the riming experiments and were then ventilated with subsaturated air at a velocity of 2 m sec^{-1} or less. The saturation ratio of the air ranged between .96 and .48. The temperature of the air for ventilation was kept at -7°C. It was found that large numbers of secondary ice particles were produced only from ice specimens with the apparent density of less than .22 g cm^{-3}. The number of secondary ice particles per unit mass, dN/dm, was as high as 200 per milligram of evaporating ice. The magnitude of dN/dm obtained in the experiment was one or two orders larger than those obtained in the riming experiment. It was concluded that the mechanical break-up of protruded parts of the surface due to ventilation and evaporation of the ice specimen was responsible for the secondary ice particle production. The combination of the ventilation velocity, subsaturation ratio of the air, and a low apparent density of the ice was essential for the production of a large number of secondary ice particles. Within the range of the experiments, a ventilation velocity of 2 m sec^{-1}, a subsaturation ratio of .65 ~ .75, and an apparent density of .08 g cm^{-3} was the optimum combination of parameters which produced the largest number of the secondary ice particles.

For these reasons, it is considered whether natural conditions are similar to those of the experiment for evaporation of rimed ice. The density of graupel, the drag forces acting on graupel, and the evaporation rate of graupel particles were considered. This lead to conclusion that graupel particles occurring in the atmosphere commonly possess similar physical characteristics. A literature survey showed that the structures of cumulus clouds were by no means uniform with respect to time and space and that subsaturated air is present throughout considerable portions of the clouds at all stages of their growth and decay. It was concluded that physical conditions which are necessary for the production of secondary ice particles by the evaporation of ice exist commonly in cumulus clouds.

A hypothetical model consideration was developed in order to examine the possibility of secondary ice particle production in real clouds by the evaporation process of graupel particles. The model was that a graupel particle with an apparent density of 0.15 g cm^{-3} encounter a subsaturated air and that the subsaturated is mixed with water saturated air resulting in the ice saturated air. The production rate of secondary ice particles and the size distribution obtained from the experiments on the evaporation of ice were used in the calculation. The assumption was made that a graupel particle was formed by pure water droplets without containing any solid impurities.

For ice multiplication in the saturated region after the mixing, the most favorable condition occurs when the saturation ratio of dry air is lower and when the mixing process takes place rather quickly. Therefore, the region, where strong mixing process between saturated air and subsaturated air is taking place, is required if ice multiplication occur by this process. A cloud grown in drier environment has a better chance of ice multiplication. In a convective cloud, there is continuous mixing of air by turbulence and by entrainment in and around a cloud. There are horizontal motions as well as vertical motion. These air motions may sometimes accelerate the process of ice multiplication by mixing the cloud air with the subsaturated air which contains secondary ice particles. If the mechanism of preactivation nuclei is incorporated with the mechanism of secondary ice particle production from an evaporating graupel, the latter could become even more effective for ice multiplication. In any case, in order for the mechanism to become effective for ice multiplication in a cloud, the presence of large graupel particles with low apparent densities and their exposure to subsaturated air are essential. It seems proper to conclude that by this process the multiplication rate of ice particles of the order of at least several per minute can be explained.

In order to verify that ice multiplication due to the evaporation of graupel particles occurs in the atmosphere, it is necessary to make the following observations:

1. The measurements of ice crystal concentration should be made in clouds with a special attention to the regions in the vicinities of subsaturated air especially near cloud edges and near the subsaturated air pockets.
2. The measurements of the concentration of large graupel particles should be conducted in clouds before ice multiplication takes place.
3. Ice nuclei concentration should be measured in the subsaturated air near cloud edges and in clouds. It is essential to take and to store samples of air in such a way as to prevent ice on solid particles from disappearing (Roberts and Hallett, 1968).
4. Graupel particles should be examined if some of the impurities contained in graupel particles can be activated as "preactivation nuclei." To do this, by taking a sample of graupel

on a clean surface the graupel particle should be evaporated, and then should be exposed to saturated air, under well-controlled condition. To avoid the migration of small particles contained as impurities, the graupel particle should be evaporated slowly.

5. Ice cystals should be examined microscopically if there is any ice crystal which has an irregualr shape in the center. If the secondary ice particles start to regrow by deposition process before having become smaller than about 5 microns, ice crystals with irregualr shape in the center can be observed.

REFERENCES

Abbas, M. A., and J. Latham, 1969: The electrofreezing of supercooled water drops. Journal of Meteorological Society of Japan, 47, 65-74.

Admirat, P., 1962: Étude des solution surfondues pour le comptage des critaux de glace. Bull. Puy de Dome 1962, 133-140.

Arenberg, D. L., 1941: The formation of small hail and snow pellets. Bulletin of the American Meteorological Society, 22, 113-116.

Aver, A. H., Jr, D. L. Veal and J. D. Marwitz, 1969: Observations of ice crystal and ice nuclei concentrations in stable cap clouds. Journal of the Atmospheric Science, 26, 1342-1342.

Aufdermaur, A. N. and D. A. Johnson, 1972: Charge separation due to riming in an electric field. Quarterly Journal of Royal Meteorological Society, 98, 369-382.

Austin, J. M. and A. Fleisher, 1948: A thermodynamic analysis of cumulus convection. Journal of Meteorology, 5, 240-243.

Bashikirova, G. M. and T. A. Pershina, 1964: On the mass of snow crystals and their fall velocity. Tr. Gl. Geofiz. Observ., 156, 83-100.

Bergeron, T., 1935: On the physics of cloud and precipitation. Proc. 5th Assembly U.G.G.I. Lisbon, Vol. 2, p. 156.

Braham, R. R., Jr., 1964: What is the role of ice in summer rain-showers? Journal of Atmospheric Science, 21, 640-645.

________, 1967: Cirrus cloud seeding as a trigger for storm development. Journal of Atmospheric Science, 24, 311-312.

Browncombe, J. L. and P. Goldsmith, 1972: On the possible production of submicron ice fragments during riming or the freezing of droplets in free fall. The International Cloud Physics Conference, London, August 1972, 143-144.

Brownscombe, J. L. and J. Hallett, 1967: Experimental and field studies of precipitation particles formed by the freezing of supercooled water. Quarterly Journal of Royal Meteorological Society, 93, 455-473.

________ and N.S.C. Throndike, 1968: Freezing and shattering of water droplets in free fall. Nature, 220, 687-689.

Byers, H. R., 1965: Elements of cloud physics. University of Chicago Press, pp. 191.

Cross, J. D., 1969: Scanning electron microscopy of evaporating ice. Science, 164, 174-175.

Cunningham, R. M., 1958: Cumulus circulation. Recent Advances in Atmospheric Electricity. (L.G. Smith, ed.). Pergamon Press. New York. 361-367.

Cunningham, M. and H. Glass, 1965: Cumulus cloud-group history and structure in relation to precipitation growth. Proceeding of International Conference of Cloud Physics, Tokyo, 109-118.

Cunningham, R. M., G. Morton and D. R. Fitzgerald, 1965: Paper presented at A.M.S. meeting on cloud physics and severe local storms, Reno, Nevada.

De Michelli, S. M. and A. R. Licenblat, 1967: Ice whiskers grown in subsaturated atmospheres. Journal of Atmospheric Science, 24, 312-315.

Dye, J. E. and P. V. Hobbs, 1968: The influence of environmental parameters on the freezing and fragmentation of suspended water drops. Journal of Atmospheric Science, 25, 82-96.

Evanse, D. G. and W. C. A. Hutchinson, 1963: The electrification of freezing water droplets and colliding ice crystals. Quarterly Journal of Royal Meteorological Society, 89, 370-375.

Fletcher, N. H., 1962: The physics of rainclouds, Cambridge University Press.

Gebhart, B., 1961: Heat transfer. McGraw-Hill. 454 p.

Gokhale, N. R. and J. Goold, Jr., 1968: Droplet freezing by surface nucleation. Journal of Applied Meteorology, 7, 870-874.

Goldstein, S., 1965: Modern developments in fluid dyanmics. Vol. II. Dover Publications, Inc., New York.

Grant, L. O. 1968: The role of ice nuclei in the formation of precipitation. Proceedings of the International Conference on Cloud Physics, Toronto, 305-312.

________, 1971: The Second International Workshop on Condensation and Ice Nuclei Report. Department of Atmospheric Science, Colorado State University, Fort Collins, Colorado.

Hallett, J., 1971: Ice crystal nucleation. The Second International Workshop on Condensation and Ice Nuclei, 10-15.

________, and A. J. Alkezweeny, 1968: The fragmentation of freezing water droplets in free fall, Journal of the Atmospheric Sciences, 25, 881-888.

Hobbs, P. V., 1969: Ice multiplication in clouds. Journal of the Atmospheric Science, 26, 315-318.

Holroyd, E. W., 1971: The meso-and microscale structure of Great Lakes snowstorm bands. Ph.D. dissertation, Department of Atmospheric Science, State University of New York, Albany.

Johnson, D. A., 1972: The production of ice splinters by the freezing of accreted water drops. The International Cloud Physics Conference, London, 27-28.

Johnson, D. and J. Hallet, 1968: Freezing and shattering of supercooled water drops. Quarterly Journal of Royal Meteorological Society of Japan, 94, 463-482.

Kachurin, L. G. and V. I. Belyaev, 1960: Investigation of the electrification of crystallizing water. Soviet Physics Dokl. Akad. Nauk., S.S.S.R., (trans. by American Institute of Physics). 5, 137-140.

Knight, C. A. and N. C. Knight, 1973: Conical Graupel. Journal of Atmospheric Science, 30, 118-124.

Kreith, F., 1973: Principles of heat transfer (3rd edition), In text Educational Publishers, New York and London, 656 p.

Koenig, L. R., 1963: The glaciating behavior of small cumulonimbus clouds. Journal of Atmospheric Science, 20, 29-47.

________, 1968: Some observations suggesting ice multiplication in the atmosphere. Journal of Atmospheric Science, 25, 460-463.

Langmuir, I., 1948: The production of rain by a chain reaction in cumulus clouds at temperature above freezing. Journal of Meteorology, 5, 175 p.

Langmuir, I. and K. B. Blodgett, 1946: A mathematical investigation of water droplet trajectories. Army Air Forces Technical Report No. 5418.

Latham, J., 1963: The electrification of frost deposits. Quarterly Journal of Royal Meteorological Society, 89, 265-270.

MacCready, P. B., Jr. and A. I. Weinstein, 1965: Paper presented at American Meteorological Society meeting on cloud physics and severe local storms, Reno, Nevada.

Macklin, W. C., 1962: The density and structure of ice formed by accretion. Quarterly Journal of Royal Meteorological Society, 88, 30-50.

Magono, C. and C. W. Lee, 1966: Meteorological classification of natural snow crystals, Journal of the Faculty of Science, Hokkaido University, Japan, Ser. VII, Vol. II, No. 4, 321-335.

________, and T. Nakamura, 1965: Aerodynamic studies of falling snowflakes. Journal of Meteorological Society of Japan, Ser.2, 43, 139-147.

Malkus, J. S., 1954: Some results of a trade-cumulus cloud investigation. Journal of Meteorology, 11, 220 p.

Morris, T. R. and R. R. Braham, Jr., 1968: The occurrence of ice particles in Minnesota cumuli. Proceedings of the First National Conference on Weather Modification, Albany, 306-315.

Maruyama, T. 1968: On conical graupel and its density. Papers in Meteorology and Geophysics, 19, 101-108.

Mason, B. J., 1971: The physics of clouds, Clarendon Press.

________, and J. Maybank, 1960: The fragmentation and electrification of freezing water drops. Quarterly Journal of Meteorological Society, 86, 176-186.

Mossop, S. C., 1968: Comparisons between concentration of ice crystals in cloud and concentration of ice nuclei. Journal de Recherches Atmospheriques, 4, 119-124.

________, 1971: The multiplication of ice crystals in clouds, Proceedings of International Conference on Weather Modification, Canberra, Australia, September. 6-11. 1-4.

________, R. E. Cottis and B. M. Bartlett, 1972: Ice crystal concentration in cumulus and stratocumulus. Quarterly Journal of Royal Meteorological Society, 98, 487-508.

________, and A. Ono, 1969: Measurements of ice crystal concentration in clouds. Journal of Atmospheric Science, 26, 130-137.

________, and ________, and K. J. Heffernan, 1967: Studies of ice crystals in natural clouds. Journal de Recherches Atmospheriques, 3, 45-64.

________, and ________, and E. R. Wishart, 1970: Ice particles in maritime clouds near Tasmania. Quarterly Journal of Royal Meteorological Society, 96, 487-508.

________, and R. E. Ruskin and K. J. Heffernan, 1968: Glaciation of a cumulus at approximately -4 C. Journal of Atmospheric Science, 25, 889-899.

Nakaya, U. and T. Terada, 1935: Simultaneous observations of the mass, falling velocity and form of individual snow crystals. Journal of Faculty of Science, Hokkaido University, Ser. II, 1, 191-201.

Ono, A., 1973: Some aspects of the ice phase development in relatively warm supercooled maritime cumulus clouds with special attention to small regular ice crystals. Paper presented at the Seminar on Cumulonimbus Modification of Tropical Nature, Miami.

Ranz, W. E. and J. B. Wong, 1952: Impaction of dust and smoke particles on surface and body collectors. Industrial and Engineering Chemistry, 44, 1371-1381.

Roberts, P. and J. Hallett, 1968: A laboratory study of the ice nucleating properties of some mineral particulates. Quarterly Journal of Royal Meteorological Society, 94, 25-34.

Ruskin, R. H., 1969: Multiplication of ice embryos by ice whisker shedding, Science, 166, 906.

Schaefer, V. J. and R. J. Cheng, 1971: The production of ice crystal fragments by sublimation and electrification. Journal de Recherches Atmospheriques, 5, 5-10.

Scorer, R. S. and Ludlam, F. H., 1953: The bubble theory of penetrative convection. Quarterly Journal of Royal Meteorological Society, 79, 96 p.

Simpson, J. and W. L. Woodley, 1969: Intensive study of three seeded clouds on May 16, 1968. ESSA Technical Memorandum, ERLTM-APCL8.

Squires, P. 1958: The spatial variation of liquid water and droplet concentration in cumuli. Tellus, 10, 372-380.

Takahashi, C. and A. Yamashita, 1970: Shattering of frozen water drops in a supercooled cloud. Journal of Meteorological Society of Japan, 48, 373-376.

Takeda, T., 1968: The effect of the time lag in the activation of atmospheric ice nuclei on the number of ice crystals in clouds. Journal of Meteorological Society of Japan, 46, 69-76.

Takeuchi, D. M., 1970: Ice phase development in cumulus clouds. Preprints of papers presented at the Conference on Cloud Physics, Fort Collins. 175, 176.

________, 1971: Precipitation development in seeded and natural cumulus clouds. Preprint of Second National Conference on Weather Modification at Santa Barbara. American Meteorological Society, 198-204.

________, 1972: Considerations of microphysical variations upon the potential for cumulus modification by the warm rain process. Proceedings of Third Conference on Weather Modification, Rapid City. American Meteorological Society, 166-170.

Vardiman, L., 1972: Ice crystal multiplication in convective elements of winter orographic cloud. Atmospheric Science Paper No. 191, Department of Atmospheric Science, Colorado State University, Fort Collins, Colorado.

________, and L. O. Grant, 1972: A case study of ice crystal multiplication by mechanical fracturing. The International Cloud Physics Conference, London, August, 1972, 22-23.

Warner, J., 1955: The water content of cumuliform cloud. Tellus, 7, 449.

________, J., 1969: The microstructure of cumulus cloud. Part II. The Effect on droplet size distribution of the cloud nucleus spectrum and updraft velocity. Journal of Atmospheric Sciences, 26, 1272-1282.

________, and T. D. Newham, 1958: Time lag in ice crystal nucleation in the atmosphere. Bulletin de l' Observatire du Pay de Dome, 1, 1-10.

Weickmann, H. K. and H. aufm Kampe, 1953: Physical properties of cumulus clouds. Journal of Meteorology, 10, 204-211.

Zikmunda, J. and G. Vali, 1972: Fall patterns and fall velocities of rimed ice crystals. Journal of Atmospheric Science, 29, 1334-1347.

APPENDIXES

APPENDIX I

DATA OF RIMING EXPERIMENTS

EXPERIMENT (1)

Temp. (°C)	ΔV(cm^3)	ρ(g/cm^3)	Δm(mg)	N	No	ΔN	dn/dm(1/mg)	KX10^6
-7.0∿ -7.4	.48X10^{-2}	.25	1.20	18	12	6	5.00	2.228
-7.3∿ -7.7	.70	.23	1.61	17	4	13	8.13	1.372
-6.7∿ -7.3	.47	.26	1.22	11	7	4	3.33	3.343
-6.9∿ -7.5	.49	.23	1.12	7	0	7	6.37	1.751
-7.0∿ -7.4	.50	.27	1.35	9	2	7	5.19	2.149
-7.2 ± .3		.25±.03					5.60±1.6	2.168±.666

EXPERIMENT (2)

Temp. (°C)	ΔV(cm^3)	ρ(g/cm^3)	Δm(mg)	N	No	ΔN	dn/dm(1/mg)	KX10^6
-6.8∿ -7.4	.24X10^{-2}	.23	0.55	15	7	8	14.55	1.532
-6.7∿ -7.1	.36	.24	.86	11	9	2	2.29	9.750
-7.0∿ -7.4	.17	.24	.41	9	2	7	17.50	1.278
-6.8∿ -7.3	.28	.25	.70	10	5	5	7.14	3.120
-6.9∿ -7.2	.17	.21	.36	12	1	11	29.33	.760
-7.0∿ -7.6	.18	.26	.47	6	1	5	10.53	2.116
-7.1± .3		.24±.02					13.6±8.6	3.092±3.067

EXPERIMENT (3)

Temp. (°C)	ΔV(cm^3)	ρ(g/cm^3)	Δm(mg)	N	No	ΔN	dn/dm(1/mg)	KX10^6
-6.8∿ -7.4	.93X10^{-2}	.27	2.50	9	6	3	1.20	7.427
-6.7∿ -7.1	.95	.27	2.56	6	2	4	1.56	5.710
-7.0∿ -7.6	.90	.25	2.25	10	3	7	3.11	2.866
-7.2∿ -7.8	.96	.26	2.50	9	5	4	1.60	5.570
-6.6∿ -7.0	.92	.28	2.56	12	0	12	4.68	1.903
-6.8∿ -7.2	.96	.29	2.78	26	4	22	7.90	3.232
-7.1± .3		.27±.01					3.3±2.3	4.451±1.923

EXPERIMENT (4)

-6.5∿ -7.1	$.24 \times 10^{-2}$	.28	.68	9	5	4	6.0	2.785×10^{6}
-7.0∿ -7.6	.26	.26	.93	10	0	10	10.7	1.560
-6.9∿ -7.5	.25	.25	.63	13	4	9	14.2	1.175
-7.2∿ -7.8	.24	.24	.57	8	3	5	8.82	1.894
-6.8∿ -7.2	.26	.25	.90	10	2	2	2.22	7.520
-6.5∿ -6.9	.25	.26	.63	9	2	7	11.05	1.511
-7.1± .3		.26±.01					8.83±3.9	2.741±2.195

EXPERIMENT (5)

-7.1∿ -7.7	$.81 \times 10^{-2}$	.32	2.58	11	4	7	2.71	4.318
-6.7∿ -7.1	1.21	.29	3.50	3	0	3	.86	7.800
-6.9∿ -7.3	.81	.34	2.76	11	8	3	1.09	6.127
-7.0∿ -7.6	.81	.31	2.50	9	0	9	3.60	1.856
-6.8∿ -7.4	.84	.33	2.76	7	1	6	2.18	3.063
-6.5∿ -7.1	1.62	.28	4.54	9	7	2	.44	15.040
-7.1± .3		.31±.01					1.81±1.11	6.367±4.336

EXPERIMENT (6)

-7.2∿ -7.7	$.29 \times 10^{-2}$	.29	.83	2	0	2	2.40	6.965
-7.1∿ -7.5	.28	.30	.83	5	1	4	4.80	3.483
-7.2∿ -7.8	.27	.30	.80	9	4	5	6.25	2.674
-6.9∿ -7.3	.40	.28	1.13	7	0	7	6.18	2.706
-7.0∿ -7.6	.29	.27	.77	8	4	4	5.22	3.203
-7.1∿ -7.7	.37	.29	1.07	6	2	4	3.75	4.457
-7.3± .3		.29±0.01					4.77±1.356	3.915±1.987

APPENDIX II

CALCULATION OF THE TIME REQUIRED FOR THE MULTIPLICATION BY THE RIMING PROCESS

The rate of mass increase of a graupel of radius R falling with velocity V through a cloud of liquid-water content w, composed of smaller droplets having terminal velocities, v, is given by

$$\frac{dm}{dt} = E\pi R^2 w(V-v) \tag{1}$$

where m is the mass of a graupel, E is the collection efficiency. If a homogeneous cloud is assumed, the following realtionships are valid

$$m = \rho_i \cdot \frac{\pi}{6} D^3 = N \cdot \frac{\pi}{6} d^3 \tag{2}$$

$$w = n \cdot \frac{\pi}{6} d^3 \tag{3}$$

where, ρ_i is the density of a graupel; D is the diameter of a graupel; N is the number of water drops composing a graupel particle; n is the concentration of water drops in a cloud; and d is the diameter of a water drop. From the equations (1) through (3), the following equation can be obtained.

$$\frac{dN}{dt} = \frac{\pi E D^2}{4} n \cdot \Delta v \tag{4}$$

where Δv is the relative velocity of a falling graupel. Combining the relationship given by Macklin (1962)

$$\rho_i = 3.64\left(-\frac{d\Delta v}{2T_s}\right)^{0.76} \tag{5}$$

and

$$\Delta v = 286D^{.44} \tag{6}$$

with the equation (4), the following equation is obtained.

$$\frac{dN}{dt} = 0.75EnN^{.73} \cdot d^{1.89} \cdot (-\frac{1}{2T_s})^{.44}$$

or

$$\int_{No}^{N} \frac{dN}{N^{.73}} = \int_{o}^{t} 0.75End^{1.69}(-\frac{1}{2T_s})^{.44}\, dt \qquad (7)$$

By using the equation (7), the times required for the ice concentration to become multiplied were calculated. The calculations were made under the assumption that

$$T_s = -7°C$$

and

$$E = 1.0.$$

The following cases are considered:

$n = 50, 100, 200, 500, 1000\ cm^{-3}$

$d = 5, 10, 15, 20$ microns

The results of calculations are given in Figure A-1 through A-4. In the figures, K is the number of collisions which produce one secondary ice particles.

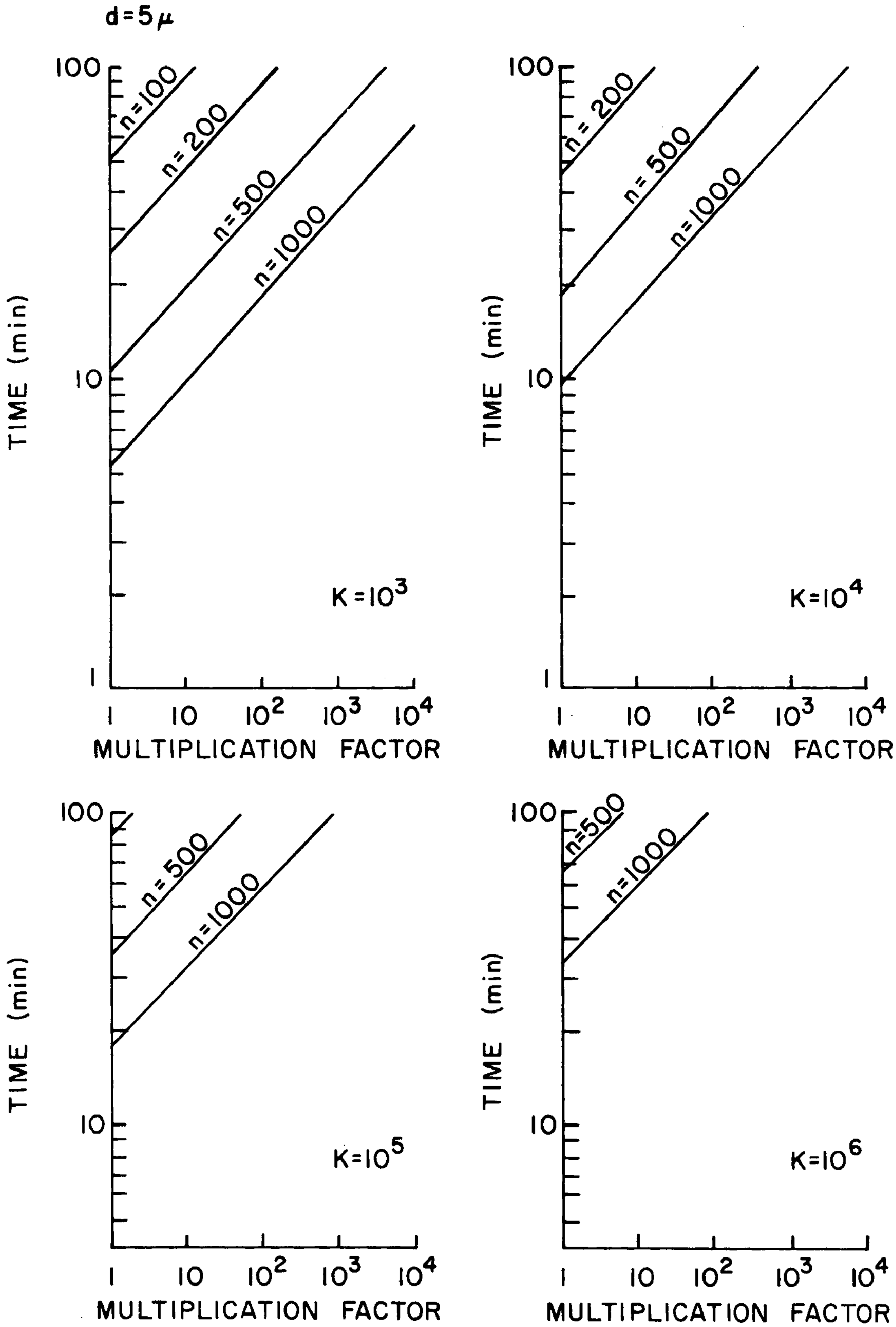

Figure A-1. Time required for ice multiplication by grazing collision (d = 5μ).

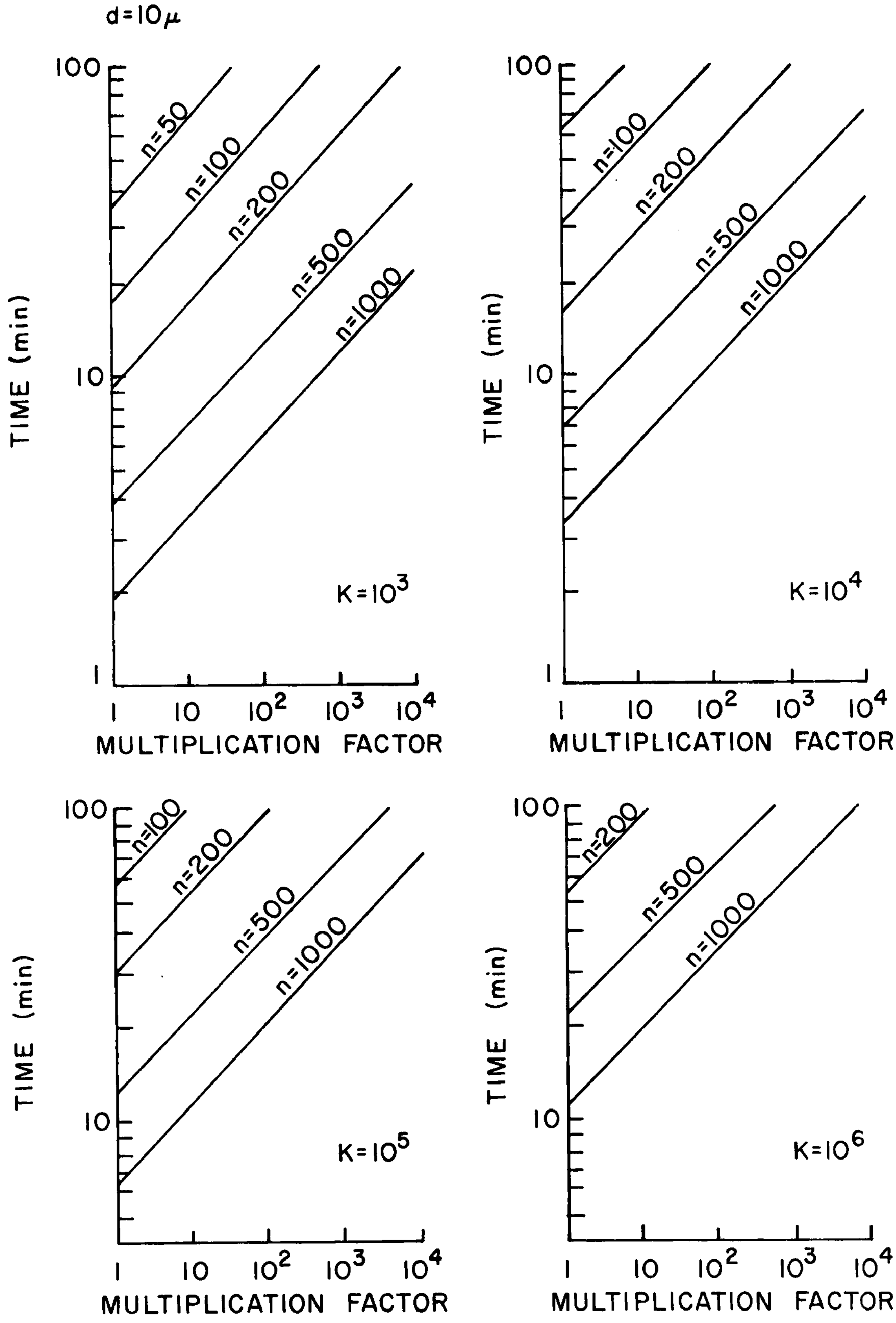

Figure A-2. Time required for ice multiplication by grazing collision (d = 10μ).

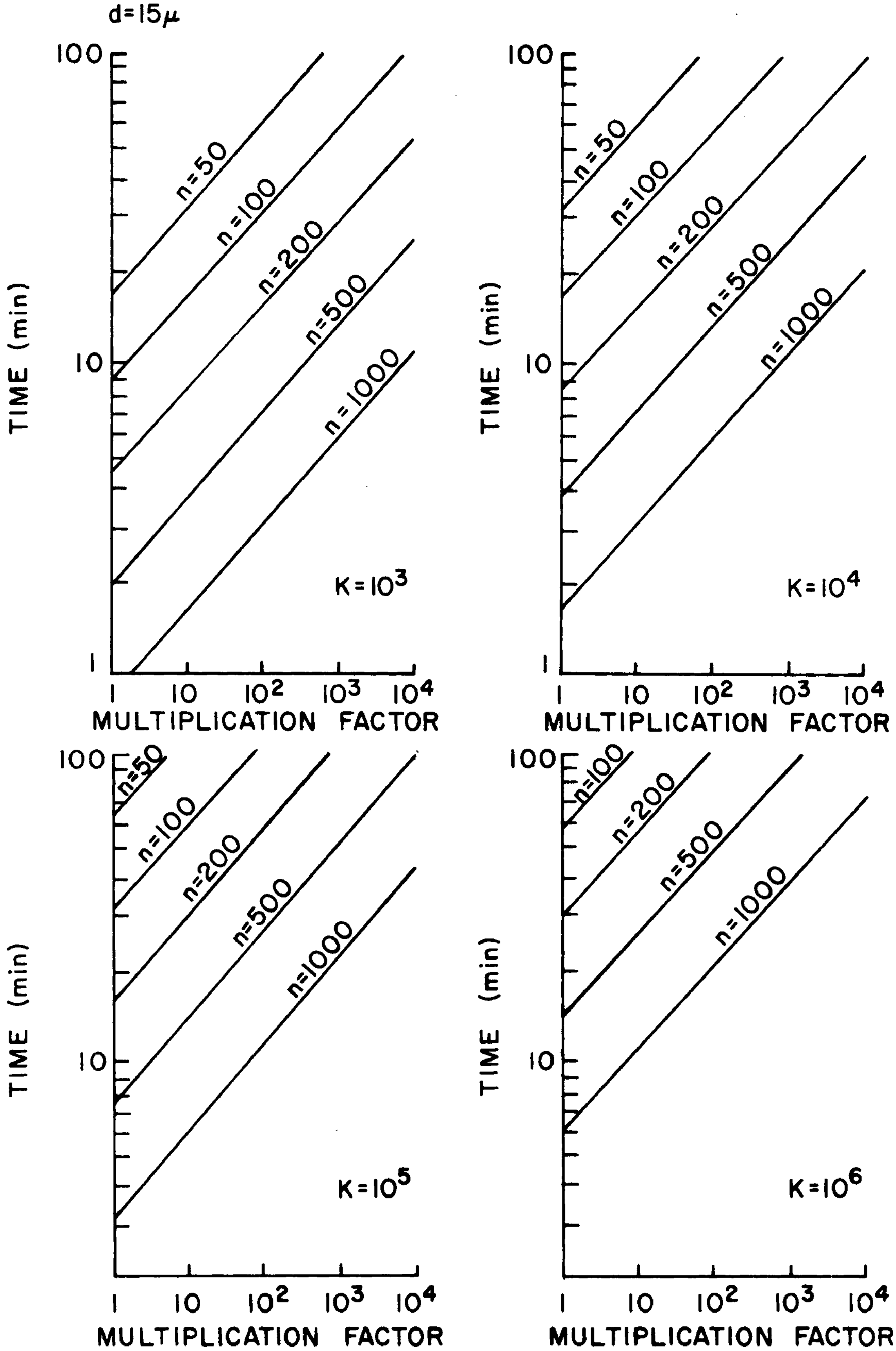

Figure A-3. Time required for ice multiplication by grazing collision (d = 15μ).

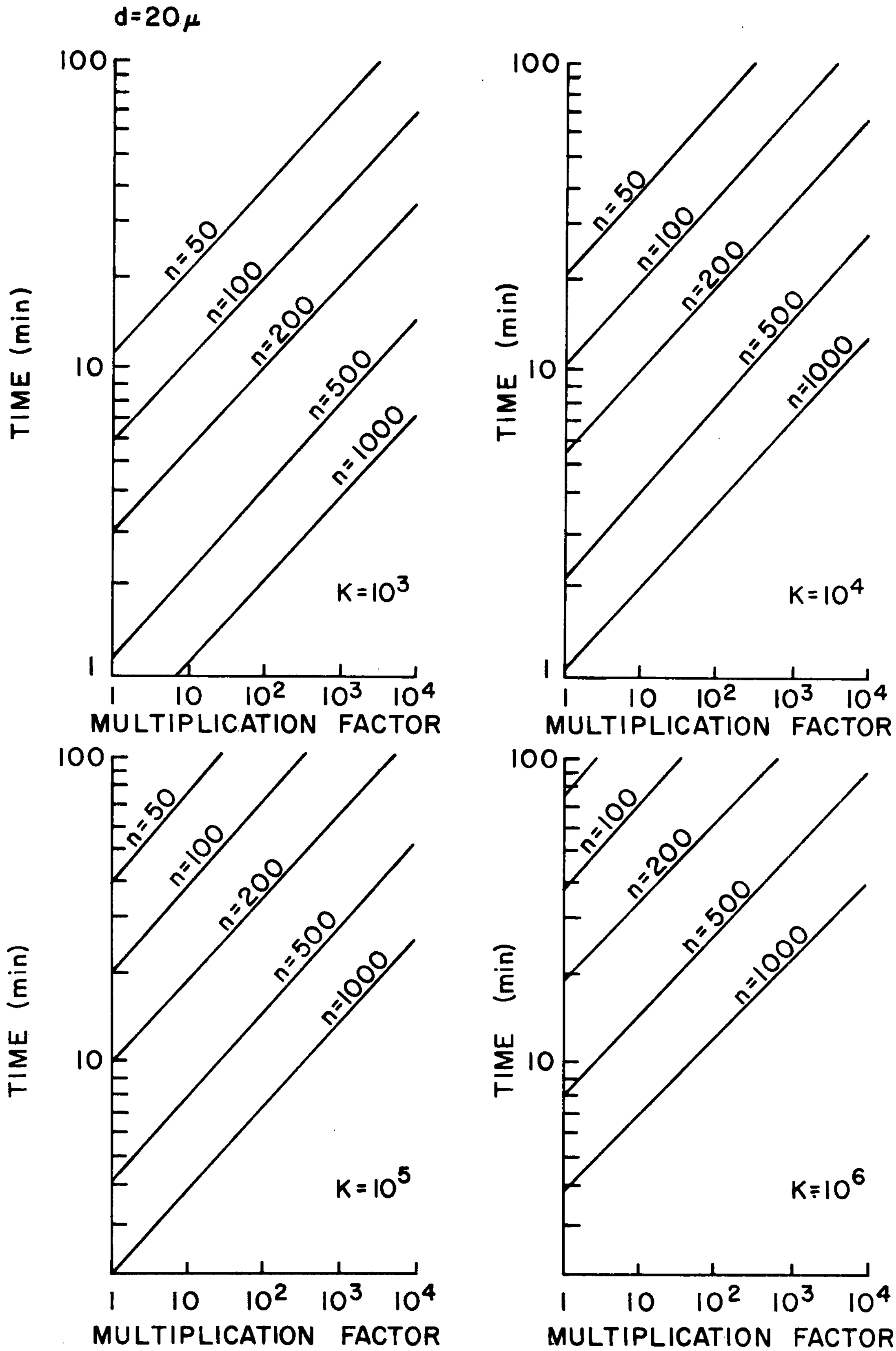

Figure A-4. Time required for ice multiplication by grazing collision (d = 20μ).

BIBLIOGRAPHIC DATA SHEET	1. Report No. CSU - ATSP - 220	2.	3. Recipient's Accession No.

4. Title and Subtitle Secondary ice particle production from rimed ice	5. Report Date June 1974
	6.
7. Author(s) Teizi Henmi	8. Performing Organization Rept. No. CSU-ATSP-220
9. Performing Organization Name and Address Colorado State University Department of Atmospheric Science	10. Project/Task/Work Unit No.
	11. Contract/Grant No. NSF GA-11574, GA-26601,GI-31460
12. Sponsoring Organization Name and Address National Science Foundation	13. Type of Report & Period Covered 1969 - 1974
	14.

15. Supplementary Notes

16. Abstracts

The roles of the riming process and of rimed ice on ice-multiplication were studied experimentally. The first experiments were to study the secondary ice particle production from ice during the growth by the riming. The number of particles produced during the growth were fewer than 10 per mg of ice. The second series of experiments were to study the secondary ice particle production due to the evaporation process of ice which had been formed by the riming process. It was found that secondary ice particles were commonly produced at the rate of 10 to 200 per mg of evaporating ice while the ice was ventilated with subsaturated air. The density of the ice effective for the production was smaller than .2 gm/cm^3. The ice multiplication rate of the order of several particles per minute in a cumulus could be explained by the production of secondary particles due to the evaporation of graupel particles.

17. Key Words and Document Analysis. 17a. Descriptors

Ice multiplication
Evaporation of ice
Rimed ice
Secondary ice particles
Graupel particles
Cumulus clouds

17b. Identifiers/Open-Ended Terms

17c. COSATI Field/Group

18. Availability Statement	19. Security Class (This Report) UNCLASSIFIED	21. No. of Pages 142
	20. Security Class (This Page UNCLASSIFIED	22. Price